UNIVERSITAT DE BARCELONA

Estimation of phylogeographic patterns and divergence times of populations of small mammals from the Iberian Peninsula using genomic data

Alfonso Balmori de la Puente

Estimation of phylogeographic patterns and divergence times of populations of small mammals from the Iberian Peninsula using genomic data

Doctoral Thesis

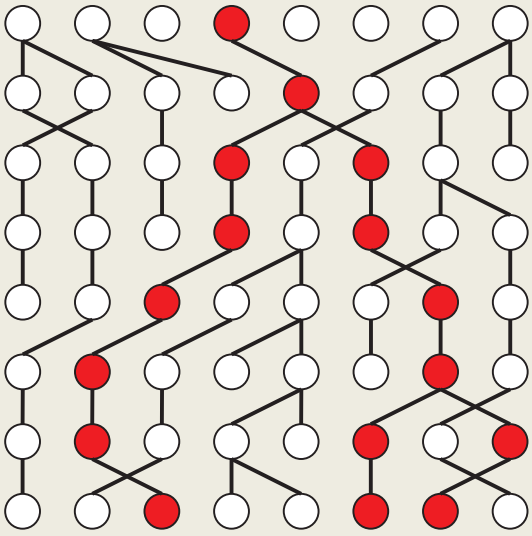

Alfonso Balmori de la Puente

Instituto de Biología Evolutiva (CSIC – UPF)

Tesis Doctoral

Universidad de Barcelona

Estimation of phylogeographic patterns and divergence times of populations of small mammals from the Iberian Peninsula using genomic data

Memoria presentada por:

Alfonso Balmori de la Puente

Para optar al grado de doctor

por la Universidad de Barcelona

Programa de Genética

Trabajo realizado en el Instituto de Biología Evolutiva (CSIC – UPF)

Director: **José Castresana Villamor**

Tutor: **Julio Rozas Liras**

Doctorando: **Alfonso Balmori de la Puente**

24 de Julio de 2020

AGRADECIMIENTOS

En primer lugar, quiero expresar mi agradecimiento a mi director de tesis, el Dr. José Castresana. Su entrega y compromiso con mi formación ha sido firme a lo largo de todos estos años. Es un privilegio que haya puesto a mi disposición su conocimiento y categoría científica, además de haberme inculcado el valor del rigor y la integridad, aspectos que ya forman parte de mí.

La redacción de esta tesis y los acertados consejos, comentarios y correcciones recibidos durante la misma me han enseñado a ser claro y conciso, y por eso agradezco en conjunto a mi tutor y coordinadores del programa de genética de la Universidad de Barcelona, coautores, colaboradores, investigadores, administración, técnicos, familia, compañeros y amigos su inestimable ayuda y aliento. Todos ellos han desempeñado un papel esencial en la preparación de este trabajo. El asesoramiento y soporte recibido desde mi llegada al laboratorio, sin apenas saber lo que era una pipeta; las reconfortantes videollamadas a kilómetros de distancia que calmaban tempestades; el crecimiento personal e intelectual de este viaje de más de cuatro años con paradas transoceánicas, gracias a la magnífica acogida del Dr. Jody Hey y su entorno en Temple University; las actividades deportivas practicadas (con mejor o peor fortuna) aquí y allá; las aventuras y experiencias en las salidas al campo, a ver bichos aéreos, terrestres, acuáticos, semi-acuáticos y subacuáticos (a veces con prismáticos, otras con lupa y siempre con gafas). Especialmente las comidas de después que finalmente se convertían en la verdadera motivación de las rutas, son algunos de los recuerdos de esta etapa que siempre me acompañarán.

Este trabajo ha contado con un contrato de investigación BES-2015-074119 obtenido por parte del Ministerio de Ciencia, Innovación y Universidades cofinanciado por el fondo europeo FEDER.

Finalmente, me gustaría agradecer a las circunstancias de la vida que me trajeron al Instituto de Biología Evolutiva, que representa un orgullo para mí, y me rodearon, una vez más, de una fantástica compañía.

Contents

I. ABSTRACT

Phylogenetic and phylogeographic methods allow studying the evolutionary relationships between populations and species, patterns of genetic structure, and historical events that have modelled the current distribution of biodiversity. Molecular markers are a fundamental complement of morphological data to accomplish these studies. The divergence time between species and populations is among the most useful parameters to place evolutionary events in the proper historical context as well as to assess population differentiation, evolutionary units and taxonomic categories, but it is difficult to estimate. The emergence of coalescent theory indicated that different genes can reflect different histories and that the coalescence of genes might have occurred much before the actual divergence between populations or species, a phenomenon that is crucial to know divergence times and evidences the importance of multilocus analysis. The Iberian Peninsula played a major role in shaping the distribution of present biodiversity as it harbored different Pleistocene refugia that were the source of recolonizations of other European areas and created internal diversity within this peninsula. In this thesis, two Eurosiberian species, *Neomys fodiens* and *Arvicola scherman*, both of which have received little attention despite their biogeographical interest, have been used to advance in this framework of study. To obtain samples of both species, an important effort to optimize laboratory protocols and bioinformatic analysis was made to enable the work with minimally invasive samples.

In chapter 1, a subspecies of the Eurasian water shrew, *Neomys fodiens niethammeri*, which is found in a narrow strip of the northern Iberian Peninsula, was studied. This subspecies presents an abrupt increase in skull size when compared to the rest of the Eurasian population, which has led to the suggestion that it is actually a different species. Skulls obtained from owl pellets collected over the last 50 years allowed us to perform a morphometric analysis in addition to an extensive multilocus analysis based on short intron fragments successfully amplified from these degraded samples. Interestingly, no genetic divergence was detected using either mitochondrial or nuclear data. Additionally, an allele frequency analysis revealed no significant genetic differentiation. The absence of genetic divergence and differentiation revealed here indicated that the large form of *N. fodiens* does

not correspond to a different species and instead represents an extreme case of size increase, of possible adaptive value, which deserves further investigation.

In chapter 2, the divergence time between two Iberian populations of the Montane water vole (*Arvicola scherman*) was estimated using double-digest restriction site-associated DNA (ddRAD) obtained through next-generation sequencing (NGS), including skulls from barn owl pellets among the samples, and applying an isolation-with-migration (IM) analysis. The Cantabrian and Pyrenean populations of *A. scherman* are geographically isolated and have subtle morphological differences between them. Thousands of single nucleotide polymorphisms (SNPs) derived from the ddRAD were used to study their genetic structure. In addition, a bioinformatic pipeline was developed to find orthologues of the ddRAD loci in other rodents and estimate specific mutation rates using a fossil calibration point (the mouse-rat split). By this means, 85 loci were calibrated. The IMa3 software was then used together with the specific mutation rates of the calibrated loci in order to estimate divergence times and other demographic parameters (population sizes and migration rates). The length of the markers used (145 base pairs) was small compared to other loci generally used with IM models, so the inclusion of only the calibrated loci did not provide enough information. However, it was demonstrated that using a set of 300 ddRAD loci, including the 85 with estimated mutation rates, resulted in good mixing and convergence of the model. The results of the analysis allowed concluding that the two Iberian populations of *A. scherman* diverged 39 thousand years (Kyr) ago with a 95% highest posterior density interval of 21 – 62 Kyr. A small amount of migration was detected between both populations. Based on this split time and the genetic structure found, it is suggested that the two populations have been present in isolated Iberian refugia at least since the last glaciation and are not the product of a recent colonization of the norther Iberian strip. The methodology developed here based on ddRAD data and coalescent theory allows estimating recent divergence times with high accuracy and comparing the results between different taxa. This can be of great help to understand the generation of diversity in a relatively small geographical area such as the Iberian Peninsula and determine whether the populations have differentiated for enough time to deserve separate taxonomic or conservation status.

II. INTRODUCTION

Evolutionary genetics aims to study the relationships between different groups of related taxa and their populations based on the differences found between their DNA sequences. These differences can be used in phylogenetic and phylogeographic analyses to address questions about the biogeography and evolutionary history of biodiversity. When using information from multiple organisms across similar areas, phylogeographic patterns can be compared and studied to identify historical events that could have modelled their current distribution. On the other hand, the estimation of population parameters such as divergence times and migration rates are useful to assess population differentiation and evolutionary units. The description of categories of related taxa in nature is fundamental for studying biodiversity. Avise (2004) discussed that molecular data have several advantages over the use of morphological, behavioral or other phenotypic features; for instance, the access to a nearly unlimited pool of genetic variability, or their ability to quantify divergence and differentiation. Molecular markers are also considered to be the key tool to provide with new insights in ecology and evolution of living beings, setting up the bases of molecular ecology (Freeland et al., 2011). The arrival of genomics and next-generation sequencing (NGS) together with the development of genetic techniques to obtain thousands of markers at reduced costs have allowed to perform studies with different organisms using a number of markers representative of their whole genome (Goodwin et al., 2016). In parallel, the use of minimally invasive samples in genetic studies is spreading quickly to sample a wide range of different taxa and allowing the study and conservation of biodiversity that would be impossible without them (Carroll et al., 2018). This is therefore a fascinating time to carry out biodiversity studies using genomic markers.

1. Minimally invasive samples in biodiversity studies

The use of minimally invasive samples in biodiversity studies has its roots in ancient DNA studies. There are several features that both research areas share, such as the use of samples with degraded DNA, so specific approaches developed to cope with small DNA fragments from ancient specimens have allowed its application in present day minimally invasive samples.

1.1. Ancient and historical DNA studies

The interest that we have in our own species has leaded the focus of genetic studies on the evolution of our lineage. Until a few decades ago, first evidences of humans could only be analyzed by morphological studies, but with the development of new genetic techniques that allow the extraction of DNA from ancient material, fossil records have enabled the discovery of surprising facts that occurred thousands of years ago. It is now even possible to sequence the complete genomes from ancient remains (Prüfer et al., 2014). Through these techniques it has been possible to know some fundamental aspects of our own species such as the hybridization events occurred between Neanderthals and modern humans (Sankararaman et al., 2012) or a better knowledge of details of our history such as the introduction of steppe-related ancestry by central European populations into Iberia (Olalde et al., 2019).

But not only humans have driven the attention of geneticists. Some genetic studies have focused on ancient DNA to analyze the impact of species domestication by human activities on horses (Librado et al., 2017), pigs (Ottoni et al., 2013) or dogs (Leonard et al., 2002). In addition, efforts have been put in emblematic species that went extinct in the past, thousands of years ago. For example, Dabney et al. (2013) recovered the mitochondrial genome of the cave bear (*Ursus deningeri*) from short fragments of ~50 base pairs of a radius bone conserved out of permafrost >300,000 years from Sima de los Huesos (Atapuerca, Spain), representing a divergent lineage of cave bears. Another phylogenetic study in which nuclear DNA was extracted from a 50,000-130,000 years old American mastodon (*Mammut americanum*) tooth, which corresponds to the outgroup of present day elephants, helped to establish that Asian elephants are the closest living relative of woolly mammoth (Rohland et al., 2010).

1.2. Extraction of genomic data from minimally invasive samples

The impressive progression of the studies based on ancient DNA led naturally to genetic studies in which other sources of degraded DNA were used, such as the retrieval of DNA from bear droppings (Höss et al., 1992), which promoted the use of non-invasive samples in biodiversity studies (Taberlet et al., 1999).

Non-invasive and minimally invasive samples are considered to be a highly valuable source of information to carry out genetic studies, since they allow researchers to assess or monitor populations of organisms without disturbing them (Morin and Woodruff, 1996; Taberlet et al., 1999; Schwartz et al., 2007; Beja-Pereira et al., 2009; Goossens and Bruford, 2009; Pauli et al., 2010). In particular, these methods allow accessing material otherwise unavailable from elusive populations as well as from endangered species in which handling can be stressful for the animals or even potentially threatening for their populations (Waits and Paetkau, 2005; McCarthy et al., 2015; Querejeta and Castresana, 2018). Thus, an important application of minimally invasive samples is conservation genetics (Taberlet and Bouvet, 1994). However, when using this source of data, some important concerns regarding genotyping accuracy should be assessed.

Sampling in which it is not necessary to kill the animal includes two different classes of samples (Taberlet et al., 1999; Mills, 2013). The first one consists in obtaining tissue samples through manipulation or capture of animals without killing or damaging them. The second category, non-invasive sampling, applies to samples left behind by the animal without catching or disturbing them. Since there is always some interference in the process of sampling, minimally invasive sampling might be a more appropriate term in general (Carroll et al., 2018). Non-invasive and minimally invasive samples, as well as other types of remains such as undigested material from small mammal prey or animals found dead in the field, share the feature of having low quantities of DNA, which is furthermore usually degraded (Rohland and Hofreiter, 2007a; Carroll et al., 2018). Although samples with degraded DNA present technical challenges, protocols have been developed and are still being improved to extract DNA from different sources of genetic material (Waits and Paetkau, 2005; Freeland et al., 2011).

1.3. Use of minimally invasive samples in conservation genetics

The improvement of laboratory techniques has enabled minimally invasive samples with degraded DNA to be used for monitoring of populations or in phylogeographic studies of rare and endangered taxa (Rohland and Hofreiter, 2007a; Carroll et al., 2018). Studies based on this sort of material to track biodiversity are increasingly common due to their non-disturbance character, enabling the emergence of conservation genetics as an important line of research (Frankham et al., 2010). The main goal of this branch of conservation biology is reducing the extinction risk of threatened species and conserving populations and species able to cope with environmental changes in the context of the sixth extinction crisis the world is facing (Leakey and Lewin, 1996; Frankham et al., 2010; IUCN, 2020).

Molecular markers are essential tools in this field to determine population structure, taxonomic status and genetic diversity of wildlife. They allow quantifying a wide range of problems that threaten biodiversity such as population bottlenecks, inbreeding or outbreeding depression and the impact of invasive species on native fauna, among others (Amos and Balmford, 2001). Ultimately, genetic results help policy makers to manage populations or take specific conservation measures.

1.4. Types of minimally invasive samples

The use of feces and hairs in particular is replacing other sample types to perform DNA-based studies in mammals but there are many other sources of minimally invasive genetic material that are becoming increasingly popular.

1.4.1. Feces

When analyzing fecal samples, it is possible to obtain either DNA information from the individual or from his diet (Kohn and Wayne, 1997). Specific primers to amplify one or the other can be used and primers should avoid the amplification of bacteria or fungi present in the excrements (Bradley and Vigilant, 2002; Walker et al., 2016; Chiou and Bergey, 2018; Egeter et al., 2019). It must be taken into account that some molecules present in feces can inhibit the Polymerase Chain Reaction (PCR), so specific extraction kits and

protocols may be required for particular sample types (Eggert et al., 2005; Broquet et al., 2007).

Several studies have been developed using DNA extracted from feces to identify species. For instance, DNA analysis from mustelid and felid excrements have been successfully used to differentiate between sympatric species, difficult to distinguish by other means (Hansen and Jacobsen, 1999; Wultsch et al., 2014).

Stool samples have been collected for performing genotyping studies from different vertebrate taxa. Molecular analysis allowed the prospection of emblematic mammalian species, such as chimpanzees or tigers, that produced reliable census estimates comparing with previous estimations based on visual or photographic surveys (Mondol et al., 2009; McCarthy et al., 2015). In the same way, a comprehensive knowledge of the number of individuals and sex ratio of small endangered populations of bears (Taberlet et al., 1997) or the genetic diversity and social structure of elephants in their ranges (Ahlering et al., 2010) has been achieved.

Phylogeographic analysis has been another application of stool samples in large animals such as elephants and chimpanzees, with implications for their conservation (Ahlering et al., 2010; McCarthy et al., 2015). For small mammals, important conclusions have also been achieved thanks to the use of feces. For instance, genetic analysis of the endangered semiaquatic Pyrenean desman let researchers know the distribution range of the species and also differentiate its stool samples from other semiaquatic mammals like water shrews (Figure 1) (Igea et al., 2013, 2015; Gillet et al., 2015). These studies also provided interesting results about the phylogeography of the Pyrenean desman, showing strong patterns with several clades of likely glacial origin distributed across the Iberian Peninsula (Igea et al., 2013). A similar phylogeographic pattern was found in the Mediterranean water shrew also using its feces (Querejeta and Castresana, 2018).

Figure 1. Stool sample (feces) of a Mediterranean water shrew (*Neomys anomalus*). Feces from this species are frequently found on emerged rocks across rivers.

Diet analysis using metabarcoding with next-generation sequencing (NGS) techniques have contributed to the knowledge of food preferences of small mammals such as the endangered Pyrenean desman (Gillet et al., 2015; Biffi et al., 2017a; Esnaola et al., 2018; Hawlitschek et al., 2018).

The presence of diseases caused by bacterial or viral pathogens and parasites have been also identified in different vertebrate taxa using stool samples, showing the full potential of this material, as dietary and disease information can be obtained at once (Xiao et al., 2004; Deagle et al., 2009; Schultz et al., 2018).

1.4.2. Hair samples

Hair material can be collected from captured specimens as it is not usually left behind with the frequency of feces (Escoda et al., 2019). Apart from the capture of specimens, several types of hair traps have been devised to obtain hair samples (Kendall and McKelvey, 2008; Pauli et al., 2008). Different studies have compared the performance between hairs and feces in mustelid species for individual identification under different circumstances, showing that they provide complementary results (Croose et al., 2016; Kubasiewicz et al., 2016). Hairs have better quality DNA than feces, but might yield less quantity of DNA, depending on the size of the mammal being studied (Morin et al., 2001; Bremmer-Harrison et al., 2006). The main advantage of hairs is that it is not contaminated with exogeneous

DNA as feces. However, some contamination with bacteria and parasites may exist and this should be taken into account in NGS studies, where the whole DNA of the sample is sequenced (Tridico et al., 2014; Escoda et al., 2019).

DNA extracted from hair follicles may have great potential once the difficulties mentioned above are overcome. For instance, multilocus approaches carried out with microsatellites amplified over hair samples were able to identify individuals and determine the sex of the Pyrenean brown bear population (Taberlet et al., 1997). Moreover, Escoda et al. (2019), using hair samples extracted from captured Pyrenean desmans, highlighted their potential to obtain SNPs through a ddRAD technique (Peterson et al., 2012) and perform kinship and connectivity analysis.

1.4.3. Skull bones from owl pellets

Another important source of DNA material for biodiversity studies are the owl pellets, that consist in regurgitated material formed in the bird's gizzard and proventriculus, which contains undigestible parts of whole vertebrates preys (bones, teeth, fur, feathers, beaks, claws, etc.) (Guimaraes et al., 2016). The regurgitation of the pellet takes several hours after swallowing and it can contain remains belonging to different individuals and from more than one species (Grimm and Whitehouse, 1963; Dodson and Wexlar, 1979).

Strigiformes, and specifically barn owls (*Tyto alba*), digest their prey to a lesser extent, and thus their pellets usually have more skeletal remains, which makes them an excellent material to perform biodiversity studies (Raczyński and Ruprecht, 1974; Guimaraes et al., 2016). Moreover, this nocturnal bird of prey usually selects nesting sites close to anthropic areas, commonly the attic of churches and abandoned houses in rural areas, making it easier the sampling of its pellets (Martin et al., 2014). Uncertainties about DNA degradation suffered during the digestion and cross-contamination between prey within pellets arose but initial studies with this material soon discarded the concerns (Taberlet and Fumagalli, 1996).

Among the different skeletal remains from the same pellet there is some heterogeneity in DNA preservation. Skull bones, including mandibles with teeth, are extensively used for its greatest quality (Buś et al., 2014; Rocha et al., 2015; Guimaraes et al., 2016).

Skull bones obtained from barn owl pellets have shown great potential to survey small mammalian species using genetic tools (Poulakakis et al., 2005; Barbosa et al., 2013). For instance, the distribution and ecological specializations of cryptic shrews in the Iberian Peninsula influenced by competitive exclusion by closely related species has been unveiled using skull samples (Biedma et al., 2018).

Another advantage of this material is the possibility to perform morphological studies (Figure 2). In fact, molecular studies of bones from pellets complementing morphological analyses have proven to be very effective to uncover hidden biodiversity of elusive taxa but they have been done only with mitochondrial DNA or a very low number of nuclear markers (Poulakakis et al., 2005; Barbosa et al., 2013; Rocha et al., 2015).

Figure 2. Pictures showing the sequential process of sampling this type of minimally invasive samples: from the starting point of collecting and opening pellets (upper row) to the determination of skull bones i.e. mandibles of interest (bottom row). Scale ruler in millimeters is placed at the bottom of the mandibles.

1.4.4. Other types of minimally invasive samples

Apart from the non-invasive samples described above there are many other types that have been used in different studies. Different parts of molted feathers from birds have been analyzed and proven good performance in genetic analyses (Segelbacher, 2002; Horváth et al., 2005). Buccal cells from chimpanzees have been extracted from their food (Takasaki and Takenaka, 1991). Fish scales and fines deposited in marine sediments, blood or embryonic residues on eggshells, deer antlers or even urine are considered a potential

source of DNA for different taxa and might perform well in DNA studies, although they have been used few times (Morin and Woodruff, 1996; Valiere and Taberlet, 2000). There are other minimally invasive sources of DNA that are being implemented in plant biodiversity studies (roots, leaves, etc.) (Freeland et al., 2011). Finally, environmental DNA from soil, air or water samples is considered to be a powerful tool in conservation biology for the detection of rare, difficult-to-sample taxa and invasive species among others due to its sensitivity and the possibility of performing time-serial samples (Ficetola et al., 2008; Taberlet et al., 2012, 2018; Bohmann et al., 2014).

1.5. Methodological problems with minimally invasive samples

As described above, minimally invasive DNA samples have several benefits both in terms of availability of samples and for the welfare of biodiversity. However, there are technical handicaps that should be overcome before working with them, specially genotyping errors and contamination, whose implications are numerous and include obtaining overestimates of the population size or performing incorrect paternity assignments (Marshall et al., 1998; Waits and Leberg, 2000; Pompanon et al., 2005; Carroll et al., 2018).

DNA quantification is an important step to determine in advance which minimally invasive samples can be used for sequencing. There are different tools that allow DNA quantification present in genomic extracts (Rohland and Hofreiter, 2007b). Among the most accurate ones is Real-Time PCR (Morin et al., 2001), in which primers for specific loci amplify DNA molecules of only the species of interest and with high sensitivity.

In any study of population genetics or individualization, genotyping errors should be considered, as they may produce misidentification of the individuals being studied. The most common genotyping errors are allelic dropout and false alleles (Taberlet et al., 1996, 1999; Mckelvey and Schwartz, 2004; Broquet et al., 2007). The former consists in sequencing only one of the alleles and the latter in the appearance of alleles not present in the sample. The different errors obtained may depend on the marker type used (microsatellites, nuclear loci, SNPs, etc.) and should be assessed specifically. Solutions to these errors include specially the analysis of several replicates (Taberlet et al., 1996; Morin et al., 2001; Beja-Pereira et al., 2009). Further analysis comparing heterozygous positions

between DNA products of non-invasive and minimally invasive samples can provide clues about the presence of allelic dropout.

The other crucial problem that may occur with minimally invasive samples is cross-contamination between samples or environmental contamination, because when DNA is extracted from samples that only have a few molecules, the chances to amplify unwished material increases (Taberlet et al., 1999; Waits and Paetkau, 2005). Therefore, it is essential to perform extractions and amplification in separated rooms in sterile conditions (Ou et al., 1991; Rohland and Hofreiter, 2007b). Finally, extraction and PCR blanks should be included to monitor contaminations (Rohland and Hofreiter, 2007b).

2. Development of genetic markers applied to biodiversity

Genetic studies can incorporate the presence of one to thousands of independent molecular markers from different types and the election of the type and number of loci have an impact on the conclusions that can be drawn from the results.

2.1. The need of multilocus analysis

Mitochondrial DNA studies have been often applied to address questions related to phylogeny and phylogeography of mammals (Skog et al., 2009; Filipi et al., 2015; Biedma et al., 2018) but this marker has drawbacks that are worth considering (Bermingham and Moritz, 1998; Hare, 2001). Their advantages are that the effective population size of mitochondrial DNA is four times smaller than nuclear DNA and the rate of molecular evolution is ~10 fold faster, making it very appropriate in studies of closely related taxa (Brown et al., 1979). However, when analyzing distant species, high rates of base substitutions may lead to saturation (Luo et al., 2011). In addition, some controversy in human arose as a result of mtDNA homoplasy, which can bias tree estimations (Hey and Machado, 2003). But the main feature of the mitogenome is that it is a single locus and only maternally inherited (Hutchison et al., 1974). Important problems may arise when using this locus alone because not all genes necessarily reflect the real evolutionary history of populations or species, giving rise to mito-nuclear discordances (Toews and Brelsford, 2012). Therefore, sequencing of multiple genetic markers is crucial in studies of phylogeny and phylogeography (Kearns et al., 2019; Amorim et al., 2020).

2.1.1. The coalescent

The coalescent theory provided with a stochastic model to track backwards in time the genealogical process of genes and developed the connection between sequence data and demographic population parameters (Kingman, 1982; Wakeley, 2006). The classical view of population geneticist was related towards future process with the aim of, for example, estimating allele frequencies, whereas the coalescent approach try to model the evolutionary processes that have led to the current genetic diversity patterns (Ewens, 1990;

Wakeley, 2006). Mutational processes and genealogies should be treated independently as they are random processes that occur in an uncertain way (Rosenberg and Nordborg, 2002).

The theory models the coalescence events occurring in the genealogy of different alleles. Two genes will follow a probability of coalesce in the previous generation of 1/N so the average time to coalesce would be N generations for those 2 genes and 2N generations for a bigger number of them (Kingman, 1982; Hudson, 1990). Coalescence of genes may have occurred much before the actual divergence between populations or species, which is crucial for the estimation of divergence times (Arbogast et al., 2002).

2.1.2. Gene flow and incomplete lineage sorting

Gene flow and incomplete lineage sorting are the processes that cause different markers to reflect different histories, thus causing the gene tree of markers not to match the species tree of the lineage (Freeland et al., 2011; Toews and Brelsford, 2012).

Incomplete lineage sorting is the process that leads to the non-monophyly of the alleles of a species as a result of ancestral alleles being inherited and lost through their evolutionary history (Fujita et al., 2012). More specifically, it occurs when lineages fail to coalesce in the ancestral populations, leading to the coalescence in a more distantly related population (Degnan and Rosenberg, 2009). Trees reconstructed from only such gene trees would lead to phylogenies being different from the species tree (Figure 3a).

Gene flow or the migration between populations (Figure 3b) is also a crucial phenomenon (Joly et al., 2009; Yannic et al., 2010). Estimating gene flow is essential for understanding population connectivity, differentiation and the diversification process (Pinho and Hey, 2010; Marko and Hart, 2011). Many studies have used post-hoc measures of gene flow, such as F_{st} (Marko and Hart, 2011) but better model-based methods exist (Chung and Hey, 2017).

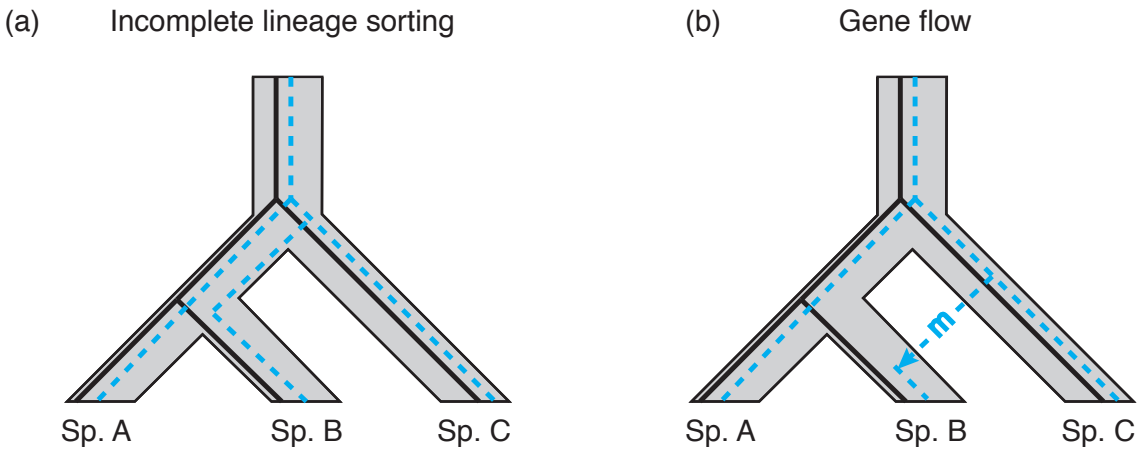

Figure 3. Two species trees representing the true evolutionary relationship between three different species ((A,B), C). Gene genealogies of two genes are represented for showing (a) incomplete lineage sorting and (b) gene flow. Continuous lines indicate congruent gene trees ((A, B), C) whereas anomalous gene genealogies (A, (B, C)) are shown with dashed lines.

2.1.3. Gene trees versus species trees

Species trees are phylogenetic trees that reproduce the branching patterns of species diversification and represent populations or species in their tips instead of alleles whereas gene trees display the coalescence events of the alleles under study (Degnan and Rosenberg, 2009; Edwards, 2009). Discrepancies found between the history of genes and species should not be obviated as they can highly overestimate divergence times, especially in recent splits (Nichols, 2001; Arbogast et al., 2002). For reconstructing species trees it is important not only to increase the number of sites but also the number of independent loci (Edwards, 2009). Edwards and Beerli (2000) concluded that increasing the number of loci will decrease uncertainty occurring around divergence time estimates. Branch length heterogeneity commonly found among gene trees causes different coalescence times for genes (Figure 4). Such differences in coalescence times can provide with information about population sizes and allow estimating better the timings of speciation events (Nichols, 2001; Arbogast et al., 2002).

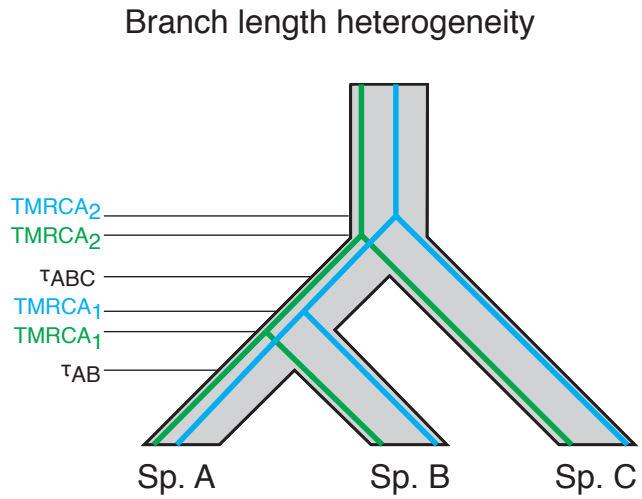

Figure 4. Two gene trees representing the genealogy of two alleles (green and blue) included within the phylogeny of the species ((A, B), C). The TMRCA (time to most recent common ancestor) between alleles for the two splits is different due to random heterogeneity and both are older than the divergence time of the species due to the effect of coalescent.

Different software making use of the coalescent theory have been developed to account for gene tree stochasticity in reconstructing species trees. One of the methods is *BEAST (Heled and Drummond, 2010; Bouckaert et al., 2014; Ogilvie et al., 2017). This software simultaneously estimates gene trees and reconstruct the species trees and divergence times using several loci and individuals per species (Heled and Drummond, 2010). Likewise, it allows estimating population sizes for different models of population evolution (constant, linear and linear with constant root).

2.2. Types of multilocus markers

Three main types of multilocus markers allow researchers to estimate population allele frequencies as well as species trees: microsatellites, sequence data and single nucleotide polymorphisms (SNPs).

2.2.1. Microsatellites

Microsatellites consist in short tandem repeat regions across the genome that vary in length (1-6 base pairs) and repeat number (typically tens of repeats). Mutations at these loci are common due to DNA polymerase slippage and unequal recombination (Debrauwere et al., 1997). Flanking regions of microsatellite loci can be conserved between related taxa, allowing primer design in closely related species.

In mammals, mutation rates (or evolutionary rates) per microsatellite locus can be up to six orders of magnitude faster than point mutation rate (Dallas, 1992; Graur and Li, 2000), making them useful to study the evolutionary history of populations (Amorim et al., 2020; Barker et al., 2020). High mutation rates make microsatellite markers also suitable for individualization and parentage analysis (Flanagan and Jones, 2019). However, when studying distant taxa, size homoplasy might occur when different lineages acquired the same length independently, and this may mislead results (Markert et al., 2001). Finally, many loci need to be used to obtain reliable results, which is time-consuming and not always feasible for microsatellites, so other kinds of markers have been developed.

2.2.2. Sequence data

DNA sequences from different loci (introns, exons or intergenic regions) can be used in studies of phylogeny and population genetics. Their amplification by PCR and subsequent sequencing allows to detect mutational differences that help to identify clades, populations and individuals.

Ultraconserved elements (UCEs) are genetic markers with an almost 100 % of identity between distantly related groups such as birds and mammals, that appear to be important for the ontogeny of vertebrates (Bejerano et al., 2004). UCEs and exons have been successfully applied for reconstructing phylogenies including high-order taxa (Weksler, 2003; McCormack et al., 2012).

However, when studying shallow phylogenies, more variable markers are needed. Intergenic regions and introns can be used for this task, as they are both variable and abundant across the genome. Nevertheless, what makes introns unique is that they are flanked by conserved exons, which is very convenient for primer design across different

taxa (Creer et al., 2005; Igea et al., 2010; Thomson et al., 2010). The main point to perform correct primer design is the selection of orthologous genes and avoid the presence of duplicates (Zhou and Mishra, 2005). It is also important to control for intron and exon length for an appropriate PCR amplification (Igea et al., 2010). Finally, the removal of loci with accelerated or conserved branches in the tree as well as sequences with incorrect alignments, will produce a convenient dataset to carry out genetic studies for shallow phylogenies (Igea et al., 2010). Pipelines to detect orthologous and highly variable introns have been successfully applied to reconstruct species trees in a coalescent framework exploiting intron markers to a greater extent (Hailer et al., 2012; Rodríguez-Prieto et al., 2014). Due to their high information content, intronic sequences have shown great potential to address questions related to the phylogeography and evolutionary history of populations, complementing mitochondrial results and resolution of contentious taxonomies (Seddon et al., 2001; Peters et al., 2008; Igea et al., 2013, 2015; Kearns et al., 2019).

2.2.3. SNPs

Single nucleotide polymorphisms (SNPs) are variable positions of nuclear DNA sequences (Morin et al., 2004). They are biparentally inherited and span millions of loci occurring approximately every 200-500 base pairs in many species, becoming the most common type of sequence variation across genomes (Brumfield et al., 2003; Morin et al., 2004).

SNP data is generally applied to perform population genetic studies for estimating genetic variation, individual genotyping, population structure, population size and change, and finally there are methods able to detect outliers that may be subject to selection (Morin et al., 2004). Although ascertainment bias can affect some SNP-based estimates related with allele frequencies, a large number of SNPs have outperformed other genetic markers such as microsatellites in terms of the data quality in studies of ecology and evolution (Brumfield et al., 2003; Morin et al., 2004; Trasher et al., 2018; Flanagan and Jones, 2019; Lemopoulos et al., 2019).

The emergence of high throughput platforms and bioinformatic pipelines for analyzing short-read sequences have eased the process of SNP discovery, as it will be described later (section 3.2.) (Peterson et al., 2012; Catchen et al., 2013).

3. Next-generation sequencing and genome reduction techniques

The replacement of traditional sequencing platforms by massive parallel sequencing has increased the robustness of molecular analysis and opened new possibilities in the study of biodiversity.

3.1. Overview of next-generation sequencing techniques

Sanger sequencing was a major discovery in the field of genetics and became the most popular method for obtaining genetic information from a wide range of species (Sanger et al., 1977). In combination with the PCR reaction for DNA amplification (Mullis and Faloona, 1987), it has been used to obtain large amounts of nucleotide sequences for the last several decades. More recently, a revolution of sequencing technologies occurred with the appearance of the sequencing by synthesis technology that allows sequencing in parallel, such as the one developed by 454 Life Sciences (Margulies et al., 2005). Indeed, Poinar et al. (2006) obtained 13 Mb of a 28,000 years old mammoth with a Roche 454 GS instrument and this advance was followed by the sequencing of ancient DNA from Neanderthals using the same approach (Green et al., 2006). The development of other platforms such as SOLiD (Applied Biosystems) and Genome Analyzer (Illumina) completed the transformation of genetics into genomics using next-generation sequencing (NGS) approaches (Schuster, 2008). The deployment of NGS together with the lowering of costs per base has led to the sequencing of a large number of genomes from non-model organisms (Michael and Jackson, 2013; Dunn and Ryan, 2015; David et al., 2019).

High throughput NGS platforms rely on parallel sequencing of spatially separated amplicons using different approaches (Pareek et al., 2011). The recent emergence of the so called third generation sequencing technologies (such as Pacbio or Nanopore), have overcome possible bias that can happen through PCR amplification, enabling single DNA molecule real-time sequencing (Liu et al., 2012; Goodwin et al., 2016).

3.2. Genome reduction techniques

The discovery of restriction site associated DNA sequencing (RADseq) has allowed the sequencing of a fraction in the genome with NGS technologies, having the advantage that

many samples can be sequenced simultaneously at a reduced cost. The method benefits from the high coverage per locus and no prior genomic information is needed. It has become a widely used genomic reduction approach for SNP discovery and genotyping (Andrews et al., 2016).

Genome reduction techniques can be divided in two main groups depending on the number of restriction enzymes cut sites used to sequence genomic fragments. The first approach started with the original RADseq and includes strategies using single restriction enzyme cut sites and reading adjacent fragments, such as 2b-RAD (Baird et al., 2008; Wang et al., 2012). The second strategy sequences fragments included in a region cut by two flanking restriction sites and rely on one or two enzymes with or without direct selection size. For instance, Genotyping by sequencing (GBS) is one of the classic methods using one enzyme and indirect size selection step with PCR preferentially amplifying short fragments (Elshire et al., 2011). Other methods that perform indirect size selection include two restriction enzymes, such as Complexity Reduction of Polymorphic Sequences (CRoPS) (van Orsouw et al., 2007). Finally, double-digest restriction site-associated DNA (ddRAD) uses two restriction enzymes with specific adaptors and performs a direct size selection, e.g. with a gel cut. Since the appearance of these techniques there have been plenty variants that include some modifications (Andrews et al., 2016).

Other genome-partitioning strategies alternative to RADseq approaches have been developed. That is the case of target capture, a pipeline that performs a parallel enrichment of previously selected genome regions. To design probes, a genome from the species of interest or a close one can be used (Jones and Good, 2016). A similar RAD capture method (Rapture) has been developed to combine RADseq protocols and produce enriched libraries with target loci of interest using oligonucleotide baits (Ali et al., 2016). Due to the capture step, these methods are useful for the sequencing of minimally invasive samples as only endogenous DNA can be retrieved and sequenced (Kidd et al., 2014). For instance, the use of fecal chimpanzees' samples in target capture approaches have produced novel analysis of genetic diversity, circumventing previous limitations (Perry et al., 2010).

As a modification of RADseq protocol, Peterson et al. (2012) developed the ddRAD protocol, which is one of the most used nowadays. First of all, two restriction enzymes (e.g. EcoRI and MspI, but could be others) break genomic DNA into pieces (Figure 5a). Once the DNA is cut, two adapters are attached to each of the ends of the genomic pieces (Figure

5b). Adapters joining the extreme cut by EcoRI are different for each individual (multiplexed with barcodes), whereas all adapters on the side of MspI are the same. The next step selects the fragments included in certain size range, so fragments for example between 200 and 400 base pairs are sliced from the gel (Figure 5c). Finally, a PCR amplification is done with primers that anneal over the adapters and can have different indexes for combining individuals with same barcodes (Figure 5d). Several PCRs can be performed and mixed to avoid biases in the number of reads between fragments. Then, sequences from different samples included in the same library are pooled together. This final library is then sequenced in an Illumina platform. The genomic information obtained contains approximately 0.1-0.5% of the total genome.

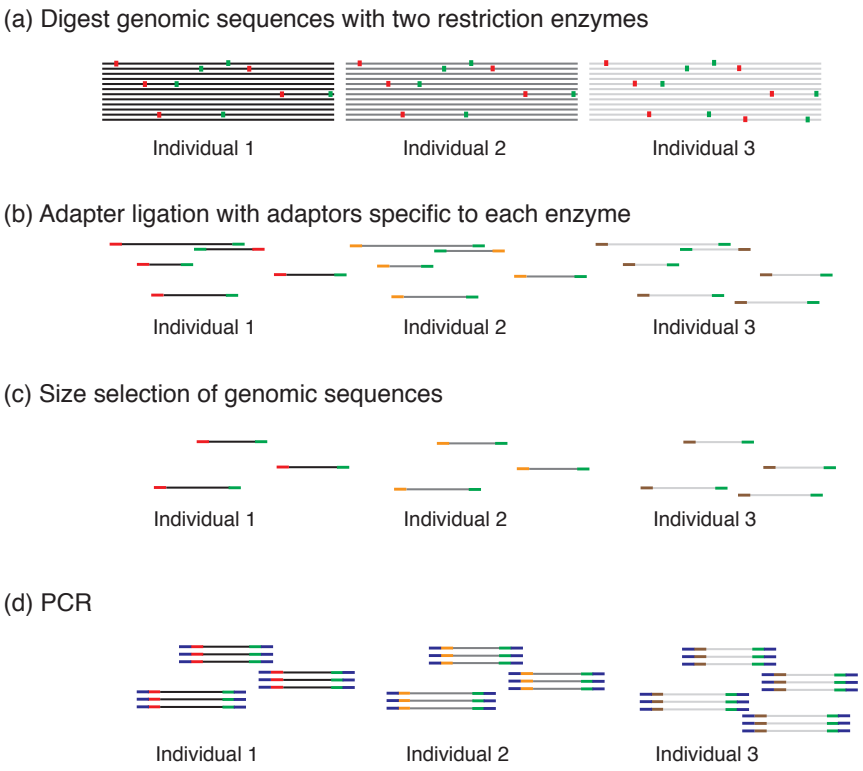

Figure 5. Protocol followed in a ddRAD library preparation. Genomic DNA is fragmented using two restriction enzymes a). Enzyme-specific adapter ligation is carried out to multiplex samples and provide with a common primer annealing region b). Size selection through gel extraction remove short and long reads c). PCR amplification of genomic fragments that fall into the size selected window d).

Bioinformatic analysis of ddRAD data includes de-multiplexing, trimming barcodes and quality sequence filtering (Catchen et al., 2013). After that, reads can be aligned to a

reference genome or assembled *de novo* using available programs, which assume that variation of similar sequence reads is attributed to sequencing errors or the presence of different alleles (Andrews et al., 2016). Finally, one last filter is recommended in order to remove individuals or loci with high amounts of missing data (Andrews et al., 2016). Simulations of digestion reads using available genomes, varying the rate and type of mutations, have shown good performance of programs specifically designed to cope with RAD sequences in SNP discovery (LaCava et al., 2020).

4. Data analysis of multilocus and NGS data

Phylogenetic and population genetic analyses can be used for a broad range of applications: estimate the topology of the tree, the divergence times of the splits and the mutation rate of sequences; infer the population sizes of the different lineages and even detect gene flow events between populations.

4.1. Phylogenetic analysis

Phylogenetic analysis allows the comparison of homologous sequences of different species or populations and the reconstruction of phylogenetic trees in which the sequences are represented by the tips, the ancestral sequences by the internal nodes, and the genetic distances between sequences by the branches, thus providing a visual description of the relationships between the sequences.

There are two main groups of phylogenetic methods depending on the type of data they use: distance and character state methods (Huelsenbeck and Hillis, 1993). The most commonly used methods today fall within the character methods and are Maximum-likelihood and Bayesian.

Maximum-likelihood methods are used to reconstruct the evolutionary tree that fits the data with the highest likelihood. This method relies on the assumption that point mutations are random events and considers the true genetic distance among sequences (Felsenstein, 1981). Several software packages such as RAxML and PHYML have been developed to optimize computations (Guindon and Gascuel, 2003; Stamatakis, 2006). Studies using maximum-likelihood phylogenetic programs for big dataset reconstruction have provided robust and reliable insights on mammal biodiversity and evolution (Meredith et al., 2011; Figueiró et al., 2017).

On the other hand, Bayesian inference methods use Markov chain Monte Carlo (MCMC) sampling to explore the parameter space of trees and create a posterior distribution based on priors given to the model (Drummond et al., 2006). Every time a new state is explored, the likelihood is estimated and accepted or rejected depending on how high it is relative to the previous step (Metropolis et al., 1953; Hastings, 1970). A percentage of samples conditioned by the prior distribution is removed (burn-in step) and the posterior distribution

is monitored to ensure reliable estimates (Nascimento et al., 2017). The programs MrBayes (Huelsenbeck and Ronquist, 2001), BEAST (Drummond and Rambaut, 2007) and BEAST2 (Bouckaert et al., 2014) reconstruct phylogenies and calibrated rooted trees using Bayesian inference.

In order to estimate the genetic distance between the sequences and to assess the likelihood, phylogenetic methods require a statistical model of nucleotide substitution (Bos and Posada, 2005). The infinite sites model proposed by Kimura (1969), considers that every new mutation occurs in different sites. However, mutations in same sites occur in divergent sequences, so that other equations to estimate the real number of substitutions are required (Strimmer and Haeseler, 2009). Jukes and Cantor formula tries to model the substitution process giving to all changes between the four nucleotides the same probability to occur (Jukes and Cantor, 1969) while more sophisticated models consider different frequencies for the four nucleotides and include a ratio of transitions and transversions such as HKY (Hasegawa et al., 1985) or GTR (Tavaré, 1986), in which all nucleotide change rates have their own value.

These models assume homogeneity in substitution rates between sites, but it is well known that some positions vary more than others, and this fact stimulated the development of new models considering rate heterogeneity (Yang, 1996). Different rates among sites can be modelled with a Gamma distribution, which can be categorized using discrete categories (Yang, 1994). Another possibility to model rate heterogeneity among sites is determining a certain proportion of invariant positions (Lockhart et al., 1996).

4.2. Population structure

Genetic properties in a population are influenced by different factors such as population size, mating system, fertility and viability, migration, recombination and mutation rate (Templeton, 2006). In an ideal population (i.e. a large random mating population where the effects of migration, mutation and selection are negligible) the frequency of each genotype can be estimated from the allele frequencies, and the population is expected to be in Hardy-Weinberg equilibrium (HWE) (Freeland et al., 2011). *F-statistics* are a group of measures that rely on HWE to estimate genetic differentiation between and within populations, comparing expected and observed patterns of heterozygosity (Shane, 2005). For instance,

the most popular index F_{st} approximates levels of population differentiation ranging from 0 (no differentiation) to 1 (complete differentiation).

Model-based clustering methods to estimate population structure in multilocus analysis (e.g. STRUCTURE) are also available (Pritchard et al., 2000). This software, which can be applied to DNA sequence data and SNPs, is not only able to estimate population differentiation, but also to assess population admixture between groups and assign individuals to populations.

4.3. Species delimitation

In the first steps of population differentiation there is no genetic divergence between populations but, if isolation continues through time, divergence appears and the need to delimit species becomes evident (Knowles, 2004; Omland et al., 2006; Richards and Knowles, 2007; Peters et al., 2016). Consequently, there is a blurred line between populations and species taxonomic status (population species continuum) and it is not always easy to determine when two populations become different species. To address this issue, multispecies coalescent models using Bayesian analysis of DNA sequences have been developed. For example, the BPP program is able to calculate posterior probabilities for different species models apart from estimating population parameters (Rannala and Yang, 2003; Yang and Rannala, 2010; Yang, 2015). This method does not take migration into account, and has received some critics related to the accuracy of delimiting species status using simulations (Jackson et al., 2017; Sukumaran and Knowles, 2017). However, different authors have shown that, when correct species simulation models are applied, BPP remains a reliable method to perform species delimitation, even considering high migration rates (Fujita et al., 2012; Leaché et al., 2019). Furthermore, BPP was recently extended to incorporate a model with introgression (Flouri et al., 2020). Other programs such as SNAPP allow species delimitation using SNP markers in a full coalescent analysis (Bryant et al., 2012; Leaché et al., 2014).

4.4. Estimation of divergence times

The theory of the molecular clock was a major contribution to understand the causes of genetic variation between and within organisms (Zuckerkandl and Pauling, 1965). Later, phylogenetic methods considering the molecular clock were refined and sophisticated to perform accurate divergence times estimates. However, it is necessary to count with fossils or biogeographic events to convert genetic distances into time.

The fossil record is commonly used to reconstruct the past of species and date the origin of new lineages (Benton et al., 2009). The presence of fossils in different sedimentary layers with known antiquity allows researchers to associate them with specific geologic times, although sometimes it is difficult to assign strict calibrations to the phylogeny (Benton et al., 2009). Fossils consist on rests of taxa that contains a common derived character of the crown group, which is constituted by the species from a monophyletic group including their common ancestor. They postdate the actual divergence of a clade and are used to estimate its divergence (Benton et al., 2009). In addition, biogeographic events can help to calibrate trees of species living on islands or at both sides of oceans formed during recent geological history (Marko, 2002). However, the fossil record is incomplete and biogeographic events are difficult to delimit, and therefore it might be difficult to date recent split times between related groups of taxa. Hence the importance of methods that manage paleontological and molecular data at the same time.

Bayesian methods can incorporate strict or relaxed clocks depending on the divergence of sequences. The appearance of relaxed phylogenetics moderated the assumptions of substitution rate homogeneity among lineages in the strict clock (Drummond et al., 2006). The relaxed clock is considered a biologically realistic model that can be applied to reconstruct phylogenies and divergence times of distant species (Drummond et al., 2006). For instance, the uncorrelated relaxed molecular clock model includes rate heterogeneity and independency among branches, which is convenient for alignments that are not clock-like.

To calibrate the trees, the use of age span is more recommended than the use of hard constraints in order to reflect the error related with the paleontological estimates (Benton et al., 2009). For instance, the use of parametric distributions including hard minimum constraints and soft maximum splitting times of the node of fossils, is a common practice.

4.5. Estimation of mutations rates

Relaxed and strict clock models with proper calibrations are able to estimate mutation rates that can vary across the tree (Drummond et al., 2006). The precise estimation of molecular rates is important as they have an impact on branch lengths and the topology of the tree.

Under the neutral theory of molecular evolution the mutation rate of sequences is the product of the total mutation rate of the sequence and the fraction of sites that are relatively neutral (Kimura, 1977), so it will be expected that mutations accumulate faster in non-coding regions (e.g. introns) than in coding regions (exons). It is also well known that there are differences in mutation rates between synonymous and non-synonymous substitution in coding genes (Li et al., 1987). Specifically, synonymous changes have higher mutation rates than non-synonymous substitution as amino acid changes may be subject to selection (Li et al., 1987). Moreover, it appears that non-coding regions (introns, intergenic regions, etc.) will typically evolve slower than synonymous sites (Andolfatto, 2005; Nikolaev et al., 2007). In addition, both synonymous and non-synonymous substitution rates have also been shown to be variable among genes (Wolfe and Sharp, 1993) and evidence has been found to suggest that large genome regions evolve at different rates (Koop, 1995). Estimation of genetic distances between humans and rodents confirmed these hypotheses, finding rapidly evolving exons together with rapidly evolving introns and slowly evolving exons with slowly evolving introns (Castresana, 2002). The idea that a mutational rate can substantially vary along the genome suggests that it is necessary to estimate specific substitution rates for the markers under study in order to obtain reliable estimates of divergence times.

4.6. Coalescent analysis and time estimation with isolation-with-migration analysis and other methods

The emergence of the coalescent theory allowed the estimation of split times between populations (Arbogast et al., 2002). The same methodologies can also be used to estimate divergence times for closely related species (Sánchez-Gracia and Castresana, 2012). Different coalescent methods to estimate divergence times using global or specific mutation rates and considering migration have been developed.

Models of population subdivision have made assumptions considering that populations diverged from an ancestral population evolving since then without gene flow (Nielsen and Wakeley, 2001). Other models infer gene flow values using measures to quantify population subdivision assuming equilibrium migration (Nielsen and Wakeley, 2001). However, it is necessary to truly distinguish between isolation and directional migration and frameworks to estimate both of them from DNA sequences. Isolation-with-migration (IM) methods accomplished that, using a complex set of analyses including both likelihood and Bayesian inference that take advantage of the MCMC approach to estimate the likelihood function and posterior distribution of the parameters (Nielsen and Wakeley, 2001; Hey and Nielsen, 2004). IM methods are multispecies coalescent models that include migration. The genealogy (gene tree) of the data is a nuisance parameter that includes information about branch length and the migration events of the sequences (Nielsen and Wakeley, 2001; Hey and Nielsen, 2004). Metropolis-Hasting criterion is then used to integrate over genealogies and approximate the posterior distribution of the parameters (Nielsen and Wakeley, 2001; Hey and Nielsen, 2004).

IM and IMa software were able to perform population parameter estimations (divergence times, migration rates and population sizes) for several loci and two populations (Hey and Nielsen, 2004, 2007). The subsequent version, IMa2, considered multiple populations and up to hundreds of loci (Figure 6) (Hey, 2010a). The most recent model, IMa3, implements a posterior probability estimation of the phylogenetic topology using a “hidden genealogy” approach that allows to have efficient updating (Hey et al., 2018). It also allows the introduction of a unsampled “ghost population” to the model that might have affected the data by, for example, experimenting gene flow with the sampled or ancestral populations (Beerli, 2004; Pinho and Hey, 2010).

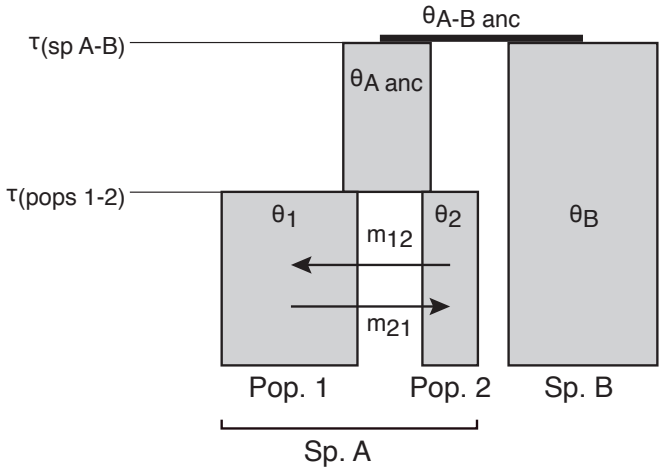

Figure 6. Isolation-with-migration model for two species and a total of three hypothetical populations. Scaled population sizes (θ), migration rates (m) and divergence times (τ) are estimated under the tree proposed. Ancestral population (anc) sizes are also displayed. In this figure, only significant migrations between the closely related populations of the present time are represented. Note that migration events are understood backwards in time, with arrows reflecting forward movement of alleles.

Approximate Bayesian Computation (ABC) is another widespread method to estimate demographic parameters (Beaumont, 2010; Csilléry et al., 2010). ABC relies on the approximation of the posterior distribution of the parameters found in demographic models via simulation, so they are considered to be a combination of simulation and data analysis studies (Bertorelle et al., 2010). ABC approaches comprise several steps: The first step is the most computationally challenging as simulations are performed, which includes obtaining parameter values from prior distribution in order to simulate the genetic data and compute the population summary statistics. A variety of software for performing backwards coalescent simulations and different models of population evolution are available for DNA sequences and SNPs (Bertorelle et al., 2010; Lopes and Boessenkool, 2010; Li and Jakobsson, 2012). The next step extracts summary statistics from the observed data and retains only those simulations with closer estimates to the observed data. The final step involves the estimation of real parameters fitting a linear regression over the retained simulations (Beaumont et al., 2002; Excoffier et al., 2005).

ABC approaches can work with genomic data although simulations of large datasets may be time-consuming (Excoffier et al., 2013). For this reason, the SFS framework was developed. SFS allows the inference of parameters such as divergence times, population bottlenecks and migration in complex models although the use of SNPs only allows to obtain relative dates due to the absence of a clear molecular clock in them (Excoffier et al., 2013). Otherwise, SFS and ABC approaches are very useful for unveiling genetic processes assessing the demography and diversity of different populations using genomic data (Li and Jakobsson, 2012; Lozier, 2014; Shafer et al., 2015; Strugnell et al., 2018).

5. Biogeographic and evolutionary framework of the studied species

The Pleistocene (~2.5 million years to ~10,000 years ago) had a strong effect on the biogeography of vertebrate species. Phylogeographic studies revealed that many extant populations and species of mammals originated during this period (Avise et al., 1998; Hewitt, 1999). Glacial periods relegated temperate adapted taxa to thermal refugia whereas interglacial periods confined cold adapted taxa to the coldest areas (Stewart et al., 2010). The use of genetic tools has allowed to reveal the impact of Pleistocene climatic cycles on the distribution and evolution of biodiversity through the biogeographic regions, and to discover different refugia that existed during these periods (Schmitt, 2007; Stewart et al., 2010). Different broad paradigms of northward expansion of lineages emerging from the Mediterranean refugia such as the Iberian Peninsula, Italy and the Balkans, have been described using model species (i.e. hedgehog, bear, butterfly and grasshopper) (Hewitt, 2000; Schmitt, 2007).

Of the several glacial and interglacial periods occurred during the Pleistocene, not all of them had the same influence on species distribution and phylogeographic patterns. Which of these periods was most relevant for the genetic differentiation of species has been a difficult question to answer in most cases. The Last Glacial Maximum (LGM) is the most recent time during which the ice sheet reached its greatest extent, starting ~33,000 years ago and arriving to its maximum coverage ~20,000 years ago (Clark et al., 2009). The LGM had a great impact on species distribution and community composition (Stewart and Lister, 2001; Sommer and Nadachowski, 2006). Previous glacial periods also affected species but determining which one affected specific biogeographic events has been difficult to achieve so far in most phylogeographic studies.

5.1. Comparative phylogeography in the Iberian Peninsula and genomic data available

The Iberian Peninsula has played a major role in shaping the distribution of present biodiversity as it has a large number of endemic species (Bilton et al., 1998). It also contains populations of species found at the edge of their European distribution, either as a consequence of recent colonization or as a source of recolonization of other European areas from Iberian refugia (Hewitt, 1999; Schmitt and Varga, 2012). Furthermore, the existence of many species with high levels of genetic differentiation between populations within the

Iberian Peninsula supports the "refugia within refugia" hypothesis (Gómez and Lunt, 2007). Understanding the impact of the Pleistocene glaciations on the genetic diversity and phylogeographic subdivision of species may be essential to detect evolutionary units and perform the best genetic management of populations and species (Schmitt, 2007).

Small mammals (insectivores and rodents) present in the Iberian Peninsula are classified as Eurosiberian or Mediterranean depending on their specific distribution (Sans-Fuentes and Ventura, 2000). Eurosiberian species are those present in the northern fringe of the Iberian Peninsula and other European areas. They include species such as *Neomys fodiens*, *Arvicola scherman*, *Sorex coronatus*, *Microtus arvalis*, *M. agrestis*, *Glis glis* and *Talpa europaea*. (Sans-Fuentes and Ventura, 2000). Whether these species have recently colonized the north of the Iberian Peninsula or they were in this area during the late glaciations is an interesting biogeographical question. Theoretical predictions have unveiled important patterns associated with range expansion processes, such as genetic diversity loss in newly colonized areas (Ibrahim et al., 1996), which allows testing this hypothesis. The Iberian populations of Eurosiberian species have generally received little attention despite their biogeographical interest. *Neomys fodiens* (order Eulipotyphla) and *Arvicola scherman* (order Rodentia) are two of these species and are the focus of this work.

The difference in available genomic data in public databases for the two groups containing these species of study is remarkable. There are no available genomes of the genus *Neomys* and genomic information have been obtained from only four species of Eulipotyphla: *Condylura cristata*, *Sorex araneus*, *Erinaceus europaeus*, and *Solenodon paradoxus*. On the contrary, there are genomic data for a minimum of 13 species of Rodentia (Liu et al., 2017). Several of them have been introduced in orthology databases (Yates et al., 2020), which allows performing thorough comparative genomic studies in this group.

5.2. *Neomys fodiens*

The Eurasian water shrew *N. fodiens* (Pennant 1771) is a small semiaquatic mammal with relatively large size compared to other species of shrews and specific adaptations to semi-aquatic life. The side of the tail has stiff hairs and posterior legs are large to facilitate swimming and diving (Hutterer, 1985; Churchfield, 1998). It generally has a grey darkish color at the dorsal view and a white ventral surface (Figure 7) (Ventura, 2007a). It is active

during day and night, feeding mainly on terrestrial and aquatic invertebrates along the shore or the bottom of rivers (Rychlik, 1997; Castién and Gosálbez, 1999; Biffi et al., 2017b). *N. fodiens* uses venomous saliva to immobilize prey and has a characterized reddish color on the tip of the teeth, shared with other species of shrews (Kowalski et al., 2017; Kowalski and Rychlik, 2018).

Figure 7. Greyscale drawing of *N. fodiens* with the typical color pattern of the species. Image source: (Ventura 2007a).

5.2.1. Distribution and subspecies

N. fodiens has a Eurasian distribution covering a wide range of northern countries from the north of the Iberian Peninsula to eastern Asia (Hutterer et al., 2016; Burgin et al., 2018). Although different subspecies have been proposed, none of them has been well studied, with the exception of the nominal subspecies (*N. f. fodiens*, Pennant 1771) present in most of its distribution, and N. *f. niethammeri* Bühler, 1963, restricted to a small population from the Iberian Peninsula (Figure 8) (Wilson and Reeder, 2005).

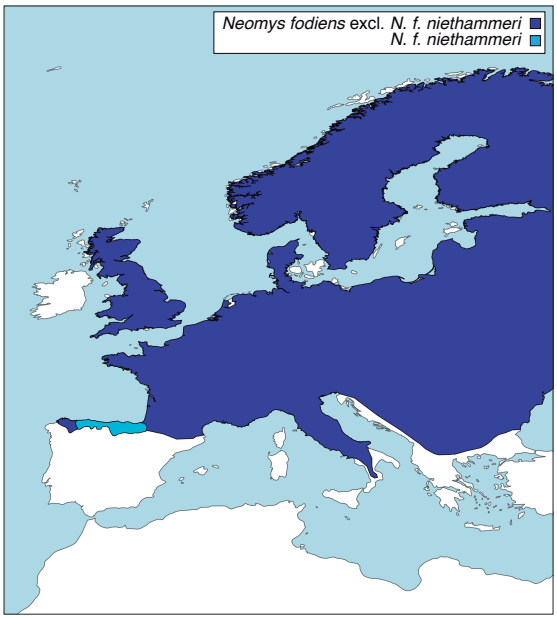

Figure 8. Map showing the range of *Neomys fodiens niethammeri* (light blue) within part of the range of *N. fodiens*. Figure source: Scientific Reports.

N. f. niethammeri is present in the north-central area of the Iberian Peninsula, from the Cantabrian mountains to the western part of the Pyrenees (Bühler, 1963, 1996; Nores et al., 1982; López-Fuster et al., 1990). It is a singular population as specimens belonging to it have the largest skull size observed throughout the whole distribution of *N. fodiens* (Bühler, 1996). This is a striking feature, considering the stable morphology that characterizes the species across other areas (Kryštufek and Quadracci, 2008). In addition, this population is flanked by populations from the nominal subspecies and live in sympatry with *N. anomalus*, another species of the genus with smaller size. That is why size has been commonly applied to differentiate *N. fodiens* in studies of past and present biodiversity (Nores et al., 1982; Blanco, 1998; Cuenca-Bescós et al., 2008; Sesé, 2017). Specifically, a length of the coronoid height (CH) higher than 5.35 mm is used to assign individuals to *N. f. niethammeri* (Figure 9) (Bühler, 1996; Blanco, 1998).

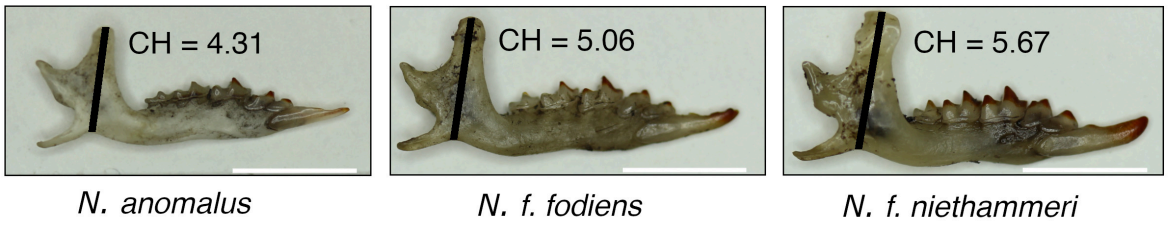

Figure 9. Mandible from the largest population of *N. fodiens*, that is *N. f. niethammeri*, marking the height of the coronoid process in mm (CH). Smaller mandibles from the nominal subspecies *N. f. fodiens* and the sister species *N. anomalus* are also shown for comparison. White scale bar: 5 mm (equal scale size for the three mandibles).

5.2.2. Habitat and ecological preferences: Interactions with other species

N. fodiens is usually associated with small water courses and ponds, although it is also able to colonize terrestrial habitats such as wet forests, grasslands and farmlands (Rychlik, 2000; Ventura, 2007a). Along its European distribution, *N. fodiens* lives in sympatry and compete with the European water shrew *N. milleri*, whereas in the Iberian Peninsula, it shares most of its distribution areas with the Cabrera water shrew *N. anomalus* (Ventura, 2007b), a species recently separated from *N. milleri* (Igea et al., 2015; Querejeta and Castresana, 2018).

Since *N. milleri* and *N. anomalus* were recently split into two species (Igea et al., 2015), the interactions of *N. fodiens* and *N. anomalus* in their European distribution have actually been studied between *N. milleri* and *N. fodiens*. In ecological studies, *N. fodiens* dominates over *N. milleri* due to its bigger body size and stronger semiaquatic adaptations, showing more aggressive behavior and even displacing *N. milleri* from aquatic habitats (Rychlik, 1997; Rychlik and Zwolak, 2006; Keckel et al., 2014). In fact, *N. fodiens* has greater preference over aquatic prey and better diving ability than *N. milleri*, which prefers wading, is present at some distance from the water and includes a larger number of terrestrial taxa into its diet (Churchfield and Rychlik, 2006; Mendes-Soares and Rychlik, 2009; Keckel et al., 2014). On the other hand, studies on allopatric populations of *N. milleri* have shown ecological displacement towards bigger size, suggesting better ability to exploit aquatic habitats in the absence of *N. fodiens* (Kryštufek and Quadracci, 2008). In the case of *N. anomalus* populations of the Iberian Peninsula, no interaction studies with *N. fodiens* exist, but it has been shown that the former can extend its ecological niche into deeper water when the latter is absent (Tapisso et al., 2013).

5.2.3. Phylogeography of *N. fodiens*

Mitochondrial DNA studies showed low divergence between haplotypes along the European distribution of *N. fodiens*, revealing a southern clade that included only two samples from Italy and the Pyrenees (Castiglia et al., 2007), but there are not any multilocus analysis developed for this species.

In addition, a correct assessment of the *N. f. niethammeri* population has never been performed using genetic data. The species category has even been proposed for this population due to its morphological distinctness (López-Fuster et al., 1990; Bühler, 1996; Wilson and Reeder, 2005; Burgin et al., 2018). It is therefore important to carry out genetic studies using samples from the Iberian Peninsula and other areas of its Palearctic distribution in order to determine its true taxonomic status.

5.3. *Arvicola scherman*

The Montane water vole *A. scherman* (Shaw, 1801) is a rodent with smaller size compared to related species of the same genus, dark brown body and grey belly (Figure 10) (Ventura, 2007c; Amori et al., 2008). It has upper incisors projected forwards (proodont) and strong bite force as an adaptation to excavation and fossorial activity (Wilson and Reeder, 2005; Amori et al., 2008; Kryštufek et al., 2015; Durão et al., 2019). It feeds on vegetation, specially roots and bulbs (Amori et al., 2008). Its sister species, the European water vole (*A. amphibius*), has larger size, orthodont incisors and lives in aquatic environments (Wilson and Reeder, 2005; Amori et al., 2008; Kryštufek et al., 2015).

Figure 10. Greyscale drawing of *A. scherman* with the typical color pattern of the species. Image source: (Ventura 2007c).

A. scherman inhabits lowlands and uplands in the north of Iberia and central Europe (reaching Poland, Ukraine and Romania in the east) isolated in certain mountain ranges such as Cantabrian Mountains, Pyrenees, Alps, Massif Central and Carpathians (Wilson and Reeder, 2005; Amori et al., 2008). In comparison, *A. amphibius* has a wider distribution extending from France and UK in the east as far as Russia in the west through much of continental Europe (Batsaikhan et al., 2016).

A. scherman uses its teeth to construct underground borrows and molehills, creating subterranean colonies (Miñarro, 2019). Due to its subterranean activity and population cycles, it can invade and damage crops and apple orchards, and for this reason it is considered a pest in some areas (Figure 11) (Amori et al., 2008; Miñarro et al., 2012; Somoano et al., 2016).

Figure 11. Picture of a damaged crop with molehills due to the subterranean activity of *Arvicola scherman*.

5.3.1. Taxonomy, phylogeography and ecological plasticity of *Arvicola*

The genus *Arvicola* has traditionally included two main lineages of water voles: The Southern water vole *A. sapidus* and the Northern water vole *A. terrestris* (Cubo et al., 2006; Ventura, 2007c, 2007d; Centeno-Cuadros et al., 2009). Whereas *A. sapidus* is restricted to freshwater habitats in the Iberian Peninsula and France, *A. terrestris* shows two ecological forms with a Paleartic distribution (Amori et al., 2008; Rigaux et al., 2008; Batsaikhan et al., 2016). Taxonomic uncertainties have accompanied *A. terrestris* since its first classification by Linnaeus, who proposed the different names *A. terrestris* and *A. amphibius*, which later were considered to be part of the same species (Amori et al., 2008; Batsaikhan et al., 2016). Nowadays, interspecific variability in mitochondrial DNA within the *A. terrestris* lineage and other morphological, ecological and biogeographic data revealed three different taxonomic entities: The European clade with fossorial and semiaquatic individuals *A. amphibius*, the Italian lineage also with the two ecotypes *A. italicus,* and the strictly fossorial morphotype *A. terrestris*, currently renamed as *A. scherman,* present mostly in the north of Iberia and central Europe (Taberlet et al., 1998; Kryštufek et al., 2015; Castiglia et al., 2016).

Phylogeographic studies of certain populations of water voles have revealed interesting events, such as two colonizations of the British Isles coming from Europe (Piertney et al., 2005; Brace et al., 2016), the high genetic differentiation between Norwegian populations assessed with multilocus analysis (Melis et al., 2013), or an inconsistent level of genetic diversity between populations, reflecting distinct reproductive and migration strategies (Aars et al., 2006; Somoano, 2017).

The fossorial form *A. scherman* is supposed to have evolved from individuals with semiaquatic requirements. In fact, the reconstruction of the ancestral size of the genus has confirmed this hypothesis, supporting genetic changes directed to an apomorphic reduction of body size and overdelopment of skull characters and long bones linked to the hypogeal activity (Cubo et al., 2006). However, the presence of both morphotypes in mitochondrial lineages in some areas hint the possibility of morphotype reversions, high plasticity of the species or possible introgression events that require further investigations (Kryštufek et al., 2015; Castiglia et al., 2016).

5.3.2. Distribution and subspecies of *A. scherman* in the Iberian Peninsula

Although there is certain confusion between the distribution of *A. scherman* and *A. amphibius* in northern areas of its distribution, in the Iberian Peninsula only the former is present (Ventura, 2007c; Amori et al., 2008).

In the Iberian Peninsula there are two subspecies of *A. scherman* that are separated geographically and can be distinguished morphologically: *A. s. monticola*, which is present along the Pyrenees and is characterized by its bigger size, and *A. s. cantabriae*, which is distributed across the Cantabrian Mountains and possess smaller size and certain differences associated with the digging activity in teeth (Ventura, 2007c; Marcolini et al., 2011). The presence of these two differentiated populations in the Iberian Peninsula suggests the existence of separated Pleistocene refugia within this relatively small area, making this species an interesting model to date the split between the Cantabrian and Pyrenean populations and to study the effects of recent glaciations in generating genetic structure.

III. OBJECTIVES

Recent theoretical advances in phylogeographic, phylogenetic and population genetics analyses have opened new possibilities in the study of the origin and evolution of populations. This fact, together with the emergence of next-generation sequencing (NGS), which allows producing thousands of sequences cost-effectively, has greatly facilitated answering questions about the evolution of biodiversity. The main objective of this thesis is the optimization of genetic and bioinformatic techniques to get information from minimally invasive samples and perform multilocus and NGS analyses to resolve questions related to the origin and evolution of different populations of small mammals from the Iberian Peninsula. To achieve this goal, two different taxa that have generally received little attention despite their biological interest will be studied, with the possibility of exporting the new laboratory and bioinformatic procedures to questions related to other species.

More specifically, the objectives of this thesis are:

1. Get the full potential of skull bones extracted from barn owl pellets in order to perform simultaneous genetic and morphometric analyses.

2. Design new variable sequence markers that allow reducing the size of the PCR product and facilitate the process of amplification of degraded samples.

3. Assess the contentious taxonomic status of the Iberian population of the Eurasian water shrew with bigger skull size (currently *Neomys fodiens niethammeri*), which is flanked by populations of the nominal subspecies (*N. f. fodiens*), using genetic and morphological information from skull bones obtained from barn owl pellets.

4. Perform multilocus genetic analyses of divergence and differentiation between the two Iberian populations of the Eurasian water shrew.

5. Understand the possible ecological consequences of a phenotypic novelty such as the large size in this Iberian population of the Eurasian water shrew.

6. Estimate the divergence between the Cantabrian and Pyrenean populations of the Montane water vole (*Arvicola scherman*) through double-digest restriction site-associated

DNA (ddRAD) data obtained by NGS in a coalescent framework, using different types of samples that include skull bones obtained from barn owl pellets.

7. Study the genomic structure of these Iberian populations using thousands of SNPs obtained from ddRAD.

8. Develop a bioinformatic pipeline to identify ddRAD orthologous loci in other rodents and estimate mutation rates of ddRAD loci in a calibrated phylogenetic tree.

9. Devise the best method to use ddRAD loci in order to estimate demographic parameters, particularly split time, in an isolation-with-migration (IM) model.

10. Put the split time obtained in the context of the Pleistocene glaciations to better understand their effects in generating genetic structure and diversity in the Iberian Peninsula.

IV. METHODS

1. Size increase without genetic divergence in the Eurasian water shrew *Neomys fodiens*

1.1. Sample collection

A total of 79 samples from the Palearctic range of the genus *Neomys*, with special emphasis on *N. f. niethammeri* and *N. f. fodiens* from the Iberian Peninsula, were analyzed (Figure 12 and Supplementary Table S1). These included 68 skull samples from barn owl pellets collected in the field, of which 65 could be used for genetics and morphometry, and 3 could only be used for genetic analysis. Some of these samples had been analyzed in a previous morphological study of *N. f. niethammeri* (Nores et al., 1982). In addition, 9 tissue samples were loaned from museums and colleagues, and 2 tissue samples were taken from our own collection.

To complete the phylogenetic analysis, cytochrome *b* and nuclear sequences of 18 *Neomys* samples were taken from Igea et al. (2015) and 39 cytochrome *b* sequences were downloaded from GenBank (Clark et al., 2016). Two of the *N. fodiens* skull samples available from Igea et al. (2015) were used for morphometry.

1.2. Measurements and geometric morphometric analysis

After cleaning the skulls extracted from the owl pellets, we used only one lower mandible per skull and the rest was stored. Images of the 67 mandibles, together with a scale, were taken with a Canon 100D camera and a Canon EF-S 60 mm f/2.8 macro objective. The ImageJ 1.50i (Schneider et al., 2012) program was then utilized to take 16 landmarks from each sample (Supplementary Figure S1 and Supplementary Table S2). Many of the mandibles were partially broken or without teeth due to the digestion process so that no landmarks were taken in teeth. Landmarks 1 and 7 were used to calculate the coronoid height (for six partial mandibles, only these two landmarks could be obtained). According to previous works, the coronoid height ranges considered to discriminate the different taxa were: ≤4.70 mm for *N. anomalus*; 4.80-5.35 mm for *N. f. fodiens*; and >5.35 mm for *N. f. niethammeri* (Bühler, 1996; Blanco, 1998). With the coordinates of the 16 landmarks, and

using MorphoJ version 1.06d (Klingenberg, 2011), we made a Procrustes fit, calculated the centroid size, and performed a principal components analysis from the covariance matrix.

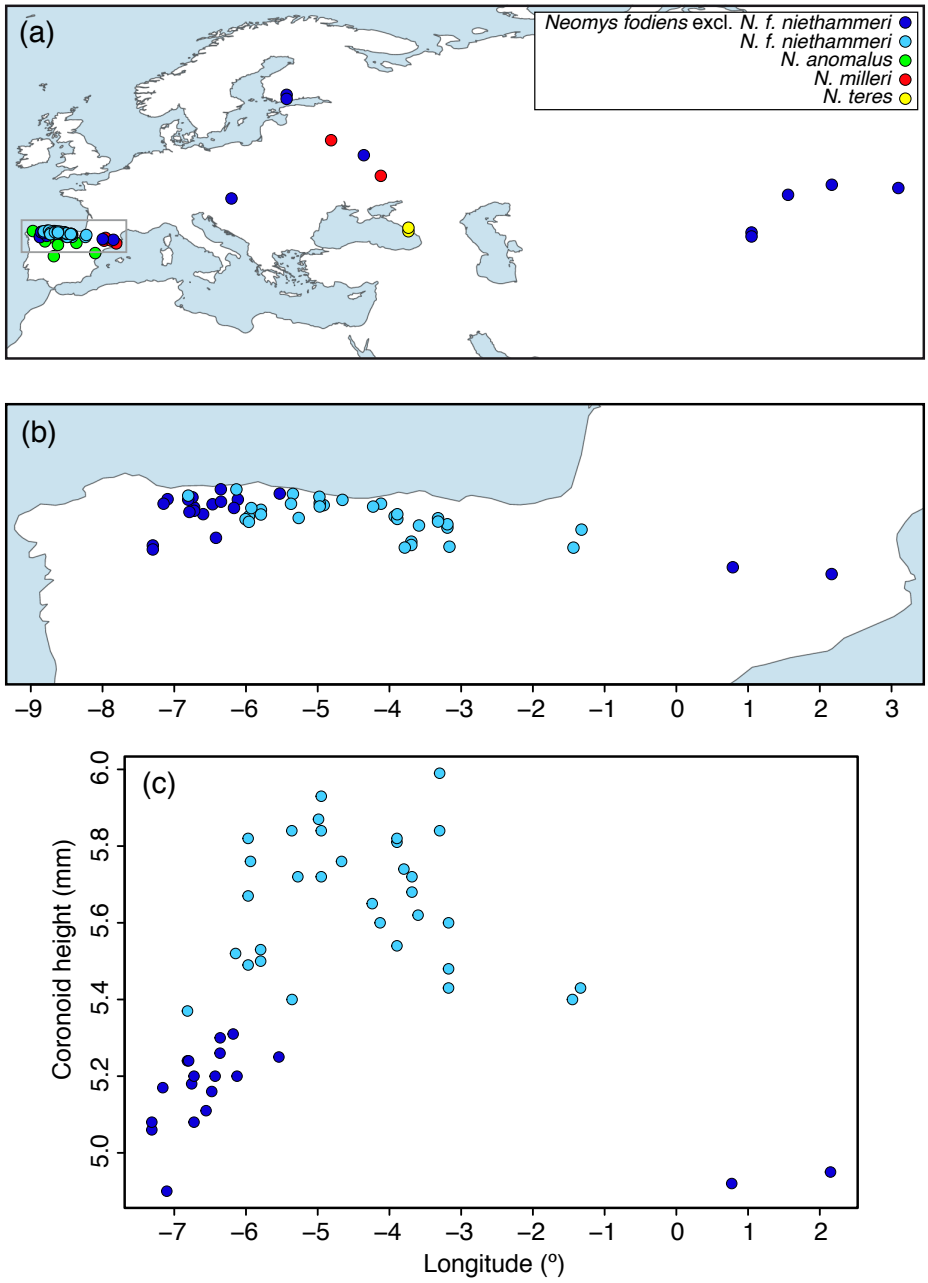

Figure 12. Distribution of the samples used in this study. (a) Map of all *Neomys* samples with the main study area highlighted, (b) enlargement of the northern Iberian Peninsula showing only *N. fodiens* specimens, and (c) plot across longitude in the Iberian Peninsula showing differences in skull size as measured using the coronoid height for *N. fodiens*. Samples from Igea et al. (2015) are included but sequences from databases are not. Note that the samples of *N. fodiens* not corresponding to *N. f. niethammeri* may include several subspecies: the European specimens most likely correspond to *N. f. fodiens* but those from Central Asia may belong to other subspecies whose ranges are not clearly delimited.

1.3. DNA extraction, PCR amplification and sequencing

The photographed mandibles were then used for DNA extraction. They were first powdered using liquid nitrogen and a mortar after which genomic DNA was extracted with a QIAamp DNA Micro kit. In the case of tissues, DNA was extracted with a DNeasy Blood & Tissue Kit (QIAGEN) following the recommended protocol. Extractions of all degraded samples were performed in a separate room with UV irradiation to avoid contamination. Extraction blanks were always present in order to detect any possible contamination at each step. Additionally, pre-PCR procedures were developed in a dedicated UV-hood, in a controlled, sterile room.

Complete cytochrome *b* sequences (1140 bp) from *N. fodiens* samples were amplified in three fragments using already published primers (Igea et al., 2015) with slight modifications to improve amplification (Supplementary Table S3). In addition, primers for a smaller fragment of 226 bp were developed with the purpose of amplifying DNA from the most degraded samples (Supplementary Table S3). The length amplified in each sample is shown in Supplementary Table S1.

For the nuclear markers, a set of six new primer pairs were designed starting from intron markers previously developed for *Neomys* (Igea et al., 2015). The primers were placed in conserved intronic regions or exons that spanned small fragments (between 153 and 229 bp) and flanked the highest possible number of polymorphic sites. Some markers were amplified with more than one primer pair in various samples, as we reduced the amplified intron length during the work to enable the amplification of degraded samples that failed with the initial primers (Supplementary Table S4). PCR reactions were performed in a final volume of 25 µl with 2-6 µl genomic DNA, 0.15 µl of Promega GoTaq DNA polymerase, and 1µM of each primer. The cycling conditions included an initial denaturation step of 30 s at 95ºC, followed by 40 cycles of denaturation (30 s at 95ºC), annealing (60 s at 54ºC for cytochrome *b* and 65ºC for introns), and extension (60 s at 72ºC), as well as a final extension of 5 min at 72ºC. For the most degraded skull samples, an alternative protocol using the QIAGEN Multiplex PCR was performed in a final volume of 50 µl with 4 µl of genomic DNA, 0.3 µM of each primer, and 25 µl of PCR Master Mix. In this case, there was an initial heat activation step of 15 min at 95ºC, the denaturation step was at 94ºC, the annealing temperature was lowered to 63ºC for the introns, and the annealing time was extended to 90 s. PCR products were purified using ExoSAP-It (Affymetrix) and sequenced

at Macrogen Inc. Sequences were assembled using Geneious Pro 5.1.7 (https://www.geneious.com).

In introns where two or more variable sites were present in a sample, PHASE version 2.1.1 (Stephens et al., 2001) with a threshold of 0.9 was used to phase the alleles. When the program did not produce results or length-heterozygous alleles were present, allele-specific primers were used to independently amplify the two alleles. Allele-specific primers consist of two primers that are identical to one another except for the last nucleotide, which is situated over a polymorphic position of the sequence to be phased. The use of this type of primers was suggested for the sequencing reaction (Scheen et al., 2012), although in this work we used them both for amplifying and sequencing. To design them, a polymorphic position was selected and two 19-20 nucleotide primers were synthetized, each of which had one of the two possible nucleotides placed at the 3' end. Then, two independent PCR reactions were performed, one for each allele-specific primer, and using the opposite original primer at the other side of the polymorphic region for amplification. In this way, two PCR products, corresponding to the two alleles, were obtained. Finally, each PCR product was sequenced with the corresponding allele-specific primer to obtain the resolved partial allele, which was then assembled with the original PCR sequence to obtain the complete allele (Scheen et al., 2012). The primers used for PCR allele-specific resolution are shown in Supplementary Table S5.

1.4. Phylogenetic analyses of cytochrome *b*

Since some cytochrome *b* sequences were completely amplified whereas others were only partial (Supplementary Table S1), they were aligned using MAFFT version 7.130 (Katoh and Standley, 2013) with the maxiterate option enabled.

A Bayesian tree of the cytochrome *b* sequences was built using BEAST version 2.5.0 (Bouckaert et al., 2014). To select a statistically appropriate model, a Bayes factors approach based on path sampling (Baele et al., 2012) was used with 96 complete sequences. Markov chain Monte Carlo analyses were based on 100 steps of 10,000,000 generations sampled each 1,000 generations, 10 % preburn-in, 10 % burn-in, and an alpha parameter of the Beta distribution to divide steps of 0.3. The convergence of each tree was checked in Tracer v1.7.1, from the same software package. Different priors were tested for each

parameter category, and a more complex model was selected only if it converged and improved the log marginal likelihood by more than 5, as recommended (Baele et al., 2012). Using these criteria, the selected model was the following: HKY substitution model with estimated base frequencies and Gamma site heterogeneity for each partition (unlinked substitution models); a strict clock model for all partitions (linked clock model); and a coalescent constant size tree model. Once the best model had been selected, it was applied to the sequences of either all *Neomys* species or only *N. fodiens*. In these cases, 50,000,000 generations were run. Consensus trees were calculated using the TreeAnnotator program (BEAST2 package) with median heights.

For comparison, a maximum-likelihood tree of all sequences was reconstructed with RAxML version 8.0.19 (Stamatakis, 2014) using a GTR substitution model (as recommended in the manual of this program), rate heterogeneity modeled with a Gamma distribution, and 100 randomized maximum-parsimony starting trees. Mid-point rooting was used to represent the tree.

1.5. Multilocus analyses

The *Neomys* alleles showed some differences in length due to small indels. They were aligned with MAFFT version 7.130 (Katoh and Standley, 2013) with the maxiterate option enabled. Then, a few gap positions as well as a few positions with unknown nucleotides were removed from each alignment.

A maximum-likelihood tree was reconstructed with RAxML (Stamatakis, 2014) from each alignment as before. For each of these trees, haplotype genealogies were constructed using Haploviewer (Salzburger et al., 2011).

In addition, we reconstructed a phylogenetic distance tree from the intron alignments, as in Igea et al. (2015). First, pairwise distances were calculated in such a way that the two alleles of each sequence were taken into account by making all possible comparisons between alleles (Freedman et al., 2014), and correcting for multiple substitutions using the Jukes-Cantor formula. The pairwise distance matrix was then utilized to construct a tree with the Fitch program of the Phylip software package (Felsenstein, 1989). Mid-point rooting was used to represent the tree.

1.6. Genetic differentiation

Intron alignments were converted to a diploid multi-allelic data format by assigning a number to each allele. Then, pairwise F_{ST} for all populations was calculated with the R package hierfstat version 0.04-22 (Goudet, 2005) using the genet.dist function with the WC84 method. Significance of the observed F_{ST} values was estimated by bootstrapping over loci using the boot.ppfst function of the same package with 100,000 replications and calculating the 95% confidence intervals. Significance was inferred if the confidence interval did not overlap zero.

1.7. Genetic diversity

Nuclear genetic diversity (π and θ) was calculated using the Bioperl library PopGen version 1.6924 (Stajich and Hahn, 2005). The number of heterozygous positions in each sample were counted across the different nuclear markers and divided by their respective lengths. A map of heterozygosity values was then represented with QGIS (QGIS Development Team, 2019).

2. Divergence time estimation of two populations of a small mammal (*Arvicola scherman*) from the Iberian Peninsula using ddRAD data and an isolation-with-migration model

2.1. Sample collection

Samples of different populations of *A. scherman* and *A. amphibius* were obtained through a combination of our own collections, loans from museums, and skull bones sampled from barn owl pellets (Supplementary Table S6). They included 32 samples belonging to two different populations of *A. scherman* from the Iberian Peninsula (19 of them from the Cantabrian Mountains and 13 from the Pyrenees), 1 sample from central Europe and 6 samples from *A. amphibius* (Figure 13). Out of the 39 samples, 9 were from skull bones. DNA extraction from tissues and skull samples was carried out as described in the previous chapter.

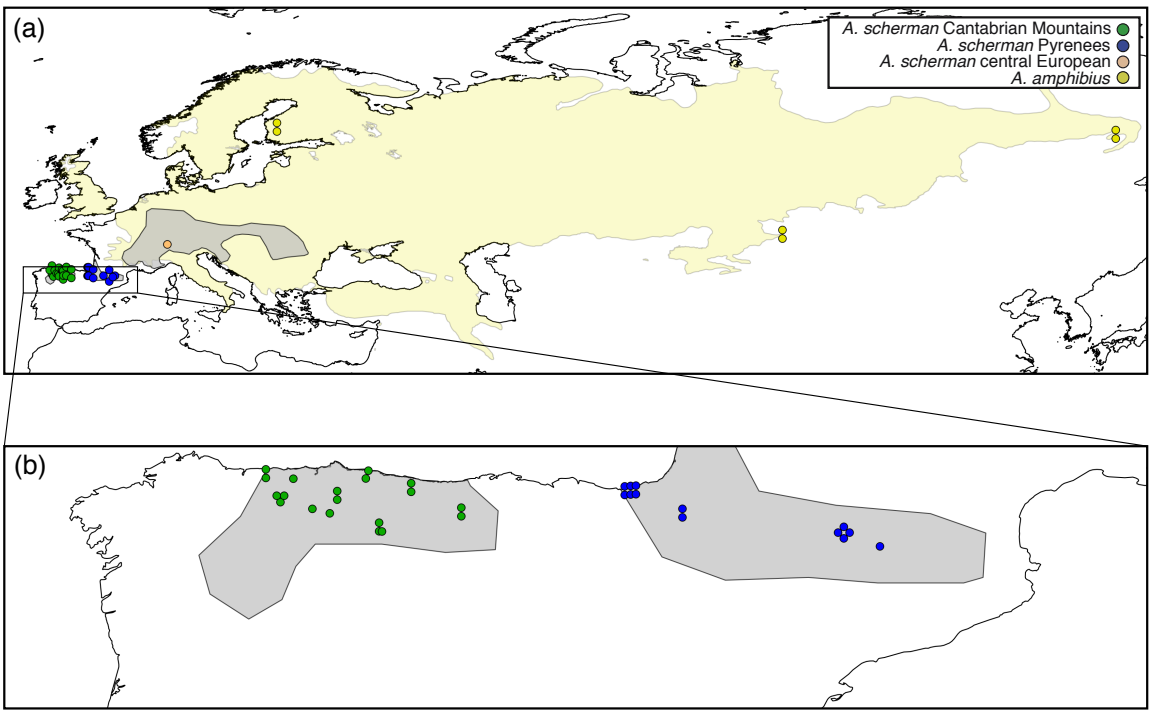

Figure 13. a) Map showing the samples used in this study superimposed over the distribution area of the two species analyzed (grey background: *A. scherman*, yellow background: *A. amphibius*) taken from the IUCN (Amori et al., 2008; Batsaikhan et al., 2016). Note that *A. scherman* is divided into three populations separated geographically (Cantabrian Mountains, Pyrenees and central European) and *A. amphibius* could include more than one species along its whole range. b) Enlargement of the Iberian populations of *A. scherman*.

2.2. ddRAD library preparation and analysis

To prepare the libraries, we followed the ddRAD protocol (Peterson et al., 2012) with modifications to process samples independently (Escoda et al., 2019). Between 50 and 200 ng of genomic DNA, estimated with qPCR as previously described (Escoda et al., 2019), was digested with EcoRI and MspI restriction enzymes. Fragments between 300 and 400 bp were selected in a precast EX 2% agarose gel using the E-Gel system (Invitrogen). Different P1 Illumina adapters for each sample (a 5 nucleotides barcode), up to a maximum of 24, and one P2 (the same for all samples) were used. When having more than 24 samples, two PCR indexes were used. A PCR of 20 cycles was performed with primers annealing over the adapters (of 24 cycles in case of having weak PCR products). Two more PCR reactions were done to avoid underrepresented loci. When there was no PCR product, samples were removed before pooling. PCR products from each sample were pooled and visualized in a gel. Finally, samples were pooled in quantities that depended on the product intensity in the gel to construct the final library. After initial bioinformatic analyses to estimate the coverage of each sample, some tissues and most of skull samples were reprocessed in subsequent libraries to increase coverage. Libraries were sequenced using the NextSeq Sequencing System (Illumina) with the 150-cycles Mid Output kit and single-read runs in the Genomics Core Facility at Pompeu Fabra University.

Library sequences were analyzed using stacks 1.35 (Catchen et al., 2013). *Process_radtags* using the recovery option (*r*) was used to filter sequences and truncate reads to 145 bp. Sample reads coming from different libraries of the same specimen were merged after this step. Using *ustacks*, the initial minimum coverage (*m*) was set to 3 and the maximum differences between stacks (*M*) to 6. Finally, a catalog of loci of all samples was built allowing for a number of differences between loci from different samples (*n*) of 6 in *cstacks*. This set of parameters was considered to be optimal after testing different values. The *populations* program of the package was finally used to create two different datasets (Supplementary Table S7**)**. One of them (dataset 1), with a minimum coverage (*m*) of 12 and a minimum proportion of individuals (*r*) of 0.51, was optimized for obtaining a large number of sequences for phylogenetic reconstruction and accurate heterozygosity rate estimation; the 145 bp sequences of this dataset were saved in FASTA format. The other (dataset 2), with m = 6 and r = 1, was optimized for obtaining a large number of reliable sequences and SNPs that were present in all individuals; the 145 bp sequences were saved in FASTA format and the first SNP of each variable locus was saved in PLINK format.

Degraded samples and old tissues may contain a large amount of exogenous DNA from bacteria, fungi, and other parasites. To filter them out, sequences from tissue samples were used to construct a database of endogenous DNA. This set was assembled using the parameters m = 12 and r = 0.51 in stacks. All sequences were then filtered with Bowtie 2.3.0 (Langmead and Salzberg, 2012) using the option "--score-min L,-0.6,-0.6", so that only reads that matched the tissue samples database were retained for further analyses. This process was performed separately for samples of *A. scherman* and *A. amphibius*.

The heterozygosity rate was calculated by counting heterozygous positions in all loci of dataset 1 and dividing by their total length.

2.3. Genomic tree and population analysis

A genomic tree of the individuals was constructed using variable loci generated in dataset 1, following Igea et al. (2015). In order to summarize the divergence of the two separate alleles of each locus, a pairwise distance matrix was calculated by including genetic distances between all possible combinations of alleles from a pair of individuals (Freedman et al., 2014). After that, the matrix was corrected for multiple substitutions using the Jukes and Cantor formula. Then, the resulting matrix of pairwise distances was used to construct a tree with the Fitch program of the Phylip package (Felsenstein, 1989). Mid-point rooting was used to represent the tree.

A principal component analysis (PCA) applied to the SNPs dataset was performed with the program SNPRelate available in R, using the genetic covariance matrix (Zheng et al., 2012).

STRUCTURE 2.3.4 (Pritchard et al., 2000) was applied to the same SNPs. An admixture and correlated allele frequency model with no prior information on population origin was used with a number of populations (K) from 2 to 4. The number of replicas was set to 500,000 with 10% of burn-in. Ten independent analyses were done. When different patterns were found, something that occurred with K=4, the most common one was used. The proportion of components from each population in every sample was represented with bar plots ordered by geographic region and longitude.

Pairwise F_{st} distances using the SNPs were estimated between different populations using the Weir and Cockerman (1984) method in the *genet.dist* function of the hierfstat R package (Goudet, 2005). Using boot.ppfst of the same package, 95% confidence intervals were then calculated with 100,000 replications bootstrapping over loci. Intervals that do not overlap zero were inferred to be significant.

2.4. Estimation of specific mutation rates of ddRAD loci from rodent sequences

Specific mutation rates were estimated for ddRAD loci using a bioinformatic pipeline applied to the loci of dataset 2 (Figure 14). The starting point were the ddRAD variable loci present in all samples (2,847). One sequence per locus was extracted and a BLAST search (Altschul et al., 1997) against the mouse genome was performed (80,352 hits). To try to ensure orthology, we used only sequences with a single hit and an E-value for reported alignments smaller than $1e^{-40}$ (118 orthologues). Using the sequence coordinates from the mouse sequences found, available mammalian orthologues were downloaded from the EPO suite of the ENSEMBL database (Yates et al., 2020) using the script *dna_getAncestralSequences.pl* from the ENSEMBL Compara API (www.ensembl.org/info/docs/api/compara/index.html) and the library bioperl-1.6.924 (Stajich and Hahn, 2005), which retrieved orthologues from 37 mammalian genomes. Only sequences with less than 10 unknown nucleotides and more than 100 bp were retained (114 orthology alignments). Additionally, only alignments that included mouse (*Mus musculus*) and rat (*Rattus norvegicus*) were kept (86 mammal alignments). After that, we selected the sequences from the *Muroidea* superfamily of each alignment: *M. pahari*, *M. caroli*, *M. spretus*, *M. musculus*, *Microtus ochrogaster*, *Cricetulus griseus*, *R. norvegicus* and *Peromyscus maniculatus* (86 *Muroidea* alignments). We then included the corresponding 86 *Arvicola sp.* sequences and realigned each set of rodent orthologues using MAFFT 7.130 (Katoh and Standley, 2013) with the combination of localpair, maxiterate and adjustdirectionaccurately parameters (to properly align the *Arvicola sp.* sequences). Gap positions from the final alignments were removed using Gblocks (Castresana, 2000). Then, we filtered out invariant alignments (remaining 85 final alignments, that is, 3% of the total loci). Subsequently, we reconstructed a phylogenetic tree from each alignment with RAxML version 8.0.19 (Stamatakis, 2014). Finally, branch lengths were estimated and the trees visually inspected to corroborate that no anomalous trees were present in the final set.

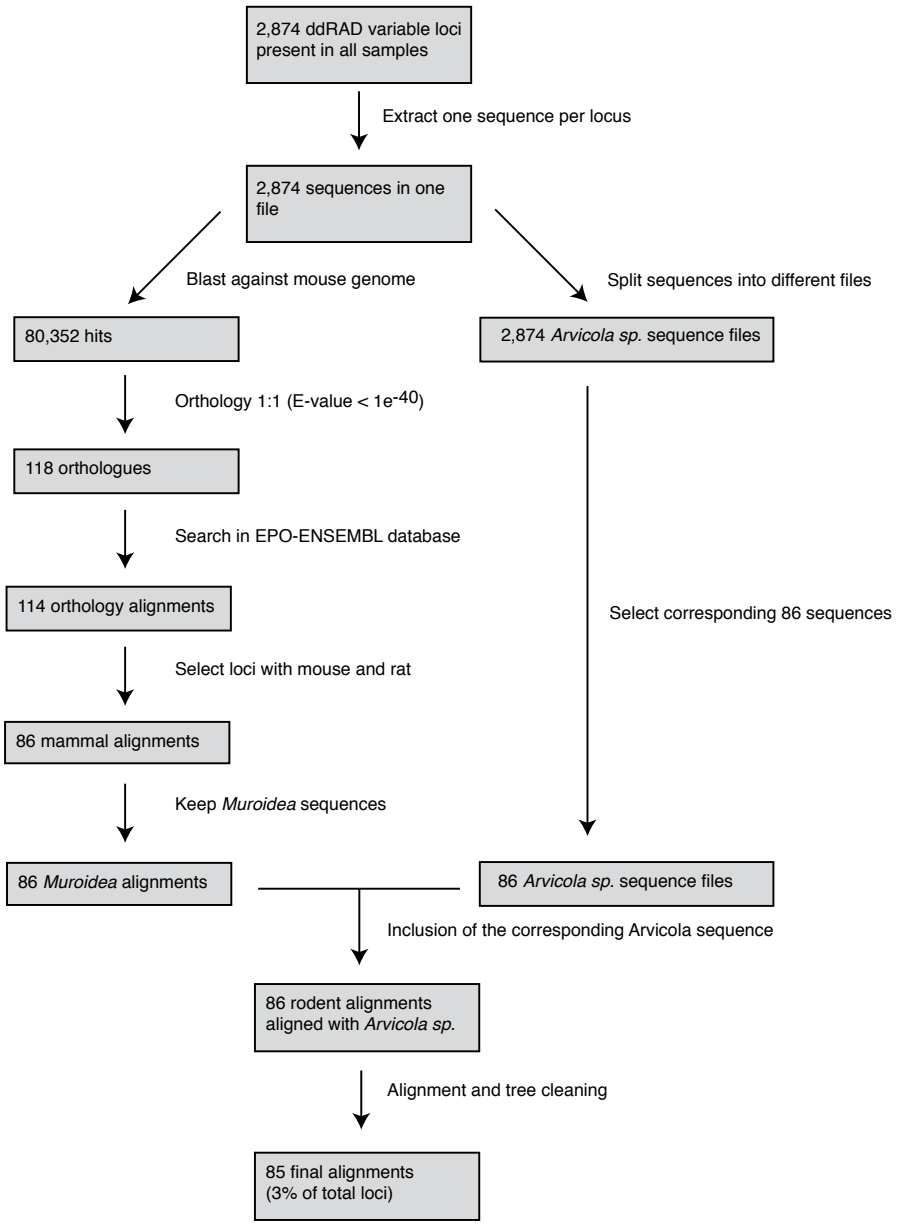

Figure 14. Scheme of the bioinformatic pipeline developed to detect *Arvicola sp.* orthologues in other rodents using ddRAD loci.

A Rodent tree was constructed with BEAST version 2.5.2 (Bouckaert et al., 2019) from all the alignments retrieved using the calibrating point of the mouse-rat split of 10.4-14.0 Myr, which is based on fossil data (Benton et al., 2009) and has been used in many other works (Steppan et al., 2004; Fabre et al., 2012; Kimura et al., 2015; Aghová et al., 2018). Unlinked site models (HKY + I) across loci, unlinked clocks (strict clock) and linked trees (Yule)

were selected. A strict clock was chosen because the analysis converged better than with a relaxed clock in initial runs, as expected when the mutation rate variation among lineages is low (Brown and Yang, 2011). The calibrated node was modelled using a lognormal prior distribution with minimum and maximum constraints in real space; we set the offset to 10.4 and the soft maximum to 14.0 Myr in order to coincide with the 95th percentil of the probability density distribution with a standard deviation of 1. The calibrated phylogeny allowed us to obtain the mutation rate for different ddRAD loci (thereafter named as calibrated loci). 75,000,000 generations were run, sampling each 1000 generations. Tracer v1.7.1 (BEAST2 package) was used to check convergence and retrieve the mutation rate of each locus. The TreeAnnotator program of the same package was used to calculate the consensus tree with median heights and 10% burn-in.

2.5. Isolation-with-migration analyses

In order to estimate divergence times in an isolation-with-migration analysis we used IMa3 (Hey et al., 2018). Four populations were considered: the Cantabrian and Pyrenean populations from the Iberian Peninsula as well as a sample from the central European distribution and *A. amphibius* samples as two outgroups. When using the four populations, the population topology was: (((Cantabrian, Pyrenean), Central European), *A. amphibius*). Runs with only the two Iberian populations, with or without a ghost population (Hey et al., 2018), were also performed. The ghost population is placed as an outgroup and represents an unsampled population that could have affected the Iberian populations by exchanging individuals (Beerli, 2004). Final analyses were carried out with 300 randomly selected loci from dataset 2 that included all calibrated loci (85). Invariable loci that appeared in the analyses of two populations when removing outgroup sequences were eliminated so that 248 loci remained (of which 64 were calibrated loci). The mutation rates estimated previously with BEAST2 were included in the corresponding loci of the input file after scaling them per alignment, as required by the program. The generation time was set to 1 year, a value that can be considered adequate for a short-lived species like *Arvicola*. However, it should be taken into account that the generation time does not affect the estimation of divergence times. The infinite sites model was used for all loci and reads that did not pass the four gametes test were trimmed, selecting the longest interval (Hey and Wang, 2019). Priors in the IMa3 model were: maximum population size $q = 1.5$, maximum

split time $t = 0.5$, and maximum migration rate $m = 2$. Runs were done with 420 chains on 14 processors. Burn-in was set to ~30,000 steps and 10,000 genealogies were sampled. ASCII plots of parameter trends and marginal posterior probability distributions of the parameters were checked to ensure proper mixing and convergence. Moreover, BEAST2 rates were compared with mutation rate scalars estimated from *Arvicola sp.* sequences by IMa3. The IMfig program (Hey, 2010b) was used to prepare a figure with the estimated demographic parameters. Significant migration rates are based on the log-likelihood-ratio test of the null hypothesis of migration being zero (Nielsen and Wakeley, 2001).

V. RESULTS

1. Size increase without genetic divergence in the Eurasian water shrew *Neomys fodiens*

1.1. Morphometric analyses of *Neomys* mandibles

Skull samples from 67 *Neomys* individuals (Supplementary Table S1) were obtained, primarily, from barn owl pellets collected over the last 50 years in the northern Iberian Peninsula. The samples came from approximately longitudes -7º to 2º, where two subspecies of *N. fodiens*, as well as *N. anomalus*, are present (Figure 12). Landmarks were taken from each mandible to measure the coronoid height and perform a geometric morphometric analysis. According to the coronoid height (Supplementary Figure S1), 32 samples were classified as *N. f. niethammeri*, 19 as *N. f. fodiens*, and 16 as *N. anomalus* (Supplementary Table S2). Plotting these measurements against longitude, we confirmed an abrupt size increase in *N. f. niethammeri* in the north-central part of the Iberian Peninsula, approximately between longitudes -6.25º and -1º (Figure 12c), corroborating previous work (Nores et al., 1982; López-Fuster et al., 1990). We found individuals of both sizes in the same locality, indicating a certain overlap in the distribution of the two groups. The skulls of the sympatric species *N. anomalus* were always smaller than those of *N. fodiens* (Supplementary Table S2). The centroid size of the mandibles provided similar results (Supplementary Figure S2 and Supplementary Table S2). A principal components analysis of the landmarks allowed *N. anomalus* to be distinguished from *N. fodiens*, but not *N. f. niethammeri* from *N. f. fodiens* (Figure 15), indicating that the two *N. fodiens* subspecies were similar in shape.

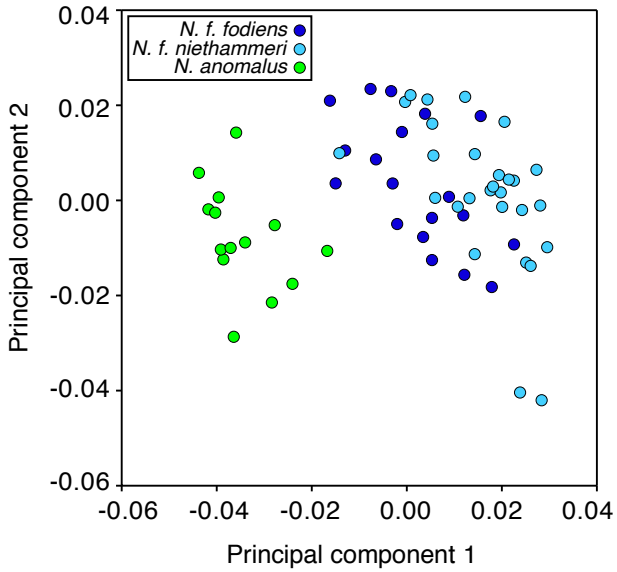

Figure 15. Principal components analysis of the mandible landmarks of Iberian *N. fodiens* and *N. anomalus* individuals.

1.2. Mitochondrial phylogeny of *Neomys*

Both complete and partial mitochondrial cytochrome *b* sequences were obtained from 85 samples of *N. fodiens*, including all the mandibles used in the morphometric analysis plus additional tissue samples from Eurasia (Figure 12 and Supplementary Table S1). Some primers were newly designed (Supplementary Table S3) so that sequences could be obtained from the majority of samples, including the oldest (Supplementary Table S1). The Bayesian mitochondrial tree reconstructed with the *N. fodiens* mitochondrial sequences can be subdivided into three main clades separated by relatively long branches and moderate or high support (Figure 16): one includes the Iberian samples and a sample from a nearby locality in France; the second consists of a single sample from southern Italy; and the third comprises samples from the remaining Eurasian range of the species. Coronoid height measurements mapped into this tree indicated that individuals classified as *N. f. niethammeri* appeared randomly across the Iberian clade, reflecting the fact that the two subspecies were indistinguishable at the mitochondrial level. When additional sequences from other *Neomys* species were included in the Bayesian phylogenetic analysis to configure a dataset of 136 sequences, the tree perfectly separated the four species in the genus, but *N. f. fodiens* and *N. f. niethammeri* were once again intermixed in the tree

(Supplementary Figure S3). Similar results were obtained with a maximum-likelihood method (Supplementary Figure S4).

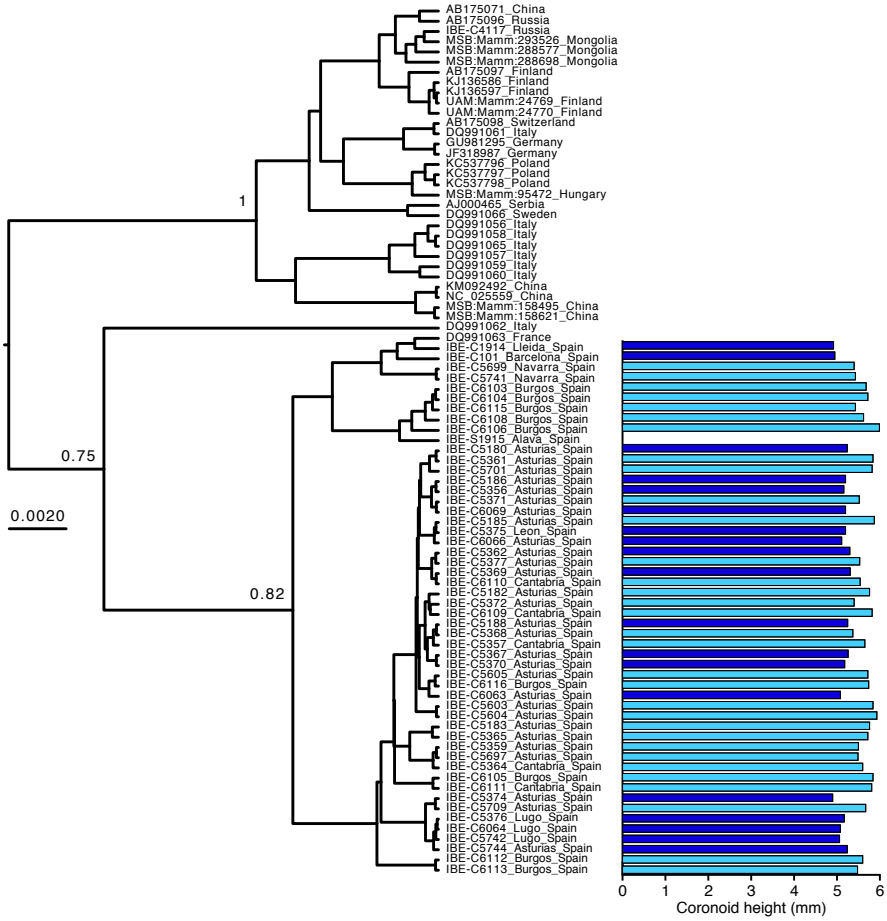

Figure 16. Bayesian tree of *N. fodiens* cytochrome *b* sequences**.** Samples with coronoid height measurement are represented with color-coded bars showing their skull size: dark blue for *N. f. fodiens* and light blue for *N. f. niethammeri*. The scale is in substitutions per position and posterior probabilities are indicated for the clades mentioned in the text.

1.3. Development of nuclear markers for degraded *Neomys* samples

We developed a set of six short intron markers (ASB6 intron 2, CSF2 intron 2, GDAP1 intron 1, JMJD intron 2, MYCBPAP intron 11, and TRAIP intron 8) that could be amplified using DNA extracted from the mandibles, despite the high degradation levels of some of them (Supplementary Table S4). For some introns, several rounds of primer design were performed to shorten the PCR product and allow the amplification of the most degraded samples (Supplementary Table S4). In this way, we obtained nuclear information from most of the recent samples, as well as from a good proportion of the older samples,

including those collected during the 1970s (Supplementary Table S1). For some introns, allele-specific primers were designed to separate heterozygous sequences (Supplementary Table S5). A total of 58 samples with a minimum of four sequenced introns were used in further analyses, including 37 mandibles and 11 tissues, together with sequences from 10 samples taken from a previous work (Igea et al., 2015) (Supplementary Table S1). Considering all the introns together, 172 sequences were used from *N. f. niethammeri*, 250 from the other *N. fodiens* specimens, 158 from *N. anomalus*, 48 from *N. milleri*, and 24 from *N. teres*, totaling 123,556 bp of nuclear sequence information after alignment cleaning.

1.4. Multilocus phylogenetic analysis of *Neomys*

Haplotype genealogies derived from the maximum-likelihood trees of the nuclear sequences showed a low degree of allele sharing between the four *Neomys* species (Figure 17a). On the other hand, *N. f. niethammeri* and the rest of *N. fodiens* shared the most frequent alleles (largest circles in Figure 17a), although most minor alleles were exclusive to one group or the other (smaller circles in Figure 17a). Since the mutational differences between the alleles were minimal, both groups were completely intermixed in the phylogenetic tree reconstructed using the concatenated intron sequences (Figure 17b). In fact, no clades within *N. fodiens* can be distinguished in the nuclear tree.

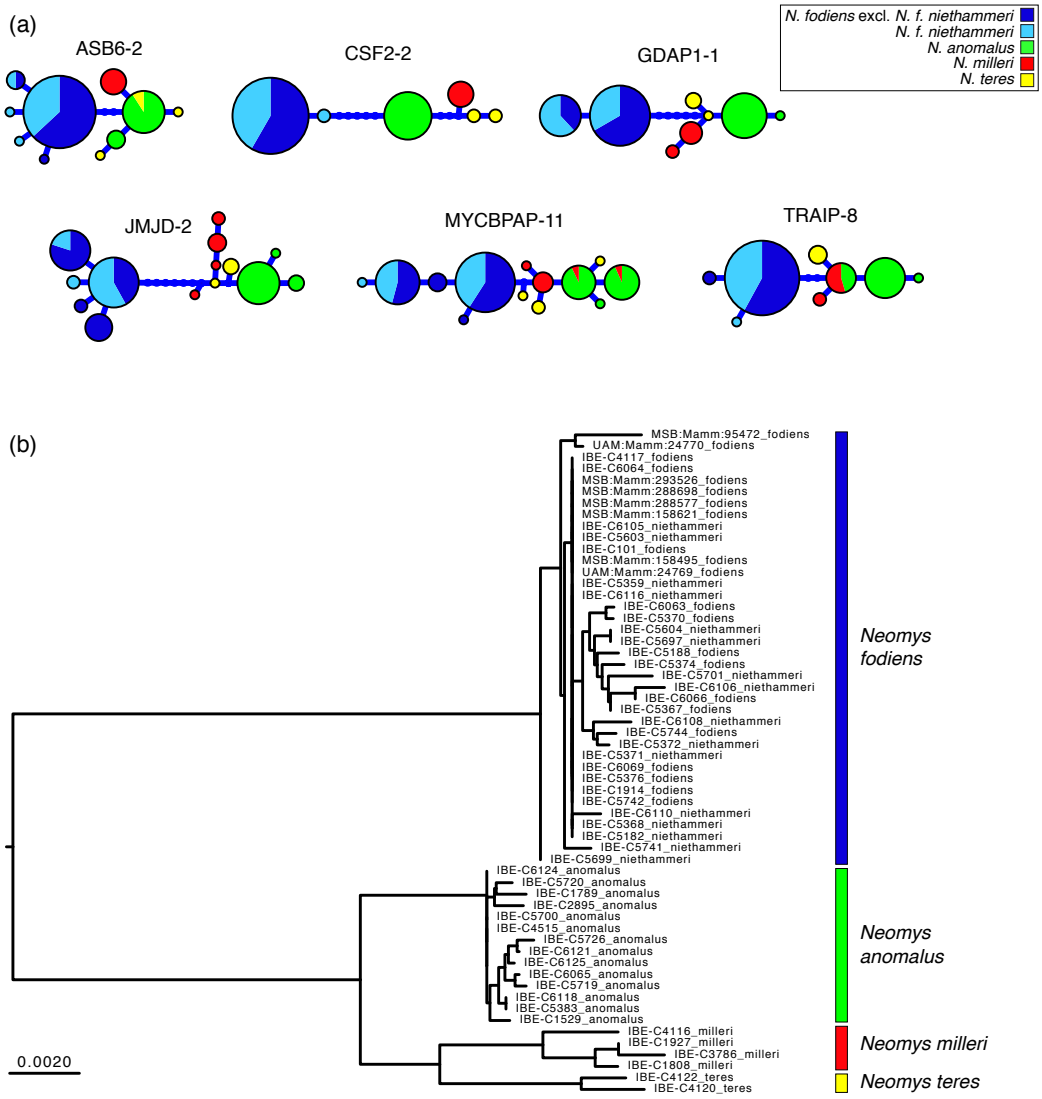

Figure 17. Phylogenetic information derived from the 6 introns amplified in the *Neomys* samples. (a) Haplotype genealogies where the size of the circles is proportional to the number of alleles detected. (b) Distance tree for the concatenated introns with the scale in substitutions per position.

1.5. Genetic differentiation

To study the possibility that differentiated groups existed within *N. fodiens*, we next converted the six intron alignments into a multi-allelic data format. There were 22 different alleles and therefore the average number of alleles per locus was 3.7. Using this information, we calculated the F_{ST} distance between *N. f. niethammeri*, *N. f. fodiens* from the northern Iberian Peninsula, and *N. fodiens* from the rest of the range. The value obtained between *N. f. niethammeri* and Iberian *N. f. fodiens* was 0.040 and it was not significant

(95% confidence intervals: -0.005 - 0.085). F_{ST} values between these and the other population were also non-significant.

1.6. Nuclear genetic diversity of *N. fodiens* populations

Individual heterozygosity estimated from the nuclear introns of *N. fodiens* specimens showed that the most heterozygous samples were from the northern Iberian Peninsula (Figure 18). Thus, we found an average of 0.0013 heterozygous positions in the Iberian samples (including both *N. f. fodiens* and *N. f. niethammeri*) versus 0.0004 in the rest of the sampled range. When the nuclear data was analyzed at the population level, the average θ values were 0.0021 and 0.0014 for these two groups, respectively (Supplementary Table S8), showing the same trend. The same was found with the π parameter (Supplementary Table S8).

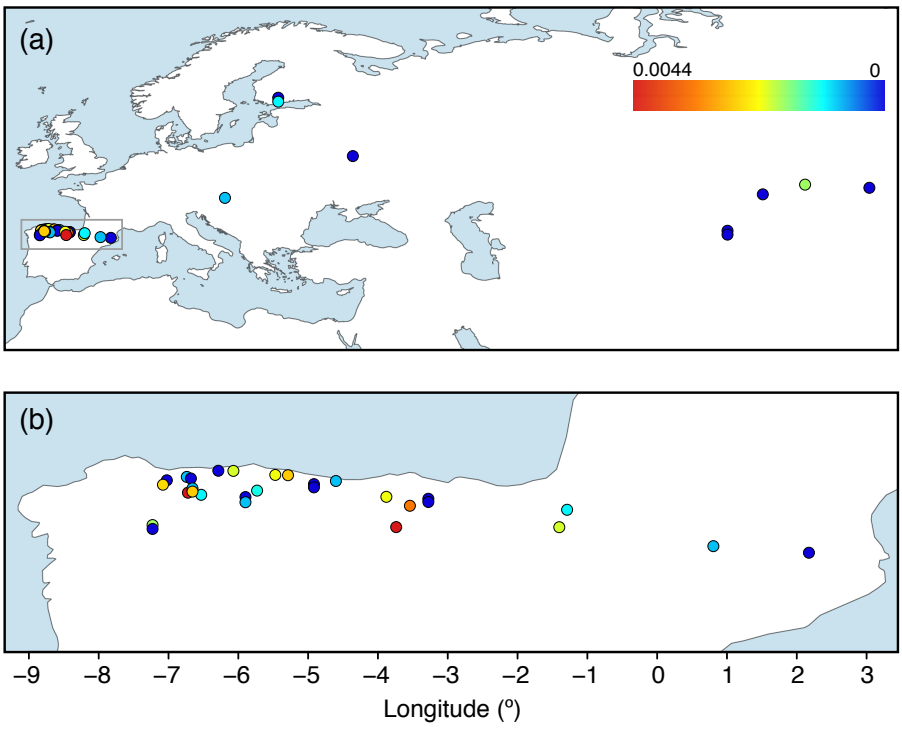

Figure 18. Map of color-coded individual heterozygosity rates in *N. fodiens*. (a) Map of all samples with the main study area highlighted, and (b) enlargement of the northern Iberian Peninsula. The scale is in number of heterozygous positions per base.

2. Divergence time estimation of two populations of a small mammal (*Arvicola scherman*) from the Iberian Peninsula using ddRAD data and an isolation-with-migration model

2.1. Sequence assembly and filtering of ddRAD reads

A total of 192,910,996 Illumina reads from 39 individuals (Supplementary Table S9) were used for assembly. After applying the filter with the tissue samples databases, 123,837,729 reads remained (71% on average for all samples). The loss of reads in this filtering process was mainly due to exogenous sequences present in the bones, where only 53% of sequences were retained (Supplementary Tables S9 and S10).

After the assembly of the remaining endogenous reads for dataset 1, 45,813 total and 39,207 variable loci were obtained (see Supplementary Table S7). The genome-wide heterozygosity rate estimated with this dataset in the Cantabrian population, where several samples of both types were available, resulted in similar values for tissues (0.001312 or 1,312 SNPs/Mb) and skull bones (0.001272 or 1,272 SNPs/Mb) (Supplementary Table S10). The fact that skull bones did not have more heterozygous sites, which could have been due to errors, indicates that bones were properly sequenced.

2.2. Genomic tree and population analyses

A genomic tree based on the variable loci (5,685,015 base pairs of dataset 1) was reconstructed (Figure 19). Apart from the *A. amphibius* and central European groups, the iberian individuals were clearly separated in two different clades, from the Cantabrian Mountains and the Pyrenees, corresponding to the two known populations.

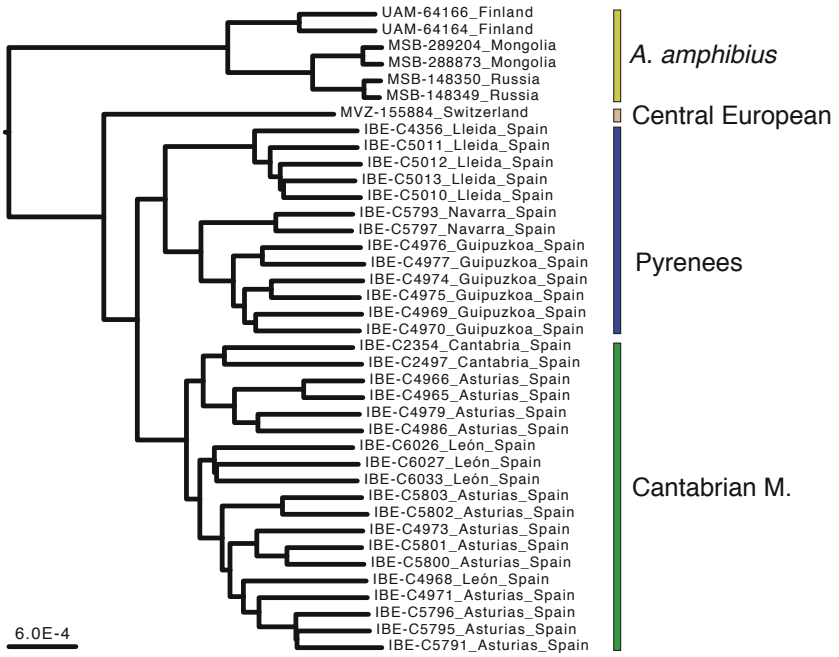

Figure 19. Genomic tree obtained from 39,207 variable loci. The scale is in substitutions per position and mid-point rooting was used to represent the tree.

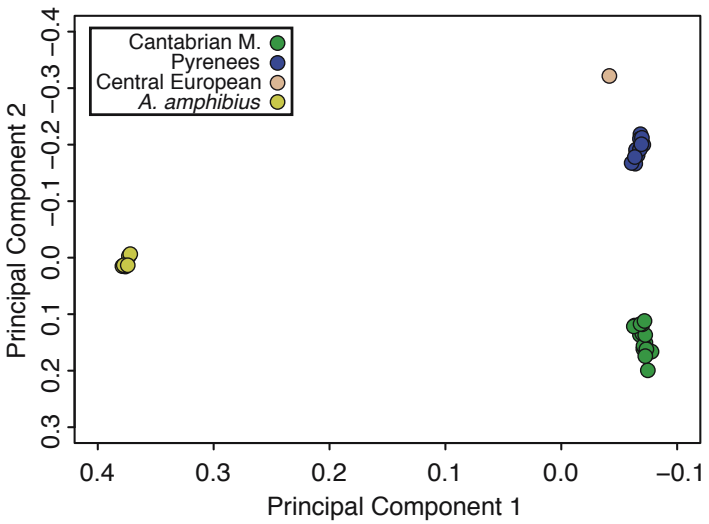

A PCA performed with 2,877 SNPs of dataset 2 separated the samples according to the species and their geographic distribution, as in the tree, corroborating the existence of four clearly delimited groups (Figure 20).

Figure 20. PCA of the 2,877 SNPs from dataset 2.

The STRUCTURE analysis considering 2 to 4 populations with the same SNPs from dataset 2 also showed a coherent subdivision in four populations. The central European sample of *A. scherman* was revealed to be admixed from other populations although this result may be affected by the fact that only one sample was in this populations (Figure 21). Increasing the K value in STRUCTURE did not reveal any additional meaningful geographical structure.

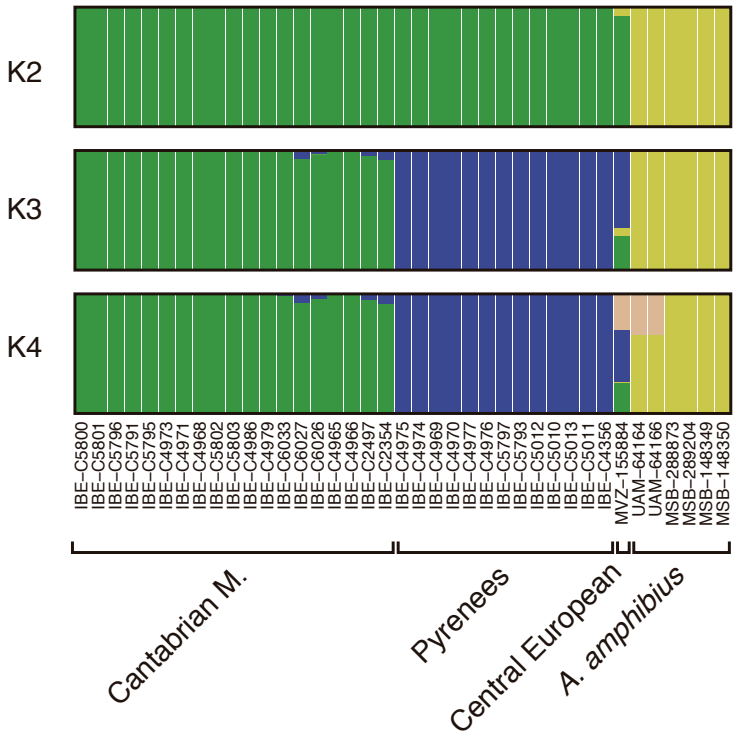

Figure 21. Bar plot of *Arvicola sp.* samples determined with a STRUCTURE analysis of the 2,877 SNPs from dataset 2 and varying the number of K populations from 2 to 4. Samples are ordered by geographic longitude and divided by populations.

F_{st} analysis revealed pronounced and significance levels of population differentiation between all four groups (>0.25) (Supplementary Table S11).

2.3. Mutation rates of ddRAD loci

We applied a pipeline to find *Muroidea* orthologues from the *Arvicola sp.* sequences, as explained in Methods, which allowed us to obtain 85 orthologues aligned with *Arvicola sp.* sequences (Figure 14).

We constructed a tree using BEAST2 with these 85 loci and the rat-mouse split as a calibration point. The calibrated phylogeny indicated that all species diverged 18 Myr ago (Figure 22). The mutation rate was obtained for each locus, with an average of 2.6 x 10^{-9} mutations/site/yr. The minimum rate was 0.3 x 10^{-9} and the maximum 5.3 x 10^{-9}, thus covering more than an order of magnitude (Supplementary Table S12).

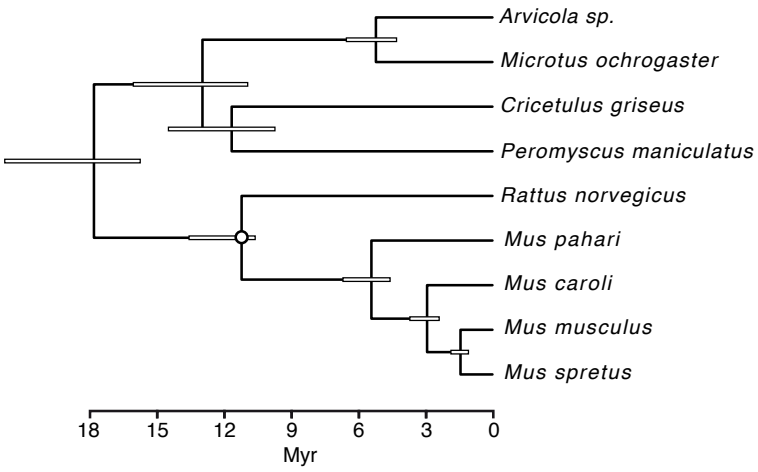

Figure 22. Calibrated BEAST2 tree reconstructed to estimate mutation rates of 85 *Arvicola sp*. ddRAD loci. The white circle shows the mouse-rat calibration prior (14.0-10.4 Myr). Node heights with bars indicate 95% highest posterior density interval.

2.4. Application of an isolation-with-migration model

We applied an isolation-with-migration model with the purpose of estimating the divergence time between the Cantabrian and Pyrenean populations of *A. scherman*. IMa3 was run with different numbers of loci, from less than 100 to 300, in which 85 of them were the loci with calibrated mutation rates and the rest of loci were randomly selected from the total pool of variable loci. In the run with 4 populations, we found that using 300 loci was enough to achieve good convergence. Probability distributions of divergence times,

populations sizes, and significant migration rates showed continuous distributions in most cases (Figure 23). Only the distribution for the oldest divergence time (t2) was noisy but the distribution of the split time of interest, that between the Cantabrian and Pyrenean populations (t0), was well defined and narrow.

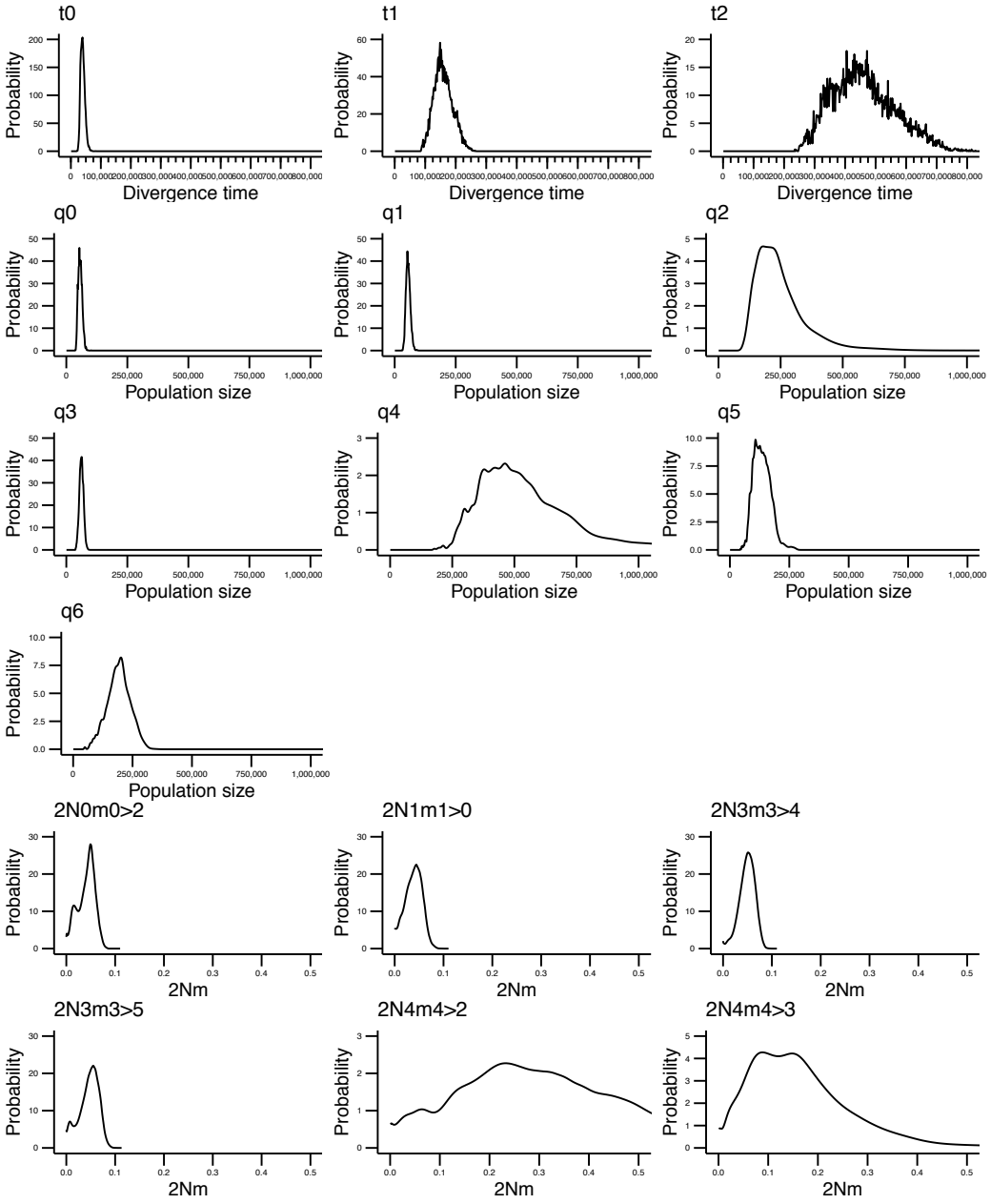

Figure 23. Marginal posterior probability histograms of the isolation-with-migration model including four populations and 300 total loci with 85 calibrated (top row: splitting time, middle rows: population size, bottom rows: population migration rate). Note that for migration rates only significant values of gene flow between populations (in the coalescent) of the log-likelihood-ratio test are shown. Population tree used: (((0,1)4,2)5,3)6; being 0: Cantabrian M., 1: Pyrenees, 2: Central European and 3: *A. amphibius.*

The run performed with 4 populations showed a divergence time between the two Iberian populations (t0) of 39 Kyr (95 % highest posterior density interval: 21 – 62 Kyr) (Figure 24 and Table 1). Six significant migration rates were found, from the central European to the Cantabrian Mountains population and within the Iberian populations (from the Cantabrian Mountains to the Pyrenees), all with values of effective number of migrant genes per generation (2Nm) << 1 (Figure 24). IMa3 analysis in which only the two Iberian populations were included, with or without a ghost population, produced slightly higher estimates for t0: 70 Kyr and 49 kyr, respectively (Table 1).

Table 1. Split times (and 95 % highest posterior density intervals) of *Arvicola sp.* populations in Kyr obtained with isolation-with-migration analyses for different number of populations and ddRAD loci. Invariable loci that appeared in the analyses of two populations with or without ghost were removed. A question mark indicates that the interval may be incorrect due to multiple peaks.

Nº of populations	**Number of total loci (calibrated loci)**	**t0: Cantabrian - Pyrenean split**	**t1: Iberian – Central European split**	**t2: *A. scherman* - *A. amphibius* split**
4	300 (85)	39 (21-62)	149 (100-223)	430 (275-668 ?)
2	248 (64)	70 (43-99)	-	-
2 + ghost	248 (64)	49 (22-76)	-	-

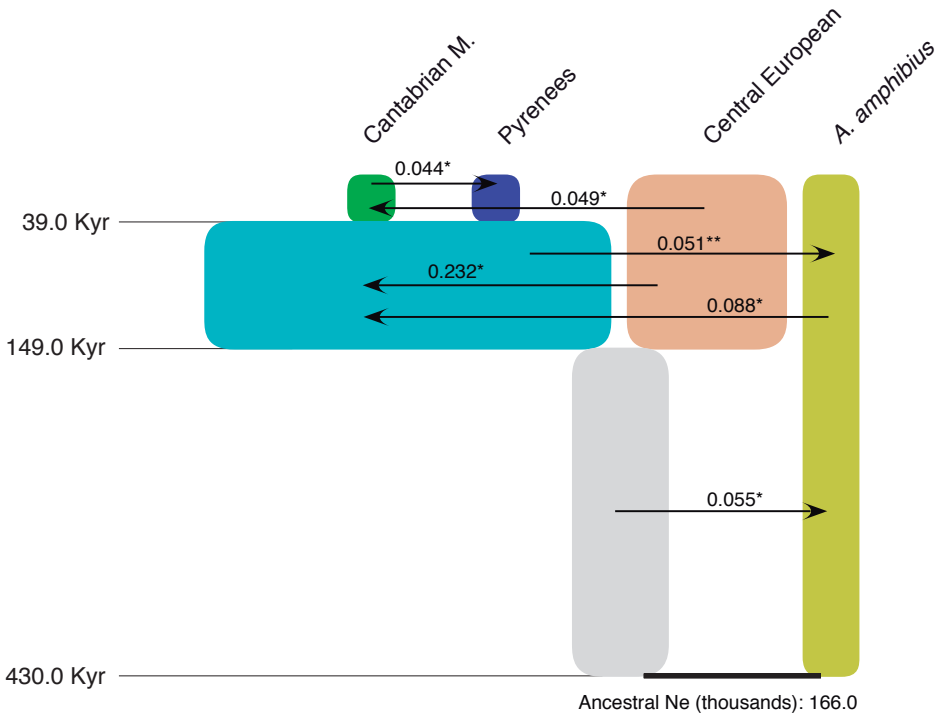

Figure 24. Isolation-with-migration model generated by IMa3 and the IMfig program using 300 loci with 85 calibrated. Splitting times are depicted as solid horizontal lines, with values on the left. Migration arrows indicate statistically significant 2Nm values (* $p < 0.05$, ** $p < 0.01$). The width of boxes is proportional to the estimated ancestral Ne.

In order to test if the loci with estimated mutation rates were more conserved, as they were selected to have orthologues in all *Muroidea*, we used the relative rates or scalars that IMa3 estimates for all loci. The means of the scalars were 1.48 and 1.69 for the calibrated and non-calibrated loci, respectively. Thus, the rates were slightly higher for the non-calibrated loci, as expected (Figure 25). Finally, a weak but significant correlation was observed between mutation rates estimated from *Muroidea* sequences by BEAST2 and the log transformed mutation rate scalars estimated for *Arvicola sp.* sequences by IMa3 ($r = 0.26$; $p = 0.02$), as expected from neutral theory.

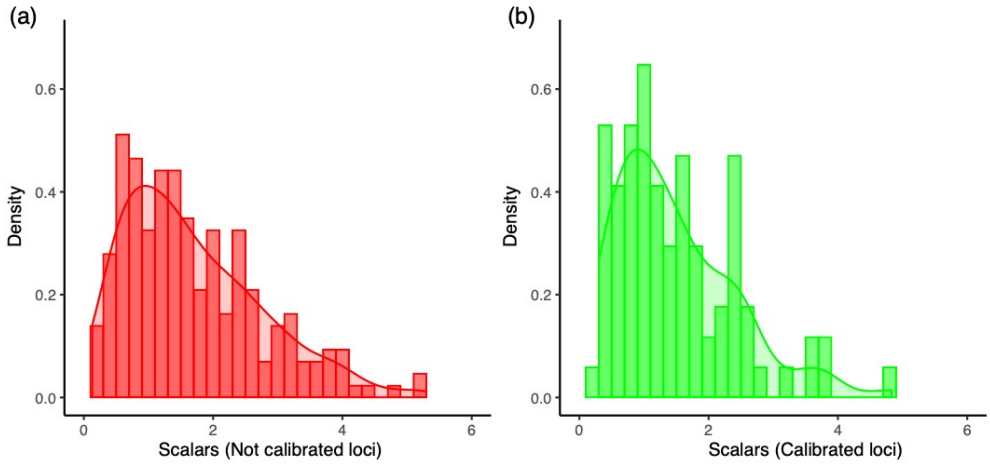

Figure 25. Histograms and smoothed density distributions of mutation rate scalars estimated by IMa3. Non-calibrated loci are shown in red (a) and calibrated loci in green (b).

VI. DISCUSSION

Skull bones from small mammals found in barn owl pellets have demonstrated to be a valuable source of DNA from minimally invasive samples to perform simultaneous morphometric and genetic studies. It has also been shown in this work that it is possible to obtain genomic information through next-generation sequencing (NGS) technologies from skull bones, opening the path to perform genomic studies of mammalian biodiversity using this material, which can be obtained relatively easily and without disturbance for the populations studied. The optimization of genetic and bioinformatic techniques to estimate genetic structure and divergence times of closely related populations using multilocus and ddRAD data have provided with new information in comparative phylogeography of small mammals in the Iberian Peninsula.

In chapter 1, morphometric and genetic analyses have clarified the taxonomic status of *Neomys fodiens niethammeri* found in the northern strip of the Iberian Peninsula, flanked by populations of the nominal subspecies. The absence of genetic divergence and differentiation revealed here indicated that the large form of *N. fodiens* does not correspond to a different species and instead represents an extreme case of size increase of possible adaptive value.

In chapter 2, the estimation of divergence times using ddRAD data with an isolation-with-migration model have helped to achieve a deeper understanding of the circumstances that have led to the current population structure at fine scale in the Iberian populations of *Arvicola scherman*. More specifically, it has been shown with statistical support that their divergence occurred during the last glacial period.

Genetic structure and diversity analyses performed in this work have uncovered high levels of intraspecific diversity for these two species in the north of the in the Iberian Peninsula, rejecting the idea of a recent colonization from the European range of the species analyzed and instead suggesting their presence in the Iberian Peninsula at least since the Last Glacial Maximum (LGM). It will be interesting to know if other Eurosiberian species follow this pattern or if some of them show lower genetic diversity levels, suggesting more recent colonizations of this area.

The methodologies used here have shown their suitability to clarify in an objective way the taxonomic status of these mammalian species. In one of the cases (*N. fodiens*), genetic data does not support any taxonomic subdivision in the populations of the Iberian Peninsula. In the other case (*A. scherman*), the existence of two subspecies coincides with the high genetic divergence and strong structure observed. These analyses could be applied to other contentious taxonomic problems as well as to help understand the possible existence of genetic structure and evolutionary conservation units in species of conservation concern.

1. Size increase without genetic divergence in the Eurasian water shrew *Neomys fodiens*

The multilocus dataset used in this study of the Eurasian water shrew *Neomys fodiens* was based on the mitochondrial cytochrome *b* gene and six small intron fragments. The lengths of the newly designed introns (153 - 229 bp) were smaller than those of previously proposed intron markers (Igea et al., 2010, 2015), in order to facilitate the amplification of degraded DNA obtained from skulls from owl pellet material. Using the novel primers, we amplified between 4 and 6 introns from 37 mandible samples of *Neomys*, many of which had been collected during the 1970s (Supplementary Table S1). Despite their relatively short lengths, the intron markers were variable enough to detect mutational differences between species. They also enabled the reconstruction of a nuclear phylogenetic tree, which was compared with the mitochondrial tree and used to detect any possible occurrence of mito-nuclear discordance in *Neomys*. Finally, once these intron markers were converted to allele frequency data, and despite the small number of markers used, they allowed us to undertake a differentiation analysis of the main populations of *N. fodiens*. Therefore, thanks to the various genetic analyses performed, these novel markers were highly useful in unraveling the evolutionary history of *N. f. niethammeri* and, specifically, assessing whether the morphological differences observed (large skull size) arose through a long period of isolation and genetic differentiation. Furthermore, to our knowledge, this is one of the first studies where multilocus genetic data as well as morphometric information of skulls obtained from owl pellets has been fully exploited, showing the enormous potential of this type of non-invasive sampling for biodiversity studies.

1.2. Mitochondrial and multilocus phylogenetic analyses

The mitochondrial sequences of *N. f. fodiens* and *N. f. niethammeri* were intermixed in the phylogenetic tree, meaning that there was no evidence to suggest genetic divergence (Figures 16 and S3). This was a highly unexpected result for two populations with important skull size differences. Without further data, a possible explanation could be that, in fact, these two forms were more divergent at the nuclear level but, due to some recent unidirectional introgression event, *N. f. niethammeri* acquired the mitochondria of *N. f. fodiens*, a phenomenon that has been observed in many other species (Hailer et al., 2012; Toews and Brelsford, 2012). With *N. anomalus* living sympatrically with *N. fodiens* in the

northern Iberian Peninsula, additional scenarios involving inter-specific introgression with this other species could not be discarded, demonstrating the need to carry out a nuclear analysis. The phylogenetic tree we obtained using nuclear data also revealed a lack of genetic divergence between the two *N. fodiens* subspecies (Figure 17b). A first conclusion from this work is, therefore, that our mitochondrial and nuclear data are consistent in highlighting a lack of support for genetic divergence between *N. f. fodiens* and *N. f. niethammeri*.

The mitochondrial and nuclear phylogenies showed that the four *Neomys* species were reciprocally monophyletic in both trees (Figures 17b and S3). This suggests that there has been no recent mitochondrial introgression, not only between *N. fodiens* groups, but also during the evolution of the *Neomys* species. Incidentally, the topological relationships between the four *Neomys* species were not coincident in the mitochondrial and nuclear trees, since *N. milleri* and *N. anomalus* group in the former, whereas *N. milleri* and *N. teres* appear as sister taxa in the latter. However, this could be a consequence of methodological difficulties in resolving old divergences in the tree or incomplete lineage sorting (Degnan and Rosenberg, 2009), and it does not affect the conclusion that there has been no recent introgression in *Neomys*. This reasonable mito-nuclear agreement enables the use of cytochrome *b* for species identification from non-invasive samples in further ecological studies of this genus (Querejeta and Castresana, 2018).

1.2. Genetic differentiation analysis

Populations that have been isolated for a short period of time may not have accumulated enough mutations to reflect phylogenetic separation, but, if the gene flow between them is low, differences in allele frequencies may appear by genetic drift (Knowles, 2004; Omland et al., 2006). To test the possibility that *N. fodiens* populations showed some degree of differentiation, we computed F_{ST} statistics. No significant genetic differentiation was found. Thus, the increase in skull size of *N. f. niethammeri* (Figure 12c) corresponded to neither a difference in shape (Figure 15) nor mitochondrial (Figure 16) or nuclear genetic divergence (Figure 17b), nor genetic differentiation of nuclear allele frequencies. In this respect, it is interesting to note that fossil data of both forms have been found at ~40 Kyr (Cuenca-Bescós et al., 2008; Sesé, 2017). This would suggest that a large amount of gene

flow must have occurred between the two forms to prevent genetic differentiation during all this time, indicating the lack of reproductive barriers between them.

1.3. Genetic diversity of *N. fodiens* in the Iberian Peninsula

The populations of *N. fodiens* of the northern Iberian Peninsula are at the edge of the Palearctic range of the species (Figure 8), which could lead to the hypothesis that this area was recently colonized from the multiple European glacial refugia that have been described for various taxa (Stewart et al., 2010; Schmitt and Varga, 2012). We found, however, that the nuclear genetic diversity was higher in the Iberian samples than in the rest of the Palearctic samples analyzed here (Figure 18), something that is not consistent with the recent colonization of the Iberian Peninsula. The existence in this area of fossil *N. fodiens* dated at ~40 Kyr (Cuenca-Bescós et al., 2008; López-García et al., 2010; Sesé, 2017) also supports the idea that the species was present in the Iberian Peninsula long before the Last Glacial Maximum and, consequently, that these populations are not the product of recent colonization. Instead, refugia in the Iberian Peninsula or nearby areas were likely to have been the source for the recolonization of at least some parts of the western Palearctic (Hewitt, 1999; Schmitt, 2007).

1.4. Taxonomic debate surrounding *N. f. niethammeri*

With regard to the taxonomic debate surrounding *N. f. niethammeri*, the phylogenetic analyses performed here, using mitochondrial and intron sequences, indicate that *N. f. niethammeri* has not accumulated measurable genetic divergence with respect to *N. f. fodiens*. There is also no significant genetic differentiation between them, meaning that also allele frequencies are similar. Taking all this information into account, it is clear that *N. f. niethammeri* cannot be considered an independent species, contradicting previous studies where it was suggested that *N. f. niethammeri* might warrant species status (López-Fuster et al., 1990; Bühler, 1996; Wilson and Reeder, 2005; Burgin et al., 2018). An alternative suggestion is that *N. f. niethammeri* is an ecotype, although further work would be required to corroborate this point.

1.5. Ecological consequences of size increase in *N. fodiens*

The lack of genetic divergence and differentiation revealed here suggests that the large skull of *N. f. niethammeri* possibly arose as an adaptation to the environment. Two main hypotheses can be used to explain this. Firstly, a previous hypothesis proposed that more calcareous substrates present in the central part of the Cantabrian Range could have resulted in rivers richer in nutrients and a consequent selection of individuals with better-developed mandibles to capture larger prey (Nores et al., 1982; López-Fuster et al., 1990). However, *N. fodiens* lives in other areas with calcareous substrates where it displays no change in body size, so this is unlikely to have been the sole driver. Alternatively, the size increase of *N. f. niethammeri* could have resulted from ecological displacement due to competition with the Iberian endemic *N. anomalus*, similar to that observed in other mammals (Hulva et al., 2004; Biedma et al., 2018). An increase in the size of *N. f. niethammeri* could have favored access to new resources, for example larger prey, thus limiting competition with *N. anomalus*. In principle, both species occupy the same aquatic habitat in the northern Iberian Peninsula and most of the range of *N. f. niethammeri* overlaps with that of *N. anomalus* (Ventura, 2007a, 2007b), making competition between the two species possible. The interaction of *N. fodiens* with *N. milleri* has been studied in Europe, where both species live sympatrically (Rychlik and Zwolak, 2006). However, the interaction of *N. fodiens* with *N. anomalus* when they live sympatrically has never before been studied, and this may be totally different to that which occurs when it coincides with *N. milleri*, so we do not know if and how this interaction could have stimulated a size increase in *N. f. niethammeri*. We therefore suggest that future studies be directed at understanding the micro-habitat and inter-specific interactions of these *Neomys* species. We hope that a combined genetic and ecological approach will help unravel why *N. f. niethammeri* experienced an abrupt increase in skull size across a narrow strip in the Iberian Peninsula, and reveal the evolutionary advantages and possible ecological consequences of this phenotypic novelty.

2. Divergence time estimation of two populations of a small mammal (*Arvicola scherman*) from the Iberian Peninsula using ddRAD data and an isolation-with-migration model

To study the genetic divergence between different Iberian populations of a small mammal (*A. scherman*), we have applied an isolation-with-migration model, considering the central European population of *A. scherman* and its sister species *A. amphibius* as outgroups. The analyses, based on short sequences obtained from ddRAD data, showed that this type of sequences work well with the IMa3 program. However, it is essential to give to the program adequate mutation rates of the loci in order to obtain accurate divergence time estimates.

2.1. Estimating specific mutation rates of ddRAD loci

Estimating diversification times is crucial to analyze the evolutionary history of species and populations, but there are several difficulties to obtain accurate measurements that need to be addressed (Arbogast et al., 2002). Divergence occurring at shallow levels are specially problematic due to the effects of coalescent and incomplete lineage sorting (Edwards and Beerli, 2000; Degnan and Rosenberg, 2009; Sánchez-Gracia and Castresana, 2012). Furthermore, migration between populations must be taken into account in order to make realistic divergence times estimations (Wakeley, 2000; Nielsen and Wakeley, 2001; Hey and Nielsen, 2004). Among the most complete methods to estimate population split times are isolation-with-migration models, which take coalescent and migration into account and allow the introduction of mutation rates for all or part of the sequence markers used (Hey and Nielsen, 2004; Carling et al., 2010; Hey et al., 2018; Marko and Zaslavskaya, 2019; Kapli et al., 2020). However, these methods have not been used so far with the sequences obtained by ddRAD and it was not clear whether, being so short, they could be used to estimate robust divergence times between recently diverged populations.

The estimation of mutation rates needed in IM models are not without problems. Extrapolating mutation rates from other species can bias divergence time estimates as it is well known that there are important variation in diversification rates in different lineages (Li et al., 1987; Welch et al., 2008). There are also important variations of mutations rates along the genome (Wolfe and Sharp, 1993; Koop, 1995; Castresana, 2002), making it necessary the estimation of rates of each locus. For this purpose, we developed a

bioinformatic pipeline to obtain orthologous sequences of mammals from public databases, something that was achieved for 85 loci. We then used the split time between mouse and rat to calibrate the tree. The average mean mutation rate obtained for rodents across all loci (2.6×10^{-9} mutations/site/yr) was similar to the average rate found in mammals (2.2×10^{-9} mutations/site/yr) (Kumar and Subramanian, 2002) but lower than the rate found in the genome of mouse using trios (5.3×10^{-9} mutations/site/yr, considering a generation time of 1 year) (Uchimura et al., 2015; Milholland et al., 2017). Among other possibilities to explain this difference is that the mouse lineage has a more accelerated rate than other rodents (Marshall et al., 1994). Additionally, it is likely that ddRAD data does not incorporate the most divergent regions of the genome and thus it is reasonable that ddRAD loci have on average smaller rates than the whole genome.

2.2. Suitability of ddRAD loci for IMa3 analysis and demographic estimates

IMa3 software uses specific rates of each locus and calculates mutation rates scalars to estimate divergence times and other demographic parameters. Mutation rate scalars can be used to compare the rates of all loci, and not only the 85 initially calibrated here with rodent orthologues. Loci with calibrated mutation rates showed slightly lower rates, as expected, as it is likely that, for the most accelerated loci, it is difficult to find its orthologues. Yet, the distributions of mutation rates of calibrated and non-calibrated loci are mostly overlapping, showing that there are no fundamental differences between them (Figure 25). Even so, the use of further loci apart from the 85 calibrated ones is justified in order to have a higher representation of the genome and add the slightly higher proportion of informative positions that they may have due to their higher mutation rates.

The length of the markers used was 145 base pairs, which is small compared to other loci generally used with isolation-with-migration models (Carling et al., 2010; Marko and Zaslavskaya, 2019). This means that a small number of loci may not converge properly, as we observed in initial runs. After increasing this number in successive runs, we could demonstrate that a set of 300 ddRAD loci resulted in good mixing and convergence in IMa3 runs and adequate distributions of most of the demographic parameters of the model (Figures 23 and 24) in a reasonable time (240 hours with 14 processors). Increasing the number of loci slows down the speed of the analysis, making it impractical.

To understand if the outgroups were necessary for the estimation of the split time between the two Iberian populations, we run independent analyses with only these two populations, without the outgroups. The runs showed higher divergence times although the presence of the ghost population made the result more similar to the run with 4 populations, showing that the model with a ghost population may help to produce more realistic results when no outgroup is available.

2.3. Phylogeographic history of populations in the Iberian Peninsula and future applications

The Iberian Peninsula was an important refuge for several species and has received much attention in phylogeographic studies (Hewitt, 1999; Schmitt, 2007). Due to the existence of different mountain ranges, the Iberian Peninsula did not constitute a unique homogeneous refuge (Gómez and Lunt, 2007). Rather, important levels of population structure were generated in different isolated refugia within this peninsula.

The isolation-with-migration analysis indicated that the two populations of *A. scherman* diverged 39 Kyr ago (Figure 24 and Table 1) with a 95% highest posterior density interval of the split time of 21 – 62 Kyr. Significant gene flow was found from the Cantabrian to the Pyrenean population but values of $2Nm << 1$ indicated that no homogenization is expected between them. These data would be consistent with the hypothesis of a divergence associated to the last glaciation (Hewitt, 2000) and, more specifically, close to the Last Glacial Maximum (LGM), which started ~33,000 years ago and arrived to its maximum coverage ~20,000 years ago (Clark et al., 2009). Based on the split time and the genetic structure found, we can conclude that these two populations have been present in the Iberian Peninsula at least since the LGM. If they had been the product of a recent colonization, they would be genetically more similar. Rather, the divergence of these populations is likely to have been associated to the last glaciation and it may have taken place in separate refugia. Thus, the coalescence-based split time obtained gives strong support to the refugia within refugia hypothesis (Gómez and Lunt, 2007) for *A. scherman*.

This work shows a novel approach for obtaining split time estimates using ddRAD data of recently diverged populations and an isolation-with-migration model, which could be extrapolated to other mammals or different vertebrate taxa. To do this, orthologous sequences and at least one calibration point to calculate mutation rates is necessary. The

application of this approach to other taxa may allow obtaining comparable divergence time results among different populations of various species, which would represent an important advance in comparative phylogeography. In addition, obtaining accurate divergence times using these methods can help to achieve a deeper understanding of the circumstances that have led to current population structure at fine scale and whether they were related to the glacial periods or to more recent events. Finally, knowing the divergence times between populations can lead to a better appreciation of intraspecific diversity and to reveal the existence of different evolutionary units and taxonomic entities.

VII. CONCLUSIONS

1. Skull bones from small mammals found in barn owl pellets have been successfully used in simultaneous morphometric and genetic studies. Specifically, genomic information from skull bones has been obtained through next-generation sequencing (NGS) techniques.

2. Genetic structure and diversity of two Eurosiberian species of small mammals with populations in the northern area of the Iberian Peninsula have been studied and clarified in some aspects. Population genetic analyses have shown high levels of intraspecific diversity in the Iberian Peninsula, rejecting the idea of a recent colonization from the European range of the populations analyzed.

3. Morphological measurements using the coronoid height of the *Neomys fodiens* mandibles allowed the assignment of samples to the *N. f. niethammeri* population. The centroid size of the mandibles provided similar results. However, a morphometric analysis revealed no differences between the two populations of *N. fodiens* of the north of the Iberian Peninsula, indicating shape similarity between them.

4. The development of six short and variable intron markers allowed the amplification of degraded DNA present in skull bones. Introns optimized in this study represent a powerful tool to carry out multilocus analyses of genetic divergence and differentiation using minimally invasive samples.

5. The subspecies *N. f. niethammeri*, of larger size, was suggested to be an independent species in references of mammalian taxonomy, but here it was found that it was not genetically different from the nominal subspecies in terms of divergence and allele frequencies. According to the genetic results of this study, *N. f. niethammeri* is not a different species, and it may rather be an ecotype with an interesting ecological adaptation that could have appeared as a result of a novel interaction with its sister species *N. anomalus*.

6. The ddRAD technique was successfully applied to samples of *Arvicola sp.*, including skull bones from barn owl pellets.

7. Orthologues of *Arvicola sp.* ddRAD loci were determined in other rodents using a bioinformatic pipeline and the EPO-ENSEMBL database. The sequential filters applied ensured that only optimal alignments were retrieved.

8. Using a Bayesian phylogenetic framework with a clock model and a fossil calibration point (mouse-rat split), the mutation rates were estimated for 85 ddRAD loci. These rates were in line with the expected ones for a mammalian genome and, accordingly, varied by more than one order of magnitude.

9. A population genetic analyses that included a genomic tree reconstructed with the ddRAD loci as well as principal component and structure analyses using thousands of SNPs confirmed the presence of two genetically different populations of *A. scherman* in the Iberian Peninsula, in agreement with previously described morphological differences.

10. Isolation-with-migration (IM) analysis, which considers the coalescent and gene flow between populations, estimated reliable divergence times using 300 ddRAD loci, including the 85 loci with estimated mutation rates. The runs performed with the IMa3 software resulted in good mixing and convergence in a reasonable computational time.

11. The IMa3 analysis indicated that the two *A. scherman* Iberian populations diverged 39 thousand years (Kyr) ago with a 95% highest posterior density interval of 21 – 62 Kyr. A small amount of migration was detected between both populations.

12. Based on the split time and the genetic structure found, these two populations of *A. scherman* have been present in the Iberian Peninsula at least since the Last Glacial Maximum (LGM) and are not the product of a recent colonization. More specifically, the split time estimated would be consistent with the hypothesis of a divergence associated to the last glaciation.

VIII. REFERENCES

Aars, J., Dallas, J.F., Piertney, S.B., Marshall, F., Gow, J.L., Telfer, S., Lambin, X., 2006. Widespread gene flow and high genetic variability in populations of water voles *Arvicola terrestris* in patchy habitats. *Molecular Ecology* 15, 1455–1466.

Aghová, T., Kimura, Y., Bryja, J., Dobigny, G., Granjon, L., Kergoat, G.J., 2018. Fossils know it best: Using a new set of fossil calibrations to improve the temporal phylogenetic framework of murid rodents (Rodentia: Muridae). *Molecular Phylogenetics and Evolution* 128, 98–111.

Ahlering, M.A., Hedges, S., Johnson, A., Tyson, M., Schuttler, S.G., Eggert, L.S., 2010. Genetic diversity, social structure, and conservation value of the elephants of the Nakai Plateau, Lao PDR, based on non-invasive sampling. *Conservation Genetics* 12, 413–422.

Ali, O.A., O'Rourke, S.M., Amish, S.J., Meek, M.H., Luikart, G., Jeffres, C., Miller, M.R., 2016. Rad capture (Rapture): Flexible and efficient sequence-based genotyping. *Genetics* 202, 389–400.

Altschul, S.F., Madden, T.L., Schäfer, A.A., Zhang, J., Zhang, Z., Miller, W., Lipman, D.J., 1997. Gapped BLAST and PSI-BLAST: A new generation of protein database search programs. *Nucleic Acids Research* 25, 3389–3402.

Amori, G., Hutterer, R., Kryštufek, B., Yigit, N., Mitsain, G., Muñoz, L.J.P., 2008. *Arvicola scherman*. *The IUCN Red List of Threatened Species* e.T136766A4337072.

Amorim, F., Razgour, O., Mata, V.A., Lopes, S., Godinho, R., Ibáñez, C., Juste, J., Rossiter, S.J., Beja, P., Rebelo, H., 2020. Evolutionary history of the European free-tailed bat, a tropical affinity species spanning across the Mediterranean Basin. *Journal of Zoological Systematics and Evolutionary Research* 58, 499–518.

Amos, W., Balmford, A., 2001. When does conservation genetics matter? *Heredity* 87, 257–265.

Andolfatto, P., 2005. Adaptive evolution of non-coding DNA in *Drosophila*. *Nature* 437, 1149–1152.

Andrews, K.R., Good, J.M., Miller, M.R., Luikart, G., Hohenlohe, P.A., 2016. Harnessing the power of RADseq for ecological and evolutionary genomics. *Nature Reviews Genetics* 17, 81–92.

Arbogast, B.S., Edwards, S. V., Wakeley, J., Beerli, P., Slowinski, J.B., 2002. Estimating divergence times from molecular data on phylogenetic and population genetic timescales. *Annual Review of Ecology and Systematics* 33, 707–740.

Avise, J.C., 2004. Molecular markers, natural history and evolution, 2nd ed. Sinauer Associates, Inc., Sunderland, MA.

Avise, J.C., Walker, D., Johns, G.C., 1998. Speciation durations and Pleistocene effects on vertebrate phylogeography. *Proceedings of the Royal Society B: Biological*

Sciences 265, 1707–1712.

Baele, G., Lemey, P., Bedford, T., Rambaut, A., Suchard, M.A., Alekseyenko, A. V., 2012. Improving the accuracy of demographic and molecular clock model comparison while accommodating phylogenetic uncertainty. *Molecular Biology and Evolution* 29, 2157–2167.

Baird, N.A., Etter, P.D., Atwood, T.S., Currey, M.C., Shiver, A.L., Lewis, Z.A., Selker, E.U., Cresko, W.A., Johnson, E.A., 2008. Rapid SNP discovery and genetic mapping using sequenced RAD markers. *PLoS ONE* 3, e3376.

Barbosa, S., Pauperio, J., Searle, J.B., Alves, P.C., 2013. Genetic identification of Iberian rodent species using both mitochondrial and nuclear loci: Application to noninvasive sampling. *Molecular Ecology Resources* 13, 43–56.

Barker, R.J., Scott, D.M., King, P.J., Overall, A.D., 2020. Genetic structure of regional water vole populations and footprints of reintroductions: A case study from southeast England. *Conservation Genetics* 21, 531–546.

Batsaikhan, N., Henttonen, H., Meinig, H., Shenbrot, G., Bukhnikashvili, A., Hutterer, R., Kryštufek, B., Yigit, N., Mitsain, G., Palomo, L., 2016. *Arvicola amphibius*. *The IUCN Red List of Threatened Species* e.T2149A115060819.

Beaumont, M.A., 2010. Approximate Bayesian computation in evolution and ecology. *Annual Review of Ecology, Evolution, and Systematics* 41, 379–406.

Beaumont, M.A., Zhang, W., Balding, D.J., 2002. Approximate Bayesian computation in population genetics. *Genetics* 162, 2025–2035.

Beerli, P., 2004. Effect of unsampled populations on the estimation of population sizes and migration rates between sampled populations. *Molecular Ecology* 13, 827–836.

Beja-Pereira, A., Oliveira, R., Alves, P.C., Schwartz, M.K., Luikart, G., 2009. Advancing ecological understandings through technological transformations in noninvasive genetics. *Molecular Ecology Resources* 9, 1279–1301.

Bejerano, G., Pheasant, M., Makunin, I., Stephen, S., Kent, W.J., Mattick, J.S., Haussler, D., 2004. Ultraconserved elements in the human genome. *Science* 304, 1321–1325.

Benton, M., Donoghue, P.C.J., Asher, R.J., 2009. Calibrating and constraining molecular clocks, in: Hedges, S.B., Kumar, S. (Eds.), *The Timetree of Life*. Oxford University Press, Oxford, UK, pp. 35–86.

Bermingham, E., Moritz, C., 1998. Comparative phylogeography: Concepts and applications. *Molecular Ecology* 7, 367–369.

Bertorelle, G., Benazzo, A., Mona, S., 2010. ABC as a flexible framework to estimate demography over space and time: Some cons, many pros. *Molecular Ecology* 19, 2609–2625.

Biedma, L., Román, J., Calzada, J., Friis, G., Godoy, J.A., 2018. Phylogeography of *Crocidura suaveolens* (Mammalia: Soricidae) in Iberia has been shaped by competitive exclusion by *C. russula*. *Biological Journal of the Linnean Society* 123, 81–95.

Biffi, M., Gillet, F., Laffaille, P., Colas, F., Aulagnier, S., Blanc, F., Galan, M., Tiouchichine, M.-L.L., Némoz, M., Buisson, L., Michaux, J.R., 2017a. Novel insights into the diet of the Pyrenean desman (*Galemys pyrenaicus*) using next-generation sequencing molecular analyses. *Journal of Mammalogy* 98, 1497–1507.

Biffi, M., Laffaille, P., Jabiol, J., André, A., Gillet, F., Lamothe, S., Michaux, J.R., Buisson, L., 2017b. Comparison of diet and prey selectivity of the Pyrenean desman and the Eurasian water shrew using next-generation sequencing methods. *Mammalian Biology* 87, 176–184.

Bilton, D.T., Mirol, P.M., Mascheretti, S., Fredga, K., Zima, J., Searle, J.B., 1998. Mediterranean Europe as an area of endemism for small mammals rather than a source for northwards postglacial colonization. *Proc. R. Soc. Lond. B.* 265, 1219–1226.

Blanco, J.C., 1998. Mamíferos de España. Vol 1. Insectívoros, Quirópteros, Primates y Carnívoros de la Península Ibérica, Baleares y Canarias. GeoPlaneta.

Bohmann, K., Evans, A., Gilbert, M.T.P., Carvalho, G.R., Creer, S., Knapp, M., Yu, D.W., de Bruyn, M., 2014. Environmental DNA for wildlife biology and biodiversity monitoring. *Trends in Ecology and Evolution* 29, 358–367.

Bos, D.H., Posada, D., 2005. Using models of nucleotide evolution to build phylogenetic trees. *Developmental and Comparative Immunology* 29, 211–227.

Bouckaert, R., Heled, J., Kühnert, D., Vaughan, T., Wu, C.H., Xie, D., Suchard, M.A., Rambaut, A., Drummond, A.J., 2014. BEAST 2: A software platform for Bayesian evolutionary analysis. *PLoS Computational Biology* 10, e1003537.

Bouckaert, R., Vaughan, T.G., Barido-Sottani, J., Duchêne, S., Fourment, M., Gavryushkina, A., Heled, J., Jones, G., Kühnert, D., De Maio, N., Matschiner, M., Mendes, F.K., Müller, N.F., Ogilvie, H.A., Du Plessis, L., Popinga, A., Rambaut, A., Rasmussen, D., Siveroni, I., Suchard, M.A., Wu, C.H., Xie, D., Zhang, C., Stadler, T., Drummond, A.J., 2019. BEAST 2.5: An advanced software platform for Bayesian evolutionary analysis. *PLoS Computational Biology* 15, e1006650.

Brace, S., Ruddy, M., Miller, R., Schreve, D.C., Stewart, J.R., Barnes, I., 2016. The colonization history of British water vole (*Arvicola amphibius* (Linnaeus, 1758)): Origins and development of the Celtic fringe. *Proceedings of the Royal Society B: Biological Sciences* 283, 20160130.

Bradley, B.J., Vigilant, L., 2002. False alleles derived from microbial DNA pose a potential source of error in microsatellite genotyping of DNA from faeces. *Molecular Ecology Notes* 2, 602–605.

Bremmer-Harrison, S., Harrison, S.W.R., Cypher, B.L., Murdoch, J.D., Maldonado, J., Darden, S.K., 2006. Development of a Single-Sampling Noninvasive Hair Snare. *Wildlife Society Bulletin* 34, 456–461.

Broquet, T., Ménard, N., Petit, E., 2007. Noninvasive population genetics: A review of sample source, diet, fragment length and microsatellite motif effects on amplification success and genotyping error rates. *Conservation Genetics* 8, 249–260.

Brown, R.P., Yang, Z., 2011. Rate variation and estimation of divergence times using strict and relaxed clocks. *BMC Evolutionary Biology* 11, 271.

Brown, W.M., George, M., Wilson, A.C., 1979. Rapid evolution of animal mitochondrial DNA. *Proceedings of the National Academy of Sciences* 76, 1967–1971.

Brumfield, R.T., Beerli, P., Nickerson, D.A., Edwards, S. V., 2003. The utility of single nucleotide polymorphisms in inferences of population history. *Trends in Ecology and Evolution* 18, 249–256.

Bryant, D., Bouckaert, R., Felsenstein, J., Rosenberg, N.A., RoyChoudhury, A., 2012. Inferring species trees directly from biallelic genetic markers: Bypassing gene trees in a full coalescent analysis. *Molecular Biology and Evolution* 29, 1917–1932.

Bühler, P., 1996. Zum taxonomischen Status der Großkopf-Wasserspitzmaus (*Neomys fodiens niethammeri* Bühler, 1963), aus Spanien nebst Festlegung und Beschreibung eines Neotypus. *Bonn. zool. Beitr.* 46, 307–314.

Bühler, P., 1963. *Neomys fodiens niethammeri* ssp. n., eine neue Wasserspitzmausform aus Nord-Spanien. *Bonner zoologische Beiträge* 14, 165–170.

Burgin, C., He, K., Haslauer, R., Sheftel, B., Jenkins, P., Ruedi, M., Hintsche, S., Motokawa, M., Hinckley, A., Hutterer, R., 2018. Species accounts of Soricidae, in: Mittermeier, R.A., Wilson, D.E. (Eds.), *Handbook of the Mammals of the World. Volume 8. Insectivores, Sloths and Colugos*. Lynx Edicions.

Buś, M.M., Żmihorski, M., Romanowski, J., Balčiauskienė, L., Cichocki, J., Balčiauskas, L., 2014. High efficiency protocol of DNA extraction from *Micromys minutus* mandibles from owl pellets: A tool for molecular research of cryptic mammal species. *Acta Theriologica* 59, 99–109.

Carling, M.D., Lovette, I.J., Brumfield, R.T., 2010. Historical divergence and gene flow: Coalescent analyses of mitochondrial, autosomal and sex-linked loci in *Passerina* buntings. *Evolution* 64, 1762–1772.

Carroll, E.L., Bruford, M.W., Dewoody, J.A., Leroy, G., Strand, A., Waits, L., Wang, J., 2018. Genetic and genomic monitoring with minimally invasive sampling methods. *Evolutionary Applications* 11, 1094–1119.

Castién, E., Gosálbez, J., 1999. Habitat and food preferences in a guild of insectivorous mammals in the Western Pyrenees. *Acta Theriologica* 44, 1–13.

Castiglia, R., Aloise, G., Amori, G., Annesi, F., Bertolino, S., Capizzi, D., Mori, E., Colangelo, P., 2016. The Italian peninsula hosts a divergent mtDNA lineage of the water vole, *Arvicola amphibius* s.l., including fossorial and aquatic ecotypes. *Hystrix* 27, 99–103.

Castiglia, R., Annesi, F., Aloise, G., Amori, G., 2007. Mitochondrial DNA reveals different phylogeographic structures in the water shrews *Neomys anomalus* and *N. fodiens* (Insectivora: Soricidae) in Europe. *Journal of Zoological Systematics and Evolutionary Research* 45, 255–262.

Castresana, J., 2002. Estimation of genetic distances from human and mouse introns. *Genome biology* 3, research0028.1–0028.7.

Castresana, J., 2000. Selection of conserved blocks from multiple alignments for their use in phylogenetic analysis. *Molecular Biology and Evolution* 17, 540–552.

Catchen, J., Hohenlohe, P.L., Bassham, S., Amores, A., Cresko, W.A., 2013. Stacks: An analysis tool set for population genomics. *Molecular Ecology* 22, 3124–31240.

Centeno-Cuadros, A., Delibes, M., Godoy, J.A., 2009. Dating the divergence between Southern and European water voles using molecular coalescent-based methods. *Journal of Zoology* 279, 404–409.

Chiou, K.L., Bergey, C.M., 2018. Methylation-based enrichment facilitates low-cost, noninvasive genomic scale sequencing of populations from feces. *Scientific Reports* 8, 1975.

Chung, Y., Hey, J., 2017. Bayesian analysis of evolutionary divergence with genomic data under diverse demographic models. *Molecular Biology and Evolution* 34, 1517–1528.

Churchfield, S., 1998. Habitat use by water shrews, the smallest of amphibious mammals, in: Dunstone, N., Gorman, M.L. (Eds.), *Behaviour and Ecology of Riparian Mammals*. Cambridge University Press, Cambridge, UK, pp. 46–68.

Churchfield, S., Rychlik, L., 2006. Diets and coexistence in *Neomys* and *Sorex* shrews in Białowieża forest, eastern Poland. *Journal of Zoology* 269, 381–390.

Clark, K., Karsch-Mizrachi, I., Lipman, D.J., Ostell, J., Sayers, E.W., 2016. GenBank. *Nucleic acids research* 44, D67–D72.

Clark, P.U., Dyke, A.S., Shakun, J.D., Carlson, A.E., Clark, J., Wohlfarth, B., Mitrovica, J.X., Hostetler, S.W., McCabe, A.M., 2009. The Last Glacial Maximum. *Science* 325, 710–714.

Creer, S., Malhotra, A., Thorpe, R.S., Pook, C.E., 2005. Targeting optimal introns for phylogenetic analyses in non-model taxa: Experimental results in Asian pitvipers. *Cladistics* 21, 390–395.

Croose, E., Birks, J.D.S., O'Reilly, C., Turner, P., Martin, J., MacLeod, E.T., 2016. Sample diversity adds value to non-invasive genetic assessment of a pine marten (*Martes martes*) population in Galloway Forest, southwest Scotland. *Mammal Research* 61, 131–139.

Csilléry, K., Blum, M.G.B., Gaggiotti, O.E., François, O., 2010. Approximate Bayesian Computation (ABC) in practice. *Trends in Ecology and Evolution* 25, 410–418.

Cubo, J., Ventura, J., Casinos, A., 2006. A heterochronic interpretation of the origin of digging adaptations in the northern water vole, *Arvicola terrestris* (Rodentia: Arvicolidae). *Biological Journal of the Linnean Society* 87, 381–391.

Cuenca-Bescós, G., Straus, L.G., González Morales, M.R., García Pimienta, J.C., 2008. Paleoclima y paisaje del final del Cuaternario en Cantabria: Los pequeños mamíferos de la cueva del Mirón (Ramales de la Victoria). *Revista Española de Paleontología* 23, 91–126.

Dabney, J., Knapp, M., Glocke, I., Gansauge, M.-T., Weihmann, A., Nickel, B.,

Valdiosera, C., García, N., Pääbo, S., Arsuaga, J.L., Meyer, M., 2013. Complete mitochondrial genome sequence of a Middle Pleistocene cave bear reconstructed from ultrashort DNA fragments. *Proceedings of the National Academy of Sciences* 110, 15758–15763.

Dallas, J.F., 1992. Estimation of microsatellite mutation rates in recombinant inbred strains of mouse. *Mammalian Genome* 3, 452–456.

David, K.T., Wilson, A.E., Halanych, K.M., 2019. Sequencing disparity in the genomic era. *Molecular Biology and Evolution* 36, 1624–1627.

Deagle, B.E., Kirkwood, R., Jarman, S.N., 2009. Analysis of Australian fur seal diet by pyrosequencing prey DNA in faeces. *Molecular Ecology* 18, 2022–2038.

Debrauwere, H., Gendrel, C.G., Lechat, S., Dutreix, M., 1997. Differences and similarities between various tandem repeat sequences: Minisatellites and microsatellites. *Biochimie* 79, 577–586.

Degnan, J.H., Rosenberg, N.A., 2009. Gene tree discordance, phylogenetic inference and the multispecies coalescent. *Trends in Ecology and Evolution* 24, 332–340.

Dodson, P., Wexlar, D., 1979. Taphonomic investigations of owl pellets. *Paleobiology* 5, 275–284.

Drummond, A.J., Ho, S.Y.W., Phillips, M.J., Rambaut, A., 2006. Relaxed phylogenetics and dating with confidence. *PLoS Biology* 4, 699–710.

Drummond, A.J., Rambaut, A., 2007. BEAST: Bayesian evolutionary analysis by sampling trees. *BMC Evolutionary Biology* 7, 214.

Dunn, C.W., Ryan, J.F., 2015. The evolution of animal genomes. *Current Opinion in Genetics and Development* 35, 25–32.

Durão, A.F., Ventura, J., Muñoz-Muñoz, F., 2019. Comparative post-weaning ontogeny of the mandible in fossorial and semi-aquatic water voles. *Mammalian Biology* 97, 95–103.

Edwards, S., Beerli, P., 2000. Perspective: Gene divergence, population divergence, and the variance in coalescence time in phylogeographic studies. *Evolution* 54, 1839–1854.

Edwards, S. V., 2009. Is a new and general theory of molecular systematics emerging? *Evolution* 63, 1–19.

Egeter, B., Roe, C., Peixoto, S., Puppo, P., Easton, L.J., Pinto, J., Bishop, P.J., Robertson, B.C., 2019. Using molecular diet analysis to inform invasive species management: A case study of introduced rats consuming endemic New Zealand frogs. *Ecology and Evolution* 9, 5032–5048.

Eggert, L.S., Maldonado, J.E., Fleischer, R.C., 2005. Nucleic acid isolation from ecological samples - Animal scat and other associated materials. *Methods in Enzymology* 395, 73–82.

Elshire, R.J., Glaubitz, J.C., Sun, Q., Poland, J.A., Kawamoto, K., Buckler, E.S.,

Mitchell, S.E., 2011. A robust, simple genotyping-by-sequencing (GBS) approach for high diversity species. *PLoS ONE* 6, e19379.

Escoda, L., Fernández-González, Á., Castresana, J., 2019. Quantitative analysis of connectivity in populations of a semi-aquatic mammal using kinship categories and network assortativity. *Molecular Ecology Resources* 19, 310–326.

Esnaola, A., Arrizabalaga-Escudero, A., González-Esteban, J., Elosegi, A., Aihartza, J., 2018. Determining diet from faeces: selection of metabarcoding primers for the insectivore Pyrenean desman (*Galemys pyrenaicus*). *PLoS ONE* 13, e0208986.

Ewens, W.J., 1990. Population genetics theory - The past and the future, in: Lessard, S. (Ed.), *Mathematical and Statistical Developments of Evolutionary Theory*. Kluwer Academic Publishers, Dordrecht, The Netherlands, pp. 177–227.

Excoffier, L., Dupanloup, I., Huerta-Sánchez, E., Sousa, V.C., Foll, M., 2013. Robust demographic inference from genomic and SNP data. *PLoS Genetics* 9, e1003905.

Excoffier, L., Estoup, A., Cornuet, J.M., 2005. Bayesian analysis of an admixture model with mutations and arbitrarily linked markers. *Genetics* 169, 1727–1738.

Fabre, P.-H., Hautier, L., Dimitrov, D., Douzery, E.J.P., 2012. A glimpse on the pattern of rodent diversification: A phylogenetic approach. *BMC Evolutionary Biology* 12, 88.

Felsenstein, J., 1989. PHYLIP-phylogeny inference package (version 3.4). *Cladistics* 5, 164–166.

Felsenstein, J., 1981. Evolutionary trees from DNA sequences: A maximum likelihood approach. *Journal of Molecular Evolution* 17, 368–376.

Ficetola, G.F., Miaud, C., Pompanon, F., Taberlet, P., 2008. Species detection using environmental DNA from water samples. *Biology Letters* 4, 423–425.

Figueiró, H. V., Li, G., Trindade, F.J., Assis, J., Pais, F., Fernandes, G., Santos, S.H.D., Hughes, G.M., Komissarov, A., Antunes, A., Trinca, C.S., Rodrigues, M.R., Linderoth, T., Bi, K., Silveira, L., Azevedo, F.C.C., Kantek, D., Ramalho, E., Brassaloti, R.A., Villela, P.M.S., Nunes, A.L.V., Teixeira, R.H.F., Morato, R.G., Loska, D., Saragüeta, P., Gabaldón, T., Teeling, E.C., O'Brien, S.J., Nielsen, R., Coutinho, L.L., Oliveira, G., Murphy, W.J., Eizirik, E., 2017. Genome-wide signatures of complex introgression and adaptive evolution in the big cats. *Science Advances* 3, e1700299.

Filipi, K., Marková, S., Searle, J.B., Kotlík, P., 2015. Mitogenomic phylogenetics of the bank vole *Clethrionomys glareolus*, a model system for studying end-glacial colonization of Europe. *Molecular Phylogenetics and Evolution* 82, 245–257.

Flanagan, S.P., Jones, A.G., 2019. The future of parentage analysis: From microsatellites to SNPs and beyond. *Molecular Ecology* 28, 544–567.

Flouri, T., Jiao, X., Rannala, B., Yang, Z., 2020. A bayesian implementation of the multispecies coalescent model with introgression for phylogenomic analysis. *Molecular Biology and Evolution* 37, 1211–1223.

Frankham, R., Ballou, J.D., Briscoe, D.A., 2010. Introduction to conservation genetics, 2nd ed. Cambridge University Press, Cambridge, UK.

Freedman, A.H., Gronau, I., Schweizer, R.M., Ortega-Del Vecchyo, D., Han, E., Silva, P.M., Galaverni, M., Fan, Z., Marx, P., Lorente-Galdos, B., Beale, H., Ramirez, O., Hormozdiari, F., Alkan, C., Vilà, C., Squire, K., Geffen, E., Kusak, J., Boyko, A.R., Parker, H.G., Lee, C., Tadigotla, V., Siepel, A., Bustamante, C.D., Harkins, T.T., Nelson, S.F., Ostrander, E.A., Marques-Bonet, T., Wayne, R.K., Novembre, J., 2014. Genome sequencing highlights the dynamic early history of dogs. *PLoS Genetics* 10, e1004016.

Freeland, J.R., Kirk, H., Petersen, S.D., 2011. Molecular Ecology, 2nd ed. John Wiley & Sons, Ltd, Chichester, UK.

Fujita, M.K., Leaché, A.D., Burbrink, F.T., McGuire, J.A., Moritz, C., 2012. Coalescent-based species delimitation in an integrative taxonomy. *Trends in Ecology and Evolution* 27, 480–488.

Gillet, F., Tiouchichine, M.L., Galan, M., Blanc, F., Némoz, M., Aulagnier, S., Michaux, J.R., 2015. A new method to identify the endangered Pyrenean desman (*Galemys pyrenaicus*) and to study its diet, using next generation sequencing from faeces. *Mammalian Biology* 80, 505–509.

Gómez, A., Lunt, D.H., 2007. Refugia within refugia: patterns of phylogeographic concordance in the Iberian Peninsula, in: Weiss, S., Ferrand, N. (Eds.), *Phylogeography of Southern European Refugia*. Springer, Dordrecht, The Netherlands, pp. 155–188.

Goodwin, S., McPherson, J.D., McCombie, W.R., 2016. Coming of age: Ten years of next-generation sequencing technologies. *Nature Reviews Genetics* 17, 333–351.

Goossens, B., Bruford, M.W., 2009. Non-invasive genetic analysis in conservation, in: Bertorelle, G., Bruford, M.W., Hauffe, H.C., Rizzoli, A., Vernesi, C. (Eds.), *Population Genetics for Animal Conservation*. Cambridge University Press, Cambridge, UK, pp. 167–201.

Goudet, J., 2005. HIERFSTAT, a package for R to compute and test hierarchical F-statistics. *Molecular Ecology Notes* 5, 184–186.

Graur, D., Li, W.-H., 2000. Fundamentals of Molecular Evolution, 2nd ed. Sinauer Associates, Inc., Sunderland, MA.

Green, R.E., Krause, J., Ptak, S.E., Briggs, A.W., Ronan, M.T., Simons, J.F., Du, L., Egholm, M., Rothberg, J.M., Paunovic, M., Pääbo, S., 2006. Analysis of one million base pairs of Neanderthal DNA. *Nature* 444, 330–336.

Grimm, R.J., Whitehouse, W.M., 1963. Pellet formation in a Great Horned Owl: A roentgenographic study. *The Auk* 80, 301–306.

Guimaraes, S., Fernandez-Jalvo, Y., Stoetzel, E., Gorgé, O., Bennett, E.A., Denys, C., Grange, T., Geigl, E.M., 2016. Owl pellets: A wise DNA source for small mammal genetics. *Journal of Zoology* 298, 64–74.

Guindon, S., Gascuel, O., 2003. A simple, fast, and accurate algorithm to estimate large

phylogenies by maximum likelihood. *Systematic Biology* 52, 696–704.

Hailer, F., Kutschera, V.E., Hallström, B.M., Klassert, D., Fain, S.R., Leonard, J.A., Arnason, U., Janke, A., 2012. Nuclear genomic sequences reveal that polar bears are an old and distinct bear lineage. *Science* 336, 344–347.

Hansen, M.M., Jacobsen, L., 1999. Identification of mustelid species: Otter (*Lutra lutra*), American mink (*Mustela vison*) and polecat (*Mustela putorius*), by analysis of DNA from faecal samples. *Journal of Zoology* 247, 177–181.

Hare, M.P., 2001. Prospects for nuclear gene phylogeography. *Trends in Ecology and Evolution* 16, 700–706.

Hasegawa, M., Kishino, H., Yano, T. aki, 1985. Dating of the human-ape splitting by a molecular clock of mitochondrial DNA. *Journal of Molecular Evolution* 22, 160–174.

Hastings, W.K., 1970. Monte Carlo sampling methods using Markov chains and their applications. *Biometrika* 57, 97–109.

Hawlitschek, O., Fernández-González, A., Balmori-de la Puente, A., Castresana, J., 2018. A pipeline for metabarcoding and diet analysis from fecal samples developed for a small semi-aquatic mammal. *PLoS ONE* 13, e0201763.

Heled, J., Drummond, A.J., 2010. Bayesian inference of species trees from multilocus data. *Molecular Biology and Evolution* 27, 570–580.

Hewitt, G., 2000. The genetic legacy of the Quaternary ice ages. *Nature* 405, 907–913.

Hewitt, G.M., 1999. Post-glacial re-colonization of European biota. *Biological Journal of the Linnean Society* 68, 87–112.

Hey, J., 2010a. Isolation with migration models for more than two populations. *Molecular Biology and Evolution* 27, 905–920.

Hey, J., 2010b. The divergence of chimpanzee species and subspecies as revealed in multipopulation isolation-with-migration analyses. *Molecular Biology and Evolution* 27, 921–933.

Hey, J., Chung, Y., Sethuraman, A., Lachance, J., Tishkoff, S., Sousa, V.C., Wang, Y., 2018. Phylogeny estimation by integration over isolation with migration models. *Molecular Biology and Evolution* 35, 2805–2818.

Hey, J., Machado, C.A., 2003. The study of structured populations - New hope for a difficult and divided science. *Nature Reviews Genetics* 4, 535–543.

Hey, J., Nielsen, R., 2007. Integration within the Felsenstein equation for improved Markov chain Monte Carlo methods in population genetics. *Proceedings of the National Academy of Sciences* 104, 2785–2790.

Hey, J., Nielsen, R., 2004. Multilocus methods for estimating population sizes, migration rates and divergence time, with applications to the divergence of *Drosophila pseudoobscura* and *D. persimilis*. *Genetics* 167, 747–760.

Hey, J., Wang, K., 2019. The effect of undetected recombination on genealogy sampling and inference under an isolation-with-migration model. *Molecular Ecology Resources* 19, 1593–1609.

Horváth, M.B., Martínez-Cruz, B., Negro, J.J., Kalmár, L., Godoy, J.A., 2005. An overlooked DNA source for non-invasive genetic analysis in birds. *Journal of Avian Biology* 36, 84–88.

Höss, M., Kohn, M., Pääbo, S., Knauer, F., Schröder, W., 1992. Excrement analysis by PCR. *Nature* 359, 199.

Hudson, R.R., 1990. Gene genealogies and the coalescent process, in: Futuyma, D., Antonovics, J. (Eds.), *Oxford Surveys of Evolutionary Biology*. Oxford University Press, Oxford, UK, Vol. 7, pp. 1–44.

Huelsenbeck, J.P., Hillis, D.M., 1993. Success of phylogenetic methods in the four-taxon case. *Systematic Biology* 42, 247–264.

Huelsenbeck, J.P., Ronquist, F., 2001. MRBAYES: Bayesian inference of phylogenetic trees. *Bioinformatics* 17, 754–755.

Hulva, P., Horáček, I., Strelkov, P.P., Benda, P., 2004. Molecular architecture of *Pipistrellus pipistrellus*/*Pipistrellus pygmaeus* complex (Chiroptera: Vespertilionidae): Further cryptic species and Mediterranean origin of the divergence. *Molecular Phylogenetics and Evolution* 32, 1023–1035.

Hutchison, C.A., Newbold, J.E., Potter, S.S., Edgell, M.H., 1974. Maternal inheritance of mammalian mitochondrial DNA. *Nature* 251, 536–538.

Hutterer, R., 1985. Anatomical adaptations of shrews. *Mammal Review* 15, 43–55.

Hutterer, R., Meinig, H., Bertolino, S., Kryštufek, B., Sheftel, B., Stubbe, M., Samiya, R., Ariunbold, J., Buuveibaatar, V., Dorjderem, V., Monkhzul, T., Otgonbaatar, M., Tsogbadrakh, M., 2016. *Neomys fodiens*. *The IUCN Red List of Threatened Species* e.T29658A115170106.

Ibrahim, K.M., Nichols, R.A., Hewitt, G.M., 1996. Spatial patterns of genetic variation generated by different forms of dispersal during range expansion. *Heredity* 77, 282–291.

Igea, J., Aymerich, P., Bannikova, A. a., Gosálbez, J., Castresana, J., 2015. Multilocus species trees and species delimitation in a temporal context: Application to the water shrews of the genus *Neomys*. *BMC Evolutionary Biology* 15, 209.

Igea, J., Aymerich, P., Fernández-González, A., González-Esteban, J., Gómez, A., Alonso, R., Gosálbez, J., Castresana, J., 2013. Phylogeography and postglacial expansion of the endangered semi-aquatic mammal *Galemys pyrenaicus*. *BMC evolutionary biology* 13, 115.

Igea, J., Juste, J., Castresana, J., 2010. Novel intron markers to study the phylogeny of closely related mammalian species. *BMC evolutionary biology* 10, 369.

IUCN, 2020. The IUCN Red List of Threatened Species. Version 2020-1. *http://www.iucnredlist.org*.

Jackson, N.D., Carstens, B.C., Morales, A.E., O'Meara, B.C., 2017. Species delimitation with gene flow. *Systematic Biology* 66, 799–812.

Joly, S., McLenachan, P.A., Lockhart, P.J., 2009. A statistical approach for distinguishing hybridization and incomplete lineage sorting. *The American Naturalist* 174, E54–E70.

Jones, M.R., Good, J.M., 2016. Targeted capture in evolutionary and ecological genomics. *Molecular Ecology* 25, 185–202.

Jukes, T.H., Cantor, C.R., 1969. Evolution of protein molecules, in: *Mammalian Protein Metabolism*. Academic Press, New York, pp. 21–132.

Kapli, P., Yang, Z., Telford, M.J., 2020. Phylogenetic tree building in the genomic age. *Nature Reviews Genetics* 21, 428–440.

Katoh, K., Standley, D.M., 2013. MAFFT multiple sequence alignment software version 7: Improvements in performance and usability. *Molecular Biology and Evolution* 30, 772–780.

Kearns, A.M., Malloy, J.F., Gobbert, M.K., Thierry, A., Joseph, L., Driskell, A.C., Omland, K.E., 2019. Nuclear introns help unravel the diversification history of the Australo-Pacific *Petroica* robins. *Molecular Phylogenetics and Evolution* 131, 48–54.

Keckel, M.R., Ansorge, H., Stefen, C., 2014. Differences in the microhabitat preferences of *Neomys fodiens* (Pennant 1771) and *Neomys anomalus* Cabrera, 1907 in Saxony, Germany. *Acta Theriologica* 59, 485–494.

Kendall, K.C., McKelvey, K.S., 2008. Hair collection, in: Long, R.A., MacKay, P., Zielinski, W.J., Ray, J.C. (Eds.), *Noninvasive Survey Methods for Carnivores*. Island Press, Washington D.C., pp. 141–182.

Kidd, J.M., Sharpton, T.J., Bobo, D., Norman, P.J., Martin, A.R., Carpenter, M.L., Sikora, M., Gignoux, C.R., Nemat-Gorgani, N., Adams, A., Guadalupe, M., Guo, X., Feng, Q., Li, Y., Liu, X., Parham, P., Hoal, E.G., Feldman, M.W., Pollard, K.S., Wall, J.D., Bustamante, C.D., Henn, B.M., 2014. Exome capture from saliva produces high quality genomic and metagenomic data. *BMC Genomics* 15, 262.

Kimura, M., 1977. Preponderance of synonymous changes as evidence for the neutral theory of molecular evolution. *Nature* 267, 275–276.

Kimura, M., 1969. The number of heterozygous nucleotide sites maintained in a finite population due to steady flux of mutations. *Genetics* 61, 893–903.

Kimura, Y., Hawkins, M.T.R., McDonough, M.M., Jacobs, L.L., Flynn, L.J., 2015. Corrected placement of *Mus-Rattus* fossil calibration forces precision in the molecular tree of rodents. *Scientific Reports* 5, 14444.

Kingman, J.F.C., 1982. The coalescent. *Stochastic Processes and their Applications* 13, 235–248.

Klingenberg, C.P., 2011. MorphoJ: An integrated software package for geometric morphometrics. *Molecular Ecology Resources* 11, 353–357.

Knowles, L.L., 2004. The burgeoning field of statistical phylogeography. *Journal of Evolutionary Biology* 17, 1–10.

Kohn, M.H., Wayne, R.K., 1997. Facts from feces revisited. *Trends in Ecology and Evolution* 12, 223–227.

Koop, B.F., 1995. Human and rodent DNA sequence comparisons: A mosaic model of genomic evolution. *Trends in Genetics* 11, 367–371.

Kowalski, K., Marciniak, P., Rosiński, G., Rychlik, L., 2017. Evaluation of the physiological activity of venom from the Eurasian water shrew *Neomys fodiens*. *Frontiers in Zoology* 14, 46.

Kowalski, K., Rychlik, L., 2018. The role of venom in the hunting and hoarding of prey differing in body size by the Eurasian water shrew, *Neomys fodiens*. *Journal of Mammalogy* 99, 351–362.

Kryštufek, B., Koren, T., Engelberger, S., Horváth, G.F., Purger, J.J., Arslan, A., Chişamera, G., Murariu, D., 2015. Fossorial morphotype does not make a species in water voles. *Mammalia* 79, 293–303.

Kryštufek, B., Quadracci, A., 2008. Effects of latitude and allopatry on body size variation in European water shrews. *Acta Theriologica* 53, 39–46.

Kubasiewicz, L.M., Minderman, J., Woodall, L.C., Quine, C.P., Coope, R., Park, K.J., 2016. Fur and faeces: An experimental assessment of non-invasive DNA sampling for the European pine marten. *Mammal Research* 61, 299–307.

Kumar, S., Subramanian, S., 2002. Mutation rates in mammalian genomes. *Proceedings of the National Academy of Sciences* 99, 803–808.

LaCava, M.E.F., Aikens, E.O., Megna, L.C., Randolph, G., Hubbard, C., Buerkle, C.A., 2020. Accuracy of de novo assembly of DNA sequences from double-digest libraries varies substantially among software. *Molecular Ecology Resources* 20, 360–370.

Langmead, B., Salzberg, S.L., 2012. Fast gapped-read alignment with Bowtie 2. *Nature Methods* 9, 357–359.

Leaché, A.D., Fujita, M.K., Minin, V.N., Bouckaert, R.R., 2014. Species delimitation using genome-wide SNP Data. *Systematic Biology* 63, 534–542.

Leaché, A.D., Zhu, T., Rannala, B., Yang, Z., 2019. The spectre of too many species. *Systematic Biology* 68, 168–181.

Leakey, R., Lewin, R., 1996. The Sixth Extinction: Patterns of life and the future of humankind. Anchor Books, New York.

Lemopoulos, A., Prokkola, J.M., Uusi Heikkilä, S., Vasemägi, A., Huusko, A., Hyvärinen, P., Koljonen, M.L., Koskiniemi, J., Vainikka, A., 2019. Comparing RADseq and microsatellites for estimating genetic diversity and relatedness — Implications for brown trout conservation. *Ecology and Evolution* 9, 2106–2120.

Leonard, J.A., Wayne, R.K., Wheeler, J., Valadez, R., Guillén, S., Vilà, C., 2002. Ancient DNA evidence for old world origin of new world dogs. *Science* 298, 1613–1616.

Li, S., Jakobsson, M., 2012. Estimating demographic parameters from large-scale population genomic data using Approximate Bayesian Computation. *BMC Genetics* 13, 22.

Li, W.H., Tanimura, M., Sharp, P.M., 1987. An evaluation of the molecular clock hypothesis using mammalian DNA sequences. *Journal of Molecular Evolution* 25, 330–342.

Librado, P., Gamba, C., Gaunitz, C., Sarkissian, C. Der, Pruvost, M., Albrechtsen, A., Fages, A., Khan, N., Schubert, M., Jagannathan, V., Serres-Armero, A., Kuderna, L.F.K., Povolotskaya, I.S., Seguin-Orlando, A., Sébastien, L., Neuditschko, M., Thèves, C., Alquraishi, S., Alfarhan, A.H., Al-Rasheid, K., Rieder, S., Samashev, Z., Francfort, H.-P., Benecke, N., Hofreiter, M., Ludwig, A., Keyser, C., Marques-Bonet, T., Ludes, B., Crubézy, E., Leeb, T., Willerslev, E., Orlando, L., 2017. Ancient genomic changes associated with domestication of the horse. *Science* 356, 442–445.

Liu, L., Li, Y., Li, S., Hu, N., He, Y., Pong, R., Lin, D., Lu, L., Law, M., 2012. Comparison of next-generation sequencing systems. *Journal of Biomedicine and Biotechnology* 2012, 251364.

Liu, L., Zhang, J., Rheindt, F.E., Lei, F., Qu, Y., Wang, Y., Zhang, Y., Sullivan, C., Nie, W., Wang, J., Yang, F., Chen, J., Edwards, S. V., Meng, J., Wu, S., 2017. Genomic evidence reveals a radiation of placental mammals uninterrupted by the KPg boundary. *Proceedings of the National Academy of Sciences* 114, E7282–E7290.

Lockhart, P.J., Larkum, A.W.D., Steel, M.A., Waddell, P.J., Penny, D., 1996. Evolution of chlorophyll and bacteriochlorophyll: The problem of invariant sites in sequence analysis. *Proceedings of the National Academy of Sciences* 93, 1930–1934.

Lopes, J.S., Boessenkool, S., 2010. The use of approximate Bayesian computation in conservation genetics and its application in a case study on yellow-eyed penguins. *Conservation Genetics* 11, 421–433.

López-Fuster, M.J., Ventura, J., Miralles, M., Castién, E., 1990. Craniometrical characteristics of *Neomys fodiens* (Pennant, 1771) (*Mammalia, Insectivora*) from the northeastern Iberian Peninsula. *Acta Theriologica* 35, 269–276.

López-García, J.M., Blain, H.A., Cuenca-Bescós, G., Ruiz-Zapata, M.B., Dorado-Valiño, M., Gil-García, M.J., Valdeolmillos, A., Ortega, A.I., Carretero, J.M., Arsuaga, J.L., de Castro, J.M.B., Carbonell, E., 2010. Palaeoenvironmental and palaeoclimatic reconstruction of the Latest Pleistocene of El Portalón Site, Sierra de Atapuerca, northwestern Spain. *Palaeogeography, Palaeoclimatology, Palaeoecology* 292, 453–464.

Lozier, J.D., 2014. Revisiting comparisons of genetic diversity in stable and declining species: Assessing genome-wide polymorphism in North American bumble bees using RAD sequencing. *Molecular Ecology* 23, 788–801.

Luo, A., Zhang, A., Ho, S.Y.W., Xu, W., Zhang, Y., Shi, W., Cameron, S.L., Zhu, C., 2011. Potential efficacy of mitochondrial genes for animal DNA barcoding: A case study using eutherian mammals. *BMC Genomics* 12, 84.

Marcolini, F., Piras, P., Kotsakis, T., Claude, J., Michaux, J., Ventura, J., Cubo, J., 2011. Phylogenetic signal and functional significance of incisor enamel microstructure in *Arvicola* (Rodentia, Arvicolinae). *Comptes Rendus Palevol* 10, 479–487.

Margulies, M., Egholm, M., Altman, W.E., Attiya, S., Bader, J.S., Bemben, L.A., Berka, J., Braverman, M.S., Chen, Y.J., Chen, Z., Dewell, S.B., Du, L., Fierro, J.M., Gomes, X. V., Godwin, B.C., He, W., Helgesen, S., Ho, C.H., Irzyk, G.P., Jando, S.C., Alenquer, M.L.I., Jarvie, T.P., Jirage, K.B., Kim, J.B., Knight, J.R., Lanza, J.R., Leamon, J.H., Lefkowitz, S.M., Lei, M., Li, J., Lohman, K.L., Lu, H., Makhijani, V.B., McDade, K.E., McKenna, M.P., Myers, E.W., Nickerson, E., Nobile, J.R., Plant, R., Puc, B.P., Ronan, M.T., Roth, G.T., Sarkis, G.J., Simons, J.F., Simpson, J.W., Srinivasan, M., Tartaro, K.R., Tomasz, A., Vogt, K.A., Volkmer, G.A., Wang, S.H., Wang, Y., Weiner, M.P., Yu, P., Begley, R.F., Rothberg, J.M., 2005. Genome sequencing in microfabricated high-density picolitre reactors. *Nature* 437, 376–380.

Markert, J.A., Danley, P.D., Arnegard, M.E., 2001. New markers for new species: Microsatellite loci and the East African cichlids. *Trends in Ecology and Evolution* 16, 100–107.

Marko, P.B., 2002. Fossil calibration of molecular clocks and the divergence times of geminate species pairs separated by the Isthmus of Panama. *Molecular Biology and Evolution* 19, 2005–2021.

Marko, P.B., Hart, M.W., 2011. The complex analytical landscape of gene flow inference. *Trends in Ecology and Evolution* 26, 448–456.

Marko, P.B., Zaslavskaya, N.I., 2019. Geographic origin and timing of colonization of the Pacific Coast of North America by the rocky shore gastropod *Littorina sitkana*. *PeerJ* 7, e7987.

Marshall, C.R., Raff, E.C., Raff, R.A., 1994. Dollo's law and the death and resurrection of genes. *Proceedings of the National Academy of Sciences* 91, 12283–12287.

Marshall, T.C., Slate, J., Kruuk, L.E.B., Pemberton, J.M., 1998. Statistical confidence for likelihood-based paternity inference in natural populations. *Molecular Ecology* 7, 639–655.

Martin, J.M., Raid, R.N., Branch, L.C., 2014. Barn Owl (*Tyto alba*). *Wildlife Ecology and Conservation Department, UF/IFAS Extension* WEC 185.

McCarthy, M.S., Lester, J.D., Howe, E.J., Arandjelovic, M., Stanford, C.B., Vigilant, L., 2015. Genetic censusing identifies an unexpectedly sizeable population of an endangered large mammal in a fragmented forest landscape. *BMC Ecology* 15, 21.

McCormack, J.E., Faircloth, B.C., Crawford, N.G., Gowaty, P.A., Brumfield, R.T., Glenn, T.C., 2012. Ultraconserved elements are novel phylogenomic markers that resolve placental mammal phylogeny when combined with species-tree analysis. *Genome Research* 22, 746–754.

Mckelvey, K.S., Schwartz, M.K., 2004. Genetic errors associated with population estimation using non-invasive molecular tagging: Problems and new solutions. *Journal of Wildlife Management* 68, 439–448.

Melis, C., Borg, Å.A., Jensen, H., Bjørkvoll, E., Ringsby, T.H., Sæther, B.E., 2013. Genetic variability and structure of the water vole *Arvicola amphibius* across four metapopulations in northern Norway. *Ecology and Evolution* 3, 770–778.

Mendes-Soares, H., Rychlik, L., 2009. Differences in swimming and diving abilities between two sympatric species of water shrews: *Neomys anomalus* and *Neomys fodiens* (Soricidae). *Journal of Ethology* 27, 317–325.

Meredith, R.W., Janečka, J.E., Gatesy, J., Ryder, O.A., Fisher, C.A., Teeling, E.C., Goodbla, A., Eizirik, E., Simão, T.L.L., Stadler, T., Rabosky, D.L., Honeycutt, R.L., Flynn, J.J., Ingram, C.M., Steiner, C., Williams, T.L., Robinson, T.J., Burk-Herrick, A., Westerman, M., Ayoub, N.A., Springer, M.S., Murphy, W.J., 2011. Impacts of the Cretaceous terrestrial revolution and KPg extinction on mammal diversification. *Science* 334, 521–524.

Metropolis, N., Rosenbluth, A.W., Rosenbluth, M.N., Teller, A.H., Teller, E., 1953. Equation of state calculations by fast computing machines. *The Journal of Chemical Physics* 21, 1087–1092.

Michael, T.P., Jackson, S., 2013. The first 50 plant genomes. *The Plant Genome* 6, 2.

Milholland, B., Dong, X., Zhang, L., Hao, X., Suh, Y., Vijg, J., 2017. Differences between germline and somatic mutation rates in humans and mice. *Nature Communications* 8, 15183.

Mills, L.S., 2013. Conservation of wildlife populations: Demography, genetics and management, 2nd ed. John Wiley & Sons, Ltd, Chichester, UK.

Miñarro, M., 2019. Rata topera *Arvicola scherman* (Shaw, 1801), in: Calzada, J., Clavero, M., Fernández, A. (Eds.), *Guía Virtual de Los Indicios de Los Mamíferos de La Península Ibérica, Islas Baleares y Canarias*. Sociedad Española para la Conservación y Estudio de los Mamíferos (SECEM).

Miñarro, M., Montiel, C., Dapena, E., 2012. Vole pests in apple orchards: Use of presence signs to estimate the abundance of *Arvicola terrestris cantabriae* and *Microtus lusitanicus*. *Journal of Pest Science* 85, 477–488.

Mondol, S., Karanth, K.U., Kumar, N.S., Gopalaswamy, A.M., Andheria, A., Ramakrishnan, U., 2009. Evaluation of non-invasive genetic sampling methods for estimating tiger population size. *Biological Conservation* 142, 2350–2360.

Morin, P.A., Chambers, K.E., Boesch, C., Vigilant, L., 2001. Quantitative polymerase chain reaction analysis of DNA from noninvasive samples for accurate microsatellite genotyping of wild chimpanzees (*Pan troglodytes verus*). *Molecular Ecology* 10, 1835–1844.

Morin, P.A., Luikart, G., Wayne, R.K., 2004. SNPs in ecology, evolution and conservation. *Trends in Ecology and Evolution* 19, 208–216.

Morin, P.A., Woodruff, D.S., 1996. Noninvasive genotyping for vertebrate conservation, in: Smith, T.B., Wayne, R.K. (Eds.), *Molecular Genetic Approaches in Conservation*. Oxford University Press, New York, pp. 298–313.

Mullis, K.B., Faloona, F.A., 1987. Specific synthesis of DNA in vitro via a polymerase-

catalyzed chain reaction. *Methods in Enzymology* 155, 335–350.

Nascimento, F.F., Reis, M. Dos, Yang, Z., 2017. A biologist's guide to Bayesian phylogenetic analysis. *Nature Ecology and Evolution* 1, 1446–1454.

Nichols, R., 2001. Gene trees and species trees are not. *Science Direct* 16, 358–364.

Nielsen, R., Wakeley, J. ohn, 2001. Distinguishing migration from isolation: A Markov chain Monte Carlo approach. *Genetics* 158, 885–896.

Nikolaev, S.I., Montoya-Burgos, J.I., Popadin, K., Parand, L., Margulies, E.H., Antonarakis, S.E., 2007. Life-history traits drive the evolutionary rates of mammalian coding and noncoding genomic elements. *Proceedings of the National Academy of Sciences* 104, 20443–20448.

Nores, C., Canals, J.L.S., Castro, A. De, Gonzalez, G.R., 1982. Variation du genre *Neomys* Kaup, 1829 (Mammalia, Insectivora) dans le secteur cantabro-galicien de la péninsule Ibérique. *Mammalia* 46, 361–373.

Ogilvie, H.A., Bouckaert, R.R., Drummond, A.J., 2017. StarBEAST2 brings faster species tree inference and accurate estimates of substitution rates. *Molecular Biology and Evolution* 34, 2101–2114.

Olalde, I., Mallick, S., Patterson, N., Rohland, N., Villalba-Mouco, V., Silva, M., Dulias, K., Edwards, C.J., Gandini, F., Pala, M., Soares, P., Ferrando-Bernal, M., Adamski, N., Broomandkhoshbacht, N., Cheronet, O., Culleton, B.J., Fernandes, D., Lawson, A.M., Mah, M., Oppenheimer, J., Stewardson, K., Zhang, Z., Jiménez Arenas, J.M., Toro Moyano, I.J., Salazar-García, D.C., Castanyer, P., Santos, M., Tremoleda, J., Lozano, M., García Borja, P., Fernández-Eraso, J., Mujika-Alustiza, J.A., Barroso, C., Bermúdez, F.J., Viguera Mínguez, E., Burch, J., Coromina, N., Vivó, D., Cebria, A., Fullola, J.M., García-Puchol, O., Morales, J.I., Oms, F.X., Majó, T., Vergés, J.M., Díaz-Carvajal, A., Ollich-Castanyer, I., López-Cachero, F.J., Silva, A.M., Alonso-Fernández, C., Delibes de Castro, G., Jiménez Echevarría, J., Moreno-Máquez, A., Pascual Berlanga, G., Ramos-García, P., Ramos-Muñoz, J., Vijande Vila, E., Aguilella Arzo, G., Esparza Arroyo, A., Lillios, K.T., Mack, J., Velasco-Vázquez, J., Waterman, A., Benítez de Lugo Enrich, L., Benito Sánchez, M., Agustí, B., Codina, F., de Prado, G., Estalrrich, A., Fernández Flores, A., Finlayson, C., Finlayson, G., Finlayson, S., Giles-Guzmán, F., Rosas, A., Barciela González, V., García Atiénzar, G., Hernández Pérez, M.S., Llanos, A., Carrión Marco, Y., Collado Beneyto, I., López-Serrano, D., Sanz Tormo, M., Valera, A.C., Blasco, C., Liesau, C., Ríos, P., Daura, J., de Pedro Micho, M.J., Diez-Castillo, A.A., Flores Fernández, R., Francès Farré, J., Garrido- Pena, R., Gonçalves, V.S., Guerra-Doce, E., Herrero-Corral, A.M., Juan-Cabanilles, J., López-Reyes, D., McClure, S.B., Merino Pérez, M., Oliver Foix, A., Sanz Borràs, M., Sousa, A.C., Vidal Encinas, J.M., Kennett, D.J., Richards, M.B., Alt, K.W., Haak, W., Pinhasi, R., Lalueza-Fox, C., Reich, D., 2019. The genomic history of the Iberian Peninsula over the past 8000 years. *Science* 363, 1230–1234.

Omland, K.E., Baker, J.M., Peters, J.L., 2006. Genetic signatures of intermediate divergence: Population history of Old and New World Holarctic ravens (*Corvus corax*). *Molecular Ecology* 15, 795–808.

Ottoni, C., Girdland Flink, L., Evin, A., Geörg, C., De Cupere, B., Van Neer, W.,

Bartosiewicz, L., Linderholm, A., Barnett, R., Peters, J., Decorte, R., Waelkens, M., Vanderheyden, N., Ricaut, F.X., Çakirlar, C., Çevik, Ö., Hoelzel, A.R., Mashkour, M., Mohaseb Karimlu, A.F., Sheikhi Seno, S., Daujat, J., Brock, F., Pinhasi, R., Hongo, H., Perez-Enciso, M., Rasmussen, M., Frantz, L., Megens, H.J., Crooijmans, R., Groenen, M., Arbuckle, B., Benecke, N., Strand Vidarsdottir, U., Burger, J., Cucchi, T., Dobney, K., Larson, G., 2013. Pig domestication and human-mediated dispersal in western eurasia revealed through ancient DNA and geometric morphometrics. *Molecular Biology and Evolution* 30, 824–832.

Ou, C.Y., Moore, J.L., Schochetman, G., 1991. Use of UV irradiation to reduce false positivity in polymerase chain reaction. *Biotechniques* 10, 442–446.

Pareek, C.S., Smoczynski, R., Tretyn, A., 2011. Sequencing technologies and genome sequencing. *Journal of Applied Genetics* 52, 413–435.

Pauli, J.N., Hamilton, M.B., Crain, E.B., Buskirk, S.W., 2008. A single-sampling hair trap for mesocarnivores. *The Journal of Wildlife Management* 72, 1650–1652.

Pauli, J.N., Whiteman, J.P., Riley, M.D., Middleton, A.D., 2010. Defining noninvasive approaches for sampling of vertebrates. *Conservation Biology* 24, 349–352.

Perry, G.H., Marioni, J.C., Melsted, P., Gilad, Y., 2010. Genomic-scale capture and sequencing of endogenous DNA from feces. *Molecular Ecology* 19, 5332–5344.

Peters, J.L., Lavretsky, P., DaCosta, J.M., Bielefeld, R.R., Feddersen, J.C., Sorenson, M.D., 2016. Population genomic data delineate conservation units in mottled ducks (*Anas fulvigula*). *Biological Conservation* 203, 272–281.

Peters, J.L., Zhuravlev, Y.N., Fefelov, I., Humphries, E.M., Omland, K.E., 2008. Multilocus phylogeography of a Holarctic duck: Colonization of North America from Eurasia by gadwall (*Anas Strepera*). *Evolution* 62, 1469–1483.

Peterson, B.K., Weber, J.N., Kay, E.H., Fisher, H.S., Hoekstra, H.E., 2012. Double digest RADseq: An inexpensive method for de novo SNP discovery and genotyping in model and non-model species. *PLoS ONE* 7, e37135.

Piertney, S.B., Stewart, W.A., Lambin, X., Telfer, S., Aars, J., Dallas, J.F., 2005. Phylogeographic structure and postglacial evolutionary history of water voles (*Arvicola terrestris*) in the United Kingdom. *Molecular Ecology* 14, 1435–1444.

Pinho, C., Hey, J., 2010. Divergence with gene flow: Models and data. *Annual Review of Ecology, Evolution, and Systematics* 41, 215–230.

Poinar, H.N., Schwarz, C., Qi, J., Shapiro, B., Macphee, R.D.E., Buigues, B., Tikhonov, A., Huson, D.H., Tomsho, L.P., Auch, A., Rampp, M., Miller, W., Schuster, S.C., 2006. Metagenomics to paleogenomics: Large-scale sequencing of mammoth DNA. *Science* 311, 392–394.

Pompanon, F., Bonin, A., Bellemain, E., Taberlet, P., 2005. Genotyping errors: Causes, consequences and solutions. *Nature Reviews Genetics* 6, 847–859.

Poulakakis, N., Lymberakis, P., Paragamian, K., Mylonas, M., 2005. Isolation and amplification of shrew DNA from barn owl pellets. *Biological Journal of the Linnean Society* 85, 331–340.

Pritchard, J.K., Stephens, M., Donnelly, P., 2000. Inference of population structure using multilocus genotype data. *Genetics* 155, 945–959.

Prüfer, K., Racimo, F., Patterson, N., Jay, F., Sankararaman, S., Sawyer, S., Heinze, A., Renaud, G., Sudmant, P.H., De Filippo, C., Li, H., Mallick, S., Dannemann, M., Fu, Q., Kircher, M., Kuhlwilm, M., Lachmann, M., Meyer, M., Ongyerth, M., Siebauer, M., Theunert, C., Tandon, A., Moorjani, P., Pickrell, J., Mullikin, J.C., Vohr, S.H., Green, R.E., Hellmann, I., Johnson, P.L.F., Blanche, H., Cann, H., Kitzman, J.O., Shendure, J., Eichler, E.E., Lein, E.S., Bakken, T.E., Golovanova, L. V., Doronichev, V.B., Shunkov, M. V., Derevianko, A.P., Viola, B., Slatkin, M., Reich, D., Kelso, J., Pääbo, S., 2014. The complete genome sequence of a Neanderthal from the Altai Mountains. *Nature* 505, 43–49.

QGIS Development Team, 2019. QGIS Geographic Information System. Open Source Geospatial Foundation Project. http://qgis.osgeo.org.

Querejeta, M., Castresana, J., 2018. Evolutionary history of the endemic water shrew *Neomys anomalus*: Recurrent phylogeographic patterns in semi-aquatic mammals of the Iberian Peninsula. *Ecology and Evolution* 8, 10138–10146.

Raczyński, J., Ruprecht, A.L., 1974. The effect of digestion on the osteological composition of owl pellets. *Acta Ornithologica* 14, 25–38.

Rannala, B., Yang, Z., 2003. Bayes estimation of species divergence times and ancestral population sizes using DNA sequences from multiple loci. *Genetics* 164, 1645–1656.

Richards, C.L., Knowles, L.L., 2007. Tests of phenotypic and genetic concordance and their application to the conservation of Panamanian golden frogs (Anura, Bufonidae). *Molecular Ecology* 16, 3119–3133.

Rigaux, P., Vaslin, M., Noblet, J.F., Amori, G., Palomo, L.J., 2008. *Arvicola sapidus*. *The IUCN Red List of Threatened Species* e.T2150A9290712.

Rocha, R.G., Justino, J., Leite, Y.L.R., Costa, L.P., 2015. DNA from owl pellet bones uncovers hidden biodiversity. *Systematics and Biodiversity* 13, 403–412.

Rodríguez-Prieto, A., Igea, J., Castresana, J., 2014. Development of rapidly evolving intron markers to estimate multilocus species trees of rodents. *PLoS ONE* 9, e96032.

Rohland, N., Hofreiter, M., 2007a. Comparison and optimization of ancient DNA extraction. *BioTechniques* 42, 343–352.

Rohland, N., Hofreiter, M., 2007b. Ancient DNA extraction from bones and teeth. *Nature Protocols* 2, 1756–1762.

Rohland, N., Reich, D., Mallick, S., Meyer, M., Green, R.E., Georgiadis, N.J., Roca, A.L., Hofreiter, M., 2010. Genomic DNA sequences from mastodon and woolly mammoth reveal deep speciation of forest and savanna elephants. *PLoS Biology* 8, e1000564.

Rosenberg, N.A., Nordborg, M., 2002. Genealogical trees, coalescent theory and the analysis of genetic polymorphisms. *Nature Reviews Genetics* 3, 380–390.

Rychlik, L., 2000. Habitat preferences of four sympatric species of shrews. *Acta Theriologica* 45, 173–190.

Rychlik, L., 1997. Differences in foraging behaviour between water shrews: *Neomys anomalus* and *Neomys fodiens*. *Acta Theriologica* 42, 351–386.

Rychlik, L., Zwolak, R., 2006. Interspecific aggression and behavioural dominance among four sympatric species of shrews. *Canadian Journal of Zoology* 84, 434–448.

Salzburger, W., Ewing, G.B., Von Haeseler, A., 2011. The performance of phylogenetic algorithms in estimating haplotype genealogies with migration. *Molecular Ecology* 20, 1952–1963.

Sánchez-Gracia, A., Castresana, J., 2012. Impact of deep coalescence on the reliability of species tree inference from different types of DNA markers in mammals. *PLoS ONE* 7, e30239.

Sanger, F., Nicklen, S., Coulson, A.R., 1977. DNA sequencing with chain-terminating inhibitors. *Proceedings of the National Academy of Sciences* 74, 5463–5467.

Sankararaman, S., Patterson, N., Li, H., Pääbo, S., Reich, D., 2012. The date of interbreeding between Neandertals and modern humans. *PLoS Genetics* 8, e1002947.

Sans-Fuentes, M.A., Ventura, J., 2000. Distribution patterns of the small mammals (Insectivora and Rodentia) in a transitional zone between the Eurosiberian and the Mediterranean regions. *Journal of Biogeography* 27, 755–764.

Scheen, A.C., Pfeil, B.E., Petri, A., Heidari, N., Nylinder, S., Oxelman, B., 2012. Use of allele-specific sequencing primers is an efficient alternative to PCR subcloning of low-copy nuclear genes. *Molecular Ecology Resources* 12, 128–135.

Schmitt, T., 2007. Molecular biogeography of Europe: Pleistocene cycles and postglacial trends. *Frontiers in Zoology* 4, 11.

Schmitt, T., Varga, Z., 2012. Extra-Mediterranean refugia: The rule and not the exception? *Frontiers in Zoology* 9, 22.

Schneider, C.A., Rasband, W.S., Eliceiri, K.W., 2012. NIH Image to ImageJ: 25 years of image analysis. *Nature Methods* 9, 671–675.

Schultz, A.J., Cristescu, R.H., Littleford-Colquhoun, B.L., Jaccoud, D., Frère, C.H., 2018. Fresh is best: Accurate SNP genotyping from koala scats. *Ecology and Evolution* 8, 3139–3151.

Schuster, S.C., 2008. Next-generation sequencing transforms today's biology. *Nature Methods* 5, 16–18.

Schwartz, M.K., Luikart, G., Waples, R.S., 2007. Genetic monitoring as a promising tool for conservation and management. *Trends in Ecology and Evolution* 22, 25–33.

Seddon, J.M., Santucci, F., Reeve, N.J., Hewitt, G.M., 2001. DNA footprints of European hedgehogs, *Erinaceus europaeus* and *E. concolor*: Pleistocene refugia, postglacial expansion and colonization routes. *Molecular Ecology* 10, 2187–2198.

Segelbacher, G., 2002. Noninvasive genetic analysis in birds: Testing reliability of feather samples. *Molecular Ecology Notes* 2, 367–369.

Sesé, C., 2017. Los micromamíferos (Eulipotyphla, Chiroptera, Rodentia y Lagomorpha) del yacimiento del Pleistoceno Superior de la cueva de El Castillo (Cantabria, España). *Estudios Geológicos* 73, e072.

Shafer, A.B.A., Gattepaille, L.M., Stewart, R.E.A., Wolf, J.B.W., 2015. Demographic inferences using short-read genomic data in an approximate Bayesian computation framework: In silico evaluation of power, biases and proof of concept in Atlantic walrus. *Molecular Ecology* 24, 328–345.

Shane, S., 2005. Shane's simple guide to F-statistics. University of Auckland, Auckland, New Zealand.

Skog, A., Zachos, F.E., Rueness, E.K., Feulner, P.G.D., Mysterud, A., Langvatn, R., Lorenzini, R., Hmwe, S.S., Lehoczky, I., Hartl, G.B., Stenseth, N.C., Jakobsen, K.S., 2009. Phylogeography of red deer (*Cervus elaphus*) in Europe. *Journal of Biogeography* 36, 66–77.

Sommer, R.S., Nadachowski, A., 2006. Glacial refugia of mammals in Europe: Evidence from fossil records. *Mammal Review* 36, 251–265.

Somoano, A., 2017. Biology and population genetics of *Arvicola scherman cantabriae* (Rodentia, Arvicolinae). PhD Thesis, University of Oviedo.

Somoano, A., Miñarro, M., Ventura, J., 2016. Reproductive potential of a vole pest (*Arvicola scherman*) in Spanish apple orchards. *Spanish Journal of Agricultural Research* 14, e1008.

Stajich, J.E., Hahn, M.W., 2005. Disentangling the effects of demography and selection in human history. *Molecular Biology and Evolution* 22, 63–73.

Stamatakis, A., 2014. RAxML version 8: A tool for phylogenetic analysis and post-analysis of large phylogenies. *Bioinformatics* 30, 1312–1313.

Stamatakis, A., 2006. RAxML-VI-HPC: Maximum likelihood-based phylogenetic analyses with thousands of taxa and mixed models. *Bioinformatics* 22, 2688–2690.

Stephens, M., Smith, N.J., Donnelly, P., 2001. A new statistical method for haplotype reconstruction from population data. *The American Journal of Human Genetics* 68, 978–989.

Steppan, S.J., Adkins, R.M., Anderson, J., 2004. Phylogeny and divergence-date estimates of rapid radiations in muroid rodents based on multiple nuclear genes. *Systematic Biology* 53, 533–553.

Stewart, J.R., Lister, A.M., 2001. Cryptic northern refugia and the origins of the modern biota. *Trends in Ecology and Evolution* 16, 608–613.

Stewart, J.R., Lister, A.M., Barnes, I., Dalén, L., 2010. Refugia revisited: Individualistic responses of species in space and time. *Proceedings of the Royal Society B: Biological Sciences* 277, 661–671.

Strimmer, K., Haeseler, A. von, 2009. Genetic distances and nucleotide substitution models, in: Lemey, P., Salemi, M., Vandamme, A.-M. (Eds.), *The Phylogenetic Handbook. A Practical Approach to Phylogenetic Analysis and Hypothesis Testing*. Cambridge University Press, New York, pp. 111–141.

Strugnell, J.M., Pedro, J.B., Wilson, N.G., 2018. Dating Antarctic ice sheet collapse: Proposing a molecular genetic approach. *Quaternary Science Reviews* 179, 153–157.

Sukumaran, J., Knowles, L.L., 2017. Multispecies coalescent delimits structure, not species. *Proceedings of the National Academy of Sciences* 114, 1607–1612.

Taberlet, P., Bonin, A., Zinger, L., Coissac, E., 2018. Environmental DNA: For biodiversity research and monitoring. Oxford University Press, Oxford, UK.

Taberlet, P., Bouvet, J., 1994. Mitochondrial DNA polymorphism, phylogeography, and conservation genetics of the brown bear *Ursus arctos* in Europe. *Proceedings of the Royal Society B: Biological Sciences* 255, 195–200.

Taberlet, P., Camarra, J.J., Griffin, S., Uhres, E., Hanotte, O., Waits, L.P., Dubois-Paganon, C., Burke, T., Bouvet, J., 1997. Noninvasive genetic tracking of the endangered Pyrenean brown bear population. *Molecular Ecology* 6, 869–876.

Taberlet, P., Coissac, E., Hajibabaei, M., Rieseberg, L.H., 2012. Environmental DNA. *Molecular Ecology* 21, 1789–1793.

Taberlet, P., Fumagalli, L., 1996. Owl pellets as a source of DNA for genetic studies of small mammals. *Molecular ecology* 5, 301–305.

Taberlet, P., Fumagalli, L., Wust-Saucy, A.G., Cosson, J.F., 1998. Comparative phylogeography and postglacial colonization routes in Europe. *Molecular Ecology* 7, 453–464.

Taberlet, P., Griffin, S., Goossens, B., Questiau, S., Manceau, V., Escaravage, N., Waits, L.P., Bouvet, J., 1996. Reliable genotyping of samples with very low DNA quantities using PCR. *Nucleic Acids Research* 24, 3189–3194.

Taberlet, P., Waits, L.P., Luikart, G., 1999. Noninvasive genetic sampling: Look before you leap. *Trends in Ecology and Evolution* 14, 323–327.

Takasaki, H., Takenaka, O., 1991. Paternity testing in chimpanzees with DNA amplification from hairs and buccal cells in wadges: A preliminary note, in: Ehara, A., Kimura, T., Takenaka, O., Iwamoto, M. (Eds.), *Primatology Today*. Proceedings of the 13th Congress of the International Primatological Society, Amsterdam: Elsevier, pp. 613–616.

Tapisso, J.T., Ramalhinho, M.G., Mathias, M.L., Rychlik, L., 2013. Ecological release: swimming and diving behavior of an allopatric population of the Mediterranean water shrew. *Journal of Mammalogy* 94, 29–39.

Tavaré, S., 1986. Some probabilistic and statistical problems on the analysis of DNA sequences. *Lectures on Mathematics in the Life Sciences* 17, 57–86.

Templeton, A.R., 2006. Population genetics and microevolutionary theory. John Wiley & Sons, Inc., Hoboken, New Jersey.

Thomson, R.C., Wang, I.J., Johnson, J.R., 2010. Genome-enabled development of DNA markers for ecology, evolution and conservation. *Molecular Ecology* 19, 2184–2195.

Toews, D.P.L., Brelsford, A., 2012. The biogeography of mitochondrial and nuclear discordance in animals. *Molecular Ecology* 21, 3907–3930.

Trasher, D.J., Butcher, B.G., Campagna, L., Webster, M.S., Lovette, I.J., 2018. Double-digest RAD sequencing outperforms microsatellite loci at assigning paternity and estimating relatedness: A proof of concept in a highly promiscuous bird. *Molecular Ecology Resources* 18, 953–965.

Tridico, S.R., Murray, D.C., Addison, J., Kirkbride, K.P., Bunce, M., 2014. Metagenomic analyses of bacteria on human hairs: A qualitative assessment for applications in forensic science. *Investigative Genetics* 5, 16.

Uchimura, A., Higuchi, M., Minakuchi, Y., Ohno, M., Toyoda, A., Fujiyama, A., Miura, I., Wakana, S., Nishino, J., Yagi, T., 2015. Germline mutation rates and the long-term phenotypic effects of mutation accumulation in wild-type laboratory mice and mutator mice. *Genome Research* 25, 1125–1134.

Valiere, N., Taberlet, P., 2000. Urine collected in the field as a source of DNA for species and individual identification. *Molecular Ecology* 9, 2150–2152.

van Orsouw, N.J., Hogers, R.C.J., Janssen, A., Yalcin, F., Snoeijers, S., Verstege, E., Schneiders, H., van der Poel, H., van Oeveren, J., Verstegen, H., van Eijk, M.J.T., 2007. Complexity reduction of polymorphic sequences (CRoPS^{TM}): A novel approach for large-scale polymorphism discovery in complex genomes. *PLoS ONE* 2, e1172.

Ventura, J., 2007a. *Neomys fodiens* (Pennant, 1771), in: Palomo, L.J., Gisbert, J., Blanco, J.C. (Eds.), *Atlas y Libro Rojo de Los Mamíferos Terrestres de España*. Dirección General para la Biodiversidad-SECEM-SECEMU, Madrid, pp. 111–113.

Ventura, J., 2007b. *Neomys anomalus* Cabrera 1907, in: Palomo, L.J., Gisbert, J., Blanco, J.C. (Eds.), *Atlas y Libro Rojo de Los Mamíferos Terrestres de España*. Dirección General para la Biodiversidad-SECEM-SECEMU, Madrid, pp. 114–116.

Ventura, J., 2007c. *Arvicola terrestris* (Linnaeus, 1758), in: Palomo, L.J., Gisbert, J., Blanco, J.C. (Eds.), *Atlas y Libro Rojo de Los Mamíferos Terrestres de España*. Dirección General para la Biodiversidad-SECEM-SECEMU, Madrid, pp. 401–404.

Ventura, J., 2007d. *Arvicola sapidus* Miller, 1908, in: Palomo, L.J., Gisbert, J., Blanco, J.C. (Eds.), *Atlas y Libro Rojo de Los Mamíferos Terrestres de España*. Dirección General para la Biodiversidad-SECEM-SECEMU, Madrid, pp. 405–407.

Waits, J.L., Leberg, P.L., 2000. Biases associated with population estimation using molecular tagging. *Animal Conservation* 3, 191–199.

Waits, L.P., Paetkau, D., 2005. Noninvasive genetic sampling tools for wildlife biologists: A review of applications and recommendations for accurate data collection. *Journal of Wildlife Management* 69, 1419–1433.

Wakeley, J., 2006. Coalescent theory: An introduction. Roberts & Co., Greenwood village, Colorado.

Wakeley, J., 2000. The effects of subdivision on the genetic divergence of populations and species. *Evolution* 54, 1092–1101.

Walker, F.M., Williamson, C.H.D., Sanchez, D.E., Sobek, C.J., Chambers, C.L., 2016. Species from feces: Order-wide identification of chiroptera from guano and other non-invasive genetic samples. *PLoS ONE* 11, e0162342.

Wang, S., Meyer, E., Mckay, J.K., Matz, M. V., 2012. 2b-RAD: A simple and flexible method for genome-wide genotyping. *Nature Methods* 9, 808–810.

Weir, B.S., Cockerham, C.C., 1984. Estimating F-statistics for the analysis of population structure. *Evolution* 38, 1358–1370.

Weksler, M., 2003. Phylogeny of Neotropical oryzomyine rodents (Muridae: Sigmodontinae) based on the nuclear IRBP exon. *Molecular Phylogenetics and Evolution* 29, 331–349.

Welch, J.J., Bininda-Emonds, O.R.P., Bromham, L., 2008. Correlates of substitution rate variation in mammalian protein-coding sequences. *BMC Evolutionary Biology* 8, 53.

Wilson, E., Reeder, D.M. (Eds.), 2005. Mammal Species of the World. A Taxonomic and Geographic Reference, 3rd ed, Johns Hopkins University Press.

Wolfe, K.H., Sharp, P.M., 1993. Mammalian gene evolution: Nucleotide sequence divergence between mouse and rat. *Journal of Molecular Evolution* 37, 441–456.

Wultsch, C., Waits, L.P., Kelly, M.J., 2014. Noninvasive individual and species identification of jaguars (*Panthera onca*), pumas (*Puma concolor*) and ocelots (*Leopardus pardalis*) in Belize, Central America using cross-species microsatellites and faecal DNA. *Molecular Ecology Resources* 14, 1171–1182.

Xiao, L., Ryan, U.M., Graczyk, T.K., Limor, J., Li, L., Kombert, M., Junge, R., Sulaiman, I.M., Zhou, L., Arrowood, M.J., Koudela, B., Modrý, D., Lal, A.A., 2004. Genetic diversity of *Cryptosporidium* spp. in captive reptiles. *Applied and Environmental Microbiology* 70, 891–899.

Yang, Z., 2015. The BPP program for species tree estimation and species delimitation. *Current Zoology* 61, 854–865.

Yang, Z., 1996. Among-site rate variation and its impact on phylogenetic analyses. *Trends in Ecology and Evolution* 11, 367–372.

Yang, Z., 1994. Maximum likelihood phylogenetic estimation from DNA sequences with variable rates over sites: Approximate methods. *Journal of Molecular Evolution* 39, 306–314.

Yang, Z., Rannala, B., 2010. Bayesian species delimitation using multilocus sequence data. *Proceedings of the National Academy of Sciences* 107, 9264–9269.

Yannic, G., Dubey, S., Hausser, J., Basset, P., 2010. Additional data for nuclear DNA give new insights into the phylogenetic position of *Sorex granarius* within the *Sorex araneus* group. *Molecular Phylogenetics and Evolution* 57, 1062–1071.

Yates, A.D., Achuthan, P., Akanni, W., Allen, James, Allen, Jamie, Alvarez-Jarreta, J.,

Amode, M.R., Armean, I.M., Azov, A.G., Bennett, R., Bhai, J., Billis, K., Boddu, S., Marugán, J.C., Cummins, C., Davidson, C., Dodiya, K., Fatima, R., Gall, A., Giron, C.G., Gil, L., Grego, T., Haggerty, L., Haskell, E., Hourlier, T., Izuogu, O.G., Janacek, S.H., Juettemann, T., Kay, M., Lavidas, I., Le, T., Lemos, D., Martinez, J.G., Maurel, T., McDowall, M., McMahon, A., Mohanan, S., Moore, B., Nuhn, M., Oheh, D.N., Parker, A., Parton, A., Patricio, M., Sakthivel, M.P., Abdul Salam, A.I., Schmitt, B.M., Schuilenburg, H., Sheppard, D., Sycheva, M., Szuba, M., Taylor, K., Thormann, A., Threadgold, G., Vullo, A., Walts, B., Winterbottom, A., Zadissa, A., Chakiachvili, M., Flint, B., Frankish, A., Hunt, S.E., IIsley, G., Kostadima, M., Langridge, N., Loveland, J.E., Martin, F.J., Morales, J., Mudge, J.M., Muffato, M., Perry, E., Ruffier, M., Trevanion, S.J., Cunningham, F., Howe, K.L., Zerbino, D.R., Flicek, P., 2020. Ensembl 2020. *Nucleic acids research* 48, D682–D688.

Zheng, X., Levine, D., Shen, J., Gogarten, S.M., Laurie, C., Weir, B.S., 2012. A high-performance computing toolset for relatedness and principal component analysis of SNP data. *Bioinformatics* 28, 3326–3328.

Zhou, Y., Mishra, B., 2005. Quantifying the mechanisms for segmental duplications in mammalian genomes by statistical analysis and modeling. *Proceedings of the National Academy of Sciences* 102, 4051–4056.

Zuckerkandl, E., Pauling, L., 1965. Evolutionary divergence and convergence in proteins, in: Bryson, V., Vogel, H.J. (Eds.), *Evolving Genes and Proteins*. Academic Press, New York, pp. 97–166.

IV. ANNEX

Table S1. Samples of *Neomys sp.* used in this study with information about sample type, collection year, locality data, morphological data (marked with XX for geometric morphometrics and X for coronoid height), cytochrome *b* length (being 226 bp the length of the Neo 1.2 fragment; 569 the length of the Neo 1.2 - Neo 2 combined fragments, which have an overlapping region; and 1140 the length of the three overlapping fragments), and number of sequenced introns in samples with nuclear information. Samples from the collection of the Department of Organisms and Systems Biology of the University of Oviedo are indicated with (UO). Samples from the Museum of Southwestern Biology (MSB) and the University of Alaska Museum (UAM) are indicated with their respective codes. The sample IBE-C4117 (2200-Briansk) is from the collection of A. Bannikova. Samples of Igea et al. (2015) are also included and indicated with (1).

Specimen Code	Species	Sample type	Year	Lat.	Lon.	Locality	Administrative Division / Country	Morphology	Cyt *b* length (bp)	Nº of introns
IBE-C5180 (UO)	*N. fodiens*	Skull	1979	43.4	-6.8	Boal	Asturias	XX	226	-
IBE-C5182 (UO)	*N. fodiens*	Skull	1970	43.4	-4.7	Vidiago	Asturias	XX	1140	6
IBE-C5183 (UO)	*N. fodiens*	Skull	1980	43.3	-5.9	Peñerudes	Asturias	XX	569	-
IBE-C5185 (UO)	*N. fodiens*	Skull	1970	43.5	-5	Cuerres	Asturias	XX	569	-
IBE-C5186 (UO)	*N. fodiens*	Skull	1979	43.4	-6.1	Rebolleda	Asturias	XX	569	-
IBE-C5188 (UO)	*N. fodiens*	Skull	1981	43.5	-5.5	Peón	Asturias	XX	1140	5
IBE-C5356 (UO)	*N. fodiens*	Skull	1980	43.3	-6.5	Obona	Asturias	XX	226	-
IBE-C5357 (UO)	*N. fodiens*	Skull	1980	43.3	-4.2	Cabezón de la Sal	Cantabria	XX	1140	-
IBE-C5359 (UO)	*N. fodiens*	Skull	1980	43.2	-5.8	Valdecuna	Asturias	XX	1140	4
IBE-C5361 (UO)	*N. fodiens*	Skull	1978	43.4	-5.4	Infiesto	Asturias	XX	226	-
IBE-C5362 (UO)	*N. fodiens*	Skull	1980	43.4	-6.4	La Millariega	Asturias	XX	226	-
IBE-C5364 (UO)	*N. fodiens*	Skull	1980	43.4	-4.1	Quijas	Cantabria	XX	226	-
IBE-C5365 (UO)	*N. fodiens*	Skull	1981	43.2	-5.3	La Foz	Asturias	XX	226	-
IBE-C5367 (UO)	*N. fodiens*	Skull	1979	43.6	-6.4	Ribón	Asturias	XX	1140	6
IBE-C5368 (UO)	*N. fodiens*	Skull	1988	43.4	-6.8	Boal	Asturias	XX	1140	6
IBE-C5369 (UO)	*N. fodiens*	Skull	1986	43.3	-6.2	Restiello	Asturias	XX	226	-
IBE-C5370 (UO)	*N. fodiens*	Skull	1983	43.4	-6.8	La Felechosa	Asturias	XX	1140	6
IBE-C5371 (UO)	*N. fodiens*	Skull	1980	43.6	-6.2	Piñera	Asturias	XX	1140	5
IBE-C5372 (UO)	*N. fodiens*	Skull	1982	43.5	-5.4	Priesca	Asturias	XX	1140	6
IBE-C5374 (UO)	*N. fodiens*	Skull	1979	43.4	-7.1	Pueblonuevo	Asturias	XX	1140	6
IBE-C5375 (UO)	*N. fodiens*	Skull	1982	42.9	-6.4	Palacios del Sil	León	XX	226	-
IBE-C5376 (UO)	*N. fodiens*	Skull	1978	43.4	-7.2	Conforto	Lugo	XX	1140	4
IBE-C5377 (UO)	*N. fodiens*	Skull	1980	43.2	-5.8	Valdecuna	Asturias	XX	226	-
IBE-C5603 (UO)	*N. fodiens*	Skull	2015	43.3	-5	Avín	Asturias	XX	1140	6
IBE-C5604 (UO)	*N. fodiens*	Skull	2015	43.3	-5	Avín	Asturias	XX	1140	6
IBE-C5605 (UO)	*N. fodiens*	Skull	2015	43.3	-5	Avín	Asturias	XX	226	-
IBE-C5697	*N. fodiens*	Skull	2017	43.1	-6	San Vicente de Nimbra	Asturias	XX	1140	6
IBE-C5699	*N. fodiens*	Skull	2017	42.7	-1.5	Iglesia Zuazu	Navarra	XX	1140	5
IBE-C5701	*N. fodiens*	Skull	2017	43.1	-6	San Vicente de Nimbra	Asturias	XX	1140	6
IBE-C5709	*N. fodiens*	Skull	2017	43.1	-6	San Vicente de Nimbra	Asturias	XX	1140	-
IBE-C5741	*N. fodiens*	Skull	2017	43	-1.3	Iglesia Burguete	Navarra	XX	1140	5
IBE-C5742	*N. fodiens*	Skull	2017	42.7	-7.3	San Martiño	Lugo	XX	1140	6
IBE-C5744	*N. fodiens*	Skull	2017	43.2	-6.8	La Figuerina	Asturias	XX	1140	6
IBE-C6063	*N. fodiens*	Skull	2017	43.3	-6.7	San Pedro de Lago	Asturias	XX	1140	6
IBE-C6064	*N. fodiens*	Skull	2017	42.7	-7.3	San Martiño	Lugo	XX	1140	4
IBE-C6066	*N. fodiens*	Skull	2017	43.2	-6.6	Santa Marina de Obanca	Asturias	XX	1140	5
IBE-C6069	*N. fodiens*	Skull	2017	43.3	-6.7	San Pedro de Lago	Asturias	XX	1140	6
IBE-C6103	*N. fodiens*	Skull	1984	42.8	-3.7	Cubillo de Butrón	Burgos	XX	569	-
IBE-C6104	*N. fodiens*	Skull	1984	42.8	-3.7	Cubillo de Butrón	Burgos	XX	569	-
IBE-C6105	*N. fodiens*	Skull	1985	43.1	-3.3	Caniego	Burgos	X	1140	5
IBE-C6106	*N. fodiens*	Skull	1985	43.1	-3.3	Caniego	Burgos	X	1140	5
IBE-C6108	*N. fodiens*	Skull	1985	43.1	-3.6	Hornillalatorre	Burgos	X	1140	5
IBE-C6109	*N. fodiens*	Skull	1986	43.2	-3.9	Entrambasmestas	Cantabria	XX	569	-
IBE-C6110	*N. fodiens*	Skull	1986	43.2	-3.9	Entrambasmestas	Cantabria	XX	1140	5
IBE-C6111	*N. fodiens*	Skull	1986	43.2	-3.9	Entrambasmestas	Cantabria	XX	1140	-
IBE-C6112	*N. fodiens*	Skull	1986	43	-3.2	Encima Angulo	Burgos	XX	226	-
IBE-C6113	*N. fodiens*	Skull	1986	43	-3.2	Encima Angulo	Burgos	XX	226	-
IBE-C6115	*N. fodiens*	Skull	1987	42.8	-3.2	Orbañanos	Burgos	X	226	-
IBE-C6116	*N. fodiens*	Skull	1993	42.7	-3.8	Covanera	Burgos	XX	1140	5
IBE-C4117 (2200-Briansk)	*N. fodiens*	Tissue		53.3	34.4	Briansk	Russia		1140	6
MSB:Mamm:95472	*N. fodiens*	Tissue	1997	47.7	17.4	Feher-to	Hungary		1140	6
MSB:Mamm:158495	*N. fodiens*	Tissue	2006	43.2	84.3	Narati	China		1140	6
MSB:Mamm:158621	*N. fodiens*	Tissue	2006	43.2	84.3	Narati	China		1140	6

MSB:Mamm:288577	*N. fodiens*	Tissue	2015	48.2	89	Songinot Gol	Mongolia		1140	6
MSB:Mamm:288698	*N. fodiens*	Tissue	2015	49.5	94.7	Han Huhnii Mountain	Mongolia		1140	6
MSB:Mamm:293526	*N. fodiens*	Tissue	2016	49	103.2	Tsachirt River	Mongolia		1140	6
UAM:Mamm:24769	*N. fodiens*	Tissue	1986	60.8	24.5	Loppi	Finland		1140	6
UAM:Mamm:24770	*N. fodiens*	Tissue	1986	60.8	24.5	Loppi	Finland		1140	5
IBE-C5187	*N. anomalus*	Skull	1980	43.2	-5.5	Rioseco	Asturias	XX	569	-
IBE-C5189	*N. anomalus*	Skull	1979	43.5	-6.1	Corias	Asturias	XX	226	-
IBE-C5190	*N. anomalus*	Skull	1980	43.5	-6.4	Muñás	Asturias	XX	1140	-
IBE-C5379	*N. anomalus*	Skull	1978	43.4	-5.4	Infiesto	Asturias	X	226	-
IBE-C5381	*N. anomalus*	Skull	1980	42.8	-3.9	Valderredible	Cantabria	XX	226	-
IBE-C5382	*N. anomalus*	Skull	1983	42.6	-6.2	Manzanal del Puerto	León	XX	226	-
IBE-C5383	*N. anomalus*	Skull	1984	43.5	-8.2	Ferrol	La Coruña	X	1140	6
IBE-C5700	*N. anomalus*	Skull	2017	43.1	-6	San Vicente de Nimbra	Asturias	XX	1140	6
IBE-C5719	*N. anomalus*	Skull	2017	43.2	-6.6	Santa Marina de Obanca	Asturias	XX	1140	6
IBE-C5720	*N. anomalus*	Skull	2017	43.2	-6.6	Santa Marina de Obanca	Asturias	XX	1140	6
IBE-C5726	*N. anomalus*	Skull	2017	43.2	-6.8	Convento de San Bruno	Asturias	XX	1140	6
IBE-C6065	*N. anomalus*	Skull	2017	43.2	-6.8	Convento de San Bruno	Asturias	XX	1140	6
IBE-C6118	*N. anomalus*	Skull	1986	42.8	-3.2	Herrán	Burgos		1140	5
IBE-C6119	*N. anomalus*	Skull	1984	42.8	-3.7	Cubillo de Butrón	Burgos	XX	226	-
IBE-C6120	*N. anomalus*	Skull	1987	43	-3.9	Cilleruelo de Bezana	Burgos	XX	569	-
IBE-C6121	*N. anomalus*	Skull	1991	43	-4.2	Barrio	Cantabria	XX	1140	5
IBE-C6122	*N. anomalus*	Skull	1986	43	-3.2	Encima Angulo	Burgos		569	-
IBE-C6124	*N. anomalus*	Skull	1986	43.2	-3.9	Entrambasmestas	Cantabria	XX	1140	5
IBE-C6125	*N. anomalus*	Skull	2015	43.1	-3.3	Caniego	Burgos		1140	4
IBE-C4515	*N. anomalus*	Tissue	2015	43.4	-6.4	La Millariega	Asturias		1140	6
IBE-C1927	*N. milleri*	Tissue	2012	42.6	1.1	Escalarre	Lleida		1140	6
IBE-C101	*N. fodiens*	(1)	2007	42.4	2.2	Queralbs	Barcelona	XX	1140	6
IBE-C1914	*N. fodiens*	(1)	2010	42.5	0.8	Coll	Lleida	XX	1140	6
IBE-S1915	*N. fodiens*	(1)	2009	42.9	-2.4	Zalduondo	Alava		1140	-
IBE-C1144	*N. anomalus*	(1)	2010	43.1	-6.7	Vega de Horreo	Asturias		1140	-
IBE-C1435	*N. anomalus*	(1)	2010	41.7	-5	Penaflor de Hornija	Valladolid		1140	-
IBE-C1529	*N. anomalus*	(1)	2010	43.3	-4.8	Tielve	Asturias		1140	6
IBE-C1662	*N. anomalus*	(1)	2010	42	-2.6	Molinos de Razón	Soria		1140	-
IBE-C1683	*N. anomalus*	(1)	2010	42.2	-6.7	Trefacio	Zamora		1140	-
IBE-C1789	*N. anomalus*	(1)	2008	40.3	-5.5	Navalguijo	Avila		1140	6
IBE-C2664	*N. anomalus*	(1)	2011	40.7	-0.2	Bergantes	Castellón		1140	-
IBE-C2895	*N. anomalus*	(1)		43.2	-4.9	Picos de Europa	León		1140	6
IBE-C1808	*N. milleri*	(1)	2010	42.3	1	La Pobla de Segur	Lleida		1140	6
IBE-C3786	*N. milleri*	(1)	2012	42.3	1.9	Guardiola de Bergueda	Barcelona		1140	6
IBE-C4115	*N. milleri*	(1)	2000	55.2	30.2	Vitebsk	Belarus		1140	-
IBE-C4116	*N. milleri*	(1)	2007	50.6	36.6	Belgorod	Russia		1140	6
IBE-S1926	*N. milleri*	(1)	2009	41.9	2.5	Osor	Girona		1140	-
IBE-C4120	*N. teres*	(1)	1999	43.9	40.1	North Caucasus	Russia		1140	6
IBE-C4122	*N. teres*	(1)	1999	43.9	40.1	North Caucasus	Russia		1140	6

Table S2. Measurements of coronoid height and centroid size of the mandibles. For broken mandibles, only coronoid height could be measured.

Specimen code	Taxon	Coronoid height (mm)	Centroid size (mm)
IBE-C5180	*N. f. fodiens*	5.24	15.2
IBE-C5182	*N. f. niethammeri*	5.76	16.3
IBE-C5183	*N. f. niethammeri*	5.76	16.1
IBE-C5185	*N. f. niethammeri*	5.87	16.1
IBE-C5186	*N. f. fodiens*	5.2	15.3
IBE-C5188	*N. f. fodiens*	5.25	14.9
IBE-C5356	*N. f. fodiens*	5.16	15.1
IBE-C5357	*N. f. niethammeri*	5.65	16.1
IBE-C5359	*N. f. niethammeri*	5.5	15.9
IBE-C5361	*N. f. niethammeri*	5.84	16.2
IBE-C5362	*N. f. fodiens*	5.3	15.4
IBE-C5364	*N. f. niethammeri*	5.6	16.2
IBE-C5365	*N. f. niethammeri*	5.72	15.8
IBE-C5367	*N. f. fodiens*	5.26	15.1
IBE-C5368	*N. f. niethammeri*	5.37	16.2
IBE-C5369	*N. f. fodiens*	5.31	15.7
IBE-C5370	*N. f. fodiens*	5.18	15.0
IBE-C5371	*N. f. niethammeri*	5.52	15.4
IBE-C5372	*N. f. niethammeri*	5.4	15.7
IBE-C5374	*N. f. fodiens*	4.9	14.6
IBE-C5375	*N. f. fodiens*	5.2	15.6
IBE-C5376	*N. f. fodiens*	5.17	14.9
IBE-C5377	*N. f. niethammeri*	5.53	15.9
IBE-C5603	*N. f. niethammeri*	5.84	16.2
IBE-C5604	*N. f. niethammeri*	5.93	16.3
IBE-C5605	*N. f. niethammeri*	5.72	16.4
IBE-C5697	*N. f. niethammeri*	5.49	15.9
IBE-C5699	*N. f. niethammeri*	5.4	16.1
IBE-C5701	*N. f. niethammeri*	5.82	15.8
IBE-C5709	*N. f. niethammeri*	5.67	15.4
IBE-C5741	*N. f. niethammeri*	5.43	15.8
IBE-C5742	*N. f. fodiens*	5.06	15.3
IBE-C5744	*N. f. fodiens*	5.24	15.1
IBE-C6063	*N. f. fodiens*	5.08	15.1
IBE-C6064	*N. f. fodiens*	5.08	14.8
IBE-C6066	*N. f. fodiens*	5.11	15.3
IBE-C6069	*N. f. fodiens*	5.2	14.6
IBE-C6103	*N. f. niethammeri*	5.68	15.6
IBE-C6104	*N. f. niethammeri*	5.72	15.8
IBE-C6105	*N. f. niethammeri*	5.84	
IBE-C6106	*N. f. niethammeri*	5.99	
IBE-C6108	*N. f. niethammeri*	5.62	
IBE-C6109	*N. f. niethammeri*	5.82	16.3
IBE-C6110	*N. f. niethammeri*	5.54	16.0
IBE-C6111	*N. f. niethammeri*	5.81	16.6

IBE-C6112	*N. f. niethammeri*	5.6	15.7
IBE-C6113	*N. f. niethammeri*	5.48	15.6
IBE-C6115	*N. f. niethammeri*	5.43	
IBE-C6116	*N. f. niethammeri*	5.74	15.9
IBE-C5187	*N. anomalus*	4.28	13.9
IBE-C5189	*N. anomalus*	4.66	14.5
IBE-C5190	*N. anomalus*	4.36	14.1
IBE-C5379	*N. anomalus*	4.27	
IBE-C5381	*N. anomalus*	4.55	15.0
IBE-C5382	*N. anomalus*	4.52	14.5
IBE-C5383	*N. anomalus*	4.62	
IBE-C5700	*N. anomalus*	4.31	14.3
IBE-C5719	*N. anomalus*	4.36	13.9
IBE-C5720	*N. anomalus*	4.22	14.1
IBE-C5726	*N. anomalus*	4.3	14.4
IBE-C6065	*N. anomalus*	4.29	14.2
IBE-C6119	*N. anomalus*	4.44	14.7
IBE-C6120	*N. anomalus*	4.48	14.4
IBE-C6121	*N. anomalus*	4.37	14.3
IBE-C6124	*N. anomalus*	4.53	14.5
IBE-C101	*N. f. fodiens*	4.95	14.9
IBE-C1914	*N. f. fodiens*	4.92	15.2

Table S3. Primers used in this work for the amplification of the different overlapping fragments of the cytochrome *b* and the special fragment employed in highly degraded samples (Neo 1.2). Fragment Neo 1.2 allowed the amplification of 26 % of the mandibles used in this study, whereas only 14 % of the available mandibles tested remained undetermined. Primer temperature (T) and length of the amplified sequences without counting primers are also shown. Newly designed primers or modified from a previous published work (Igea et al., 2015) are marked with an asterisk. For fresh tissue or recent skull samples the whole cytochrome *b* sequence could be obtained in a single PCR reaction using flanking primers (1).

Fragment	Name	Primer sequence	T (ºC)	Length (bp)
Neo1	Neomys_tRNAGlu (1)	ATCGTTGTTATTCAACTATAAGAAC	64	404
	Neomys_cytb _R1.2 *	CCYCARAATGATATTTGYCCTCA	65	
Neo2	Neomys_cytb _F2.3 *	CAGTTATAGCYACTGCCTTTATA	63	358
	Neomys_cytb _R2.1 *	AATTRTCYGGGTCTCCGAGTA	62	
Neo3	Neomys_cytb_614F	TWTTCCTYCATGAAACAGGATC	61	544
	Neomys_tRNAThr (1)	TTTTGGTTTACAAGACCAGTGTAT	64	
Neo1.2	Neomys_cytb_F1.1 *	TAGCAATACATTAYACTTCMGACAC	68	226
	Neomys_cytb_403R	YCCYCARAATGATATTTGYCCTCA	68	

Table S4. Primer pairs used to sequence intron fragments in *Neomys* species. For some introns, more than one pair was designed and the final established set is shown with an asterisk. Amplification of degraded samples with shorter fragments allowed a gain of 12 % of amplified loci. Primer temperature (T), amplified length without counting primer sequence, and number of samples sequenced with each pair are shown. Primer design tried to homogenize hybridization temperature of the different markers, which was set to 65º in conventional PCR reactions and 63º when using Multiplex, as higher temperatures were not recommended in this protocol.

Nuclear marker	Name	Primer sequence	T (ºC)	Length (bp)	Samples sequenced
ASB6-2	ASB6-2-F2	TCCTGGGTGATAACAAAGGCCT *	66	215	54
	ASB6-2-R2	CAGGTGCGTCAGTGCCTGCT *	66		
CSF2-2	CSF2-2-F2	GGCACTGGTGGTAGTCAGTGA *	66	229	57
	CSF2-2-R2	TGGACATGAGTCTGAATCTTGCT *	66		
GDAP1-1	GDAP1-F2	CAGCACCAGGACAGCTCCCA	66	229	8
	GDAP1-R2	ATGCTAAAGGAGGTAACTGTGGA	66		
	GDAP1-F3	ACCAGGACAGCTCCCAGGGT *	66	198	44
	GDAP1-R3	GCGTTTCTCTCTGCATCTCTCT *	66		
JMJD-2	JMJD2-F2	TGCGGTCAGCGGCCATCTCA	66	225	10
	JMJD2-R2	CAAGGTTCCTGCTGGCCAGCT	68		
	JMJD2-F3	CTCCACCCTGGYAGAACCCT *	65	153	41
	JMJD2-R3	TCACAGCACCTGCTCTGTGCT *	66		
MYCBPAP-11	MYCBPAP-F2	CAGTTTTATTTTGACAACCGGGAA	66	344	8
	MYCBPAP-R2	CGTYTCTTCAGGCAGAATCACA	65		
	MYCBPAP-F3	CCCAGGGAGCAGGAGCATTCT	68	200	6
	MYCBPAP-R2	CGTYTCTTCAGGCAGAATCACA	65		
	MYCBPAP-F5	ATTCTAGGGGTTYAGCTGCTTCT *	67	182	43
	MYCBPAP-R2	CGTYTCTTCAGGCAGAATCACA *	65		
TRAIP-8	TRAIP-F3	GCTCCTGGCTCCTAGACATCT *	66	198	55
	TRAIP-R3	CCCAGGCTGAACTCTCCACAA *	66		

Table S5. Allele-specific primers used for amplification and sequencing of nuclear introns. Primer temperature (T) and polymorphic position of the sequence (SNP position) are also shown. PCRs were performed with an annealing temperature of 65º or 63º with conventional or Multiplex reactions, respectively. 14 % of samples were phased for MYCBPAP-11 introns using these primers.

Primer name	Primer sequence	T (ºC)	SNP position
MYCBPAP-F5_A	TGGGCCCGGGGCTCCCTTA	66	123
MYCBPAP-F5_T	TGGGCCCGGGGCTCCCTTT	66	123
MYCBPAP-R2_C	GGCAGAAGCCAGCTGAGGCC	68	134
MYCBPAP-R2_G	GGCAGAAGCCAGCTGAGGCG	68	134

Table S6. Samples of *Arvicola sp.* used in the study including species name, sample type and geographic information. Samples from the Museum of Southwestern Biology (MSB), the University of Alaska Museum (UAM) and the Museum of Vertebrate Zoology (MVZ) are indicated with their respective codes.

Specimen Code	Species	Sample type	Lat	Lon	Locality	Administrative Division / Country
IBE_C5800	*A. scherman*	Tissue	43.5	-6.7	Coaña	Asturias
IBE_C5801	*A. scherman*	Tissue	43.5	-6.7	Coaña	Asturias
IBE_C5796	*A. scherman*	Skull	43.2	-6.6	Santa Marina de Obanca	Asturias
IBE_C5791	*A. scherman*	Skull	43.2	-6.6	Santa Marina de Obanca	Asturias
IBE_C5795	*A. scherman*	Skull	43.2	-6.6	Santa Marina de Obanca	Asturias
IBE_C4973	*A. scherman*	Tissue	43.4	-6.4	La Fajera	Asturias
IBE_C4971	*A. scherman*	Tissue	43.0	-6.1	Valle de Lago	Asturias
IBE_C4968	*A. scherman*	Tissue	43.0	-5.9	La Cubilla	León
IBE_C5802	*A. scherman*	Tissue	43.2	-5.8	Mieres	Asturias
IBE_C5803	*A. scherman*	Tissue	43.2	-5.8	Mieres	Asturias
IBE_C4986	*A. scherman*	Tissue	43.4	-5.4	Poreño	Asturias
IBE_C4979	*A. scherman*	Tissue	43.5	-5.4	Santa Marina	Asturias
IBE_C6033	*A. scherman*	Skull	42.8	-5.3	La Ercina	León
IBE_C6027	*A. scherman*	Skull	42.8	-5.3	La Ercina	León
IBE_C6026	*A. scherman*	Skull	42.8	-5.2	Valporquero de Rueda	León
IBE_C4965	*A. scherman*	Tissue	43.3	-4.9	Asiego	Asturias
IBE_C4966	*A. scherman*	Tissue	43.3	-4.9	Asiego	Asturias
IBE_C2497	*A. scherman*	Skull	43.0	-4.2	Villacantid	Cantabria
IBE_C2354	*A. scherman*	Skull	43.0	-4.2	Villacantid	Cantabria
IBE_C4975	*A. scherman*	Tissue	43.3	-2.1	Usurbil	Gipuzkoa
IBE_C4974	*A. scherman*	Tissue	43.3	-2.1	Usurbil	Gipuzkoa
IBE_C4969	*A. scherman*	Tissue	43.3	-2.0	Ibaeta	Gipuzkoa
IBE_C4970	*A. scherman*	Tissue	43.3	-2.0	Ibaeta	Gipuzkoa
IBE_C4977	*A. scherman*	Tissue	43.3	-1.9	Astigarraga	Gipuzkoa
IBE_C4976	*A. scherman*	Tissue	43.3	-1.9	Astigarraga	Gipuzkoa
IBE_C5797	*A. scherman*	Tissue	43.0	-1.3	Burguete	Navarra
IBE_C5793	*A. scherman*	Skull	43.0	-1.3	Burguete	Navarra
IBE_C5012	*A. scherman*	Tissue	42.7	0.8	Arrós	Lleida
IBE_C5010	*A. scherman*	Tissue	42.7	0.8	Arrós	Lleida
IBE_C5013	*A. scherman*	Tissue	42.7	0.8	Arrós	Lleida
IBE_C5011	*A. scherman*	Tissue	42.7	0.8	Arrós	Lleida
IBE_C4356	*A. scherman*	Tissue	42.6	1.2	Ribera de Cardós	Lleida
MVZ_155884	*A. scherman*	Tissue	46.8	8.4	Engelberg	Switzerland
UAM_64164	*A. amphibius*	Tissue	62.2	22.8	Alkkia	Finland
UAM_64166	*A. amphibius*	Tissue	62.2	22.8	Alkkia	Finland
MSB_288873	*A. amphibius*	Tissue	48.2	89.0	Songinot Gol	Mongolia
MSB_289204	*A. amphibius*	Tissue	48.2	89.0	Songinot Gol	Mongolia
MSB_148349	*A. amphibius*	Tissue	61.2	132.7	Amga River	Russia
MSB_148350	*A. amphibius*	Tissue	61.2	132.7	Amga River	Russia

Table S7. Parameters used in stacks for the different datasets analyzed and number of loci and base pairs obtained in each case. Number of loci and SNPs in dataset 2 slightly differs due to the use of two population export formats for the *populations* program.

	Dataset 1	Dataset 2
Parameters in *populations* of Stacks	*m* = 12 *r* = 0.51	*m* = 6 *r* = 1
Total loci	45,813 loci	3,361 loci
Total sequence length	6,642,885 base pairs	487,345 base pairs
Variable loci / SNPs	39,207 loci	2,874 loci / 2877 SNPs
Length in variable loci	5,685,015 base pairs	416,730 base pairs

Table S8. Genetic diversity parameters (π and θ) of the different introns estimated for all *N. fodiens* samples and the two different populations considered.

	All		Iberian		Eurasian	
	π	θ	π	θ	π	θ
ASB6-2	0.0009	0.0034	0.0010	0.0027	0.0005	0.0011
CSF2-2	0.0002	0.0009	0.0003	0.0009	0.0000	0.0000
GDAP1-1	0.0023	0.0010	0.0024	0.0010	0.0021	0.0013
JMJD-2	0.0054	0.0050	0.0036	0.0040	0.0069	0.0032
MYCBPAP-11	0.0055	0.0040	0.0058	0.0032	0.0006	0.0014
TRAIP-8	0.0004	0.0019	0.0002	0.0010	0.0010	0.0012
Nuclear average	0.0025	0.0027	0.0022	0.0021	0.0019	0.0014

Table S9. Basic statistics of the bioinformatic analyses of the genomic libraries before and after filtering the exogenous sequences present in every sample.

	PREFILTERED			FILTERED			
Specimen Code	Assembled reads	Assembled loci	Coverage	Assembled reads	Assembled loci	Coverage	Percentage of endogenous DNA
IBE-C5800	3,426,361	87,674	39.1	2,815,345	51,244	54.9	82.2
IBE-C5801	3,799,579	81,871	46.4	3,223,915	51,114	63.1	84.8
IBE-C5796	15,660,996	112,436	139.3	1,342,487	48,108	27.9	8.6
IBE-C5791	8,251,001	245,821	33.6	4,517,558	52,230	86.5	54.8
IBE-C5795	11,122,396	131,273	84.7	7,130,304	51,550	138.3	64.1
IBE-C4973	3,299,873	83,466	39.5	2,698,496	50,987	52.9	81.8
IBE-C4971	3,448,010	87,047	39.6	2,679,942	50,979	52.6	77.7
IBE-C4968	3,290,333	77,114	42.7	2,846,154	50,932	55.9	86.5
IBE-C5802	3,471,619	89,083	39.0	2,832,729	51,462	55.0	81.6
IBE-C5803	4,185,777	87,169	48.0	3,500,468	52,053	67.2	83.6
IBE-C4986	2,295,282	97,802	23.5	1,676,338	51,098	32.8	73.0
IBE-C4979	2,913,053	81,270	35.8	2,411,892	50,148	48.1	82.8
IBE-C6033	3,462,082	101,741	34.0	1,842,996	49,982	36.9	53.2
IBE-C6027	11,799,850	93,577	126.1	1,369,570	44,944	30.5	11.6
IBE-C6026	6,618,081	145,709	45.4	4,690,568	50,731	92.5	70.9
IBE-C4965	2,232,377	80,341	27.8	1,763,455	49,600	35.6	79.0
IBE-C4966	2,976,810	93,960	31.7	2,120,171	49,994	42.4	71.2
IBE-C2497	4,341,737	139,354	31.2	3,063,097	53,665	57.1	70.6
IBE-C2354	6,420,061	126,652	50.7	4,776,479	53,273	89.7	74.4
IBE-C4975	3,236,023	79,867	40.5	2,596,083	50,195	51.7	80.2
IBE-C4974	1,948,901	86,981	22.4	1,366,608	47,991	28.5	70.1
IBE-C4969	2,693,192	82,608	32.6	2,229,766	51,417	43.4	82.8
IBE-C4970	3,019,630	86,390	35.0	2,426,066	51,681	46.9	80.3
IBE-C4977	2,076,792	91,064	22.8	1,520,958	50,286	30.2	73.2
IBE-C4976	1,760,633	74,562	23.6	1,455,469	49,704	29.3	82.7
IBE-C5797	3,785,135	92,407	41.0	2,942,600	51,069	57.6	77.7
IBE-C5793	10,306,646	176,053	58.5	7,212,609	56,014	128.8	70.0
IBE-C5012	2,891,562	96,721	29.9	2,208,599	51,682	42.7	76.4
IBE-C5010	2,029,993	82,628	24.6	1,539,931	48,875	31.5	75.9
IBE-C5013	6,520,367	168,006	38.8	4,754,722	52,057	91.3	72.9
IBE-C5011	7,500,393	124,048	60.5	5,757,512	53,542	107.5	76.8
IBE-C4356	1,985,169	76,003	26.1	1,566,069	48,586	32.2	78.9
MVZ-155884	8,010,044	106,245	75.4	6,434,560	53,952	119.3	80.3
UAM-64164	6,352,507	137,650	46.1	3,964,195	43,649	90.8	62.4
UAM-64166	1,167,434	54,473	21.4	659,945	29,914	22.1	56.5
MSB-288873	4,716,459	79,076	59.6	3,435,332	44,860	76.6	72.8
MSB-289204	5,779,469	72,191	80.1	3,982,328	42,853	92.9	68.9
MSB-148349	8,358,565	98,527	84.8	6,117,091	46,011	132.9	73.2
MSB-148350	5,756,804	84,216	68.4	4,365,322	45,416	96.1	75.8
Average	4,946,436	102,387	47.4	3,175,326	49,586	63.4	71.3
Sum	192,910,996	3,993,076		123,837,729	1,933,848		

Table S10. Statistics obtained for the library samples depending on the sample type. Values in brackets for the average heterozygosity rate include only individuals from the Cantabrian Mountains population.

	Tissue	Skull
Number of samples	30	9
Average reads before filtering	3,830,938	8,664,761
Average assembled loci before filtering	90,682	141,402
Average reads	2,929,735	3,993,963
Average loci	49,112	51,166
Endogenous DNA (%)	77	53
Coverage	59	76
Average heterozygosity rate	1,134 (1,312)	1,225 (1,272)
Average missing loci (%)	23	22

Table S11. Pairwise F_{st} values obtained between the different populations analyzed.

	Pyrenees	Cantabrian Mountains	Central European
Cantabrian Mountains	0.27 (0.26 - 0.29)		
Central European	0.30 (0.26 - 0.33)	0.34 (0.30 - 0.37)	
A. amphibius	0.65 (0.63 - 0.67)	0.65 (0.63 - 0.67)	0.66 (0.63 - 0.68)

Table S12. Mutation rates estimated in the BEAST2 analysis using orthologues loci from other species of rodents and a fossil calibration point.

Locus name	Rate (mutations/site/yr)
*Arvicola*_45428	2.98E-10
*Arvicola*_42847	5.11E-10
*Arvicola*_27128	7.91E-10
*Arvicola*_40724	8.69E-10
*Arvicola*_3538	9.46E-10
*Arvicola*_13117	9.84E-10
*Arvicola*_21281	1.06E-09
*Arvicola*_27599	1.16E-09
*Arvicola*_6155	1.23E-09
*Arvicola*_11376	1.25E-09
*Arvicola*_1295	1.29E-09
*Arvicola*_25554	1.34E-09
*Arvicola*_22032	1.51E-09
*Arvicola*_15252	1.52E-09
*Arvicola*_45150	1.57E-09
*Arvicola*_34719	1.57E-09
*Arvicola*_8255	1.60E-09
*Arvicola*_25127	1.64E-09
*Arvicola*_5164	1.67E-09
*Arvicola*_45270	1.75E-09
*Arvicola*_2503	1.82E-09
*Arvicola*_36177	1.89E-09
*Arvicola*_38973	1.91E-09
*Arvicola*_539	1.91E-09
*Arvicola*_29000	1.94E-09
*Arvicola*_323	1.96E-09
*Arvicola*_35426	2.01E-09
*Arvicola*_14647	2.13E-09
*Arvicola*_27258	2.14E-09
*Arvicola*_27347	2.15E-09
*Arvicola*_43484	2.16E-09
*Arvicola*_16676	2.17E-09
*Arvicola*_45394	2.20E-09
*Arvicola*_13652	2.23E-09
*Arvicola*_45826	2.28E-09
*Arvicola*_8901	2.35E-09
*Arvicola*_11509	2.36E-09
*Arvicola*_49832	2.36E-09
*Arvicola*_32730	2.38E-09
*Arvicola*_40032	2.39E-09
*Arvicola*_8735	2.39E-09
*Arvicola*_46446	2.43E-09
*Arvicola*_21065	2.45E-09
*Arvicola*_50749	2.46E-09

*Arvicola*_2944	2.47E-09
*Arvicola*_18146	2.49E-09
*Arvicola*_50803	2.52E-09
*Arvicola*_11593	2.58E-09
*Arvicola*_5283	2.60E-09
*Arvicola*_22238	2.63E-09
*Arvicola*_45768	2.71E-09
*Arvicola*_28997	2.72E-09
*Arvicola*_9776	2.79E-09
*Arvicola*_25695	2.80E-09
*Arvicola*_23832	2.93E-09
*Arvicola*_15494	2.95E-09
*Arvicola*_14543	2.95E-09
*Arvicola*_17227	3.02E-09
*Arvicola*_46856	3.04E-09
*Arvicola*_23384	3.14E-09
*Arvicola*_7123	3.18E-09
*Arvicola*_40876	3.25E-09
*Arvicola*_17389	3.29E-09
*Arvicola*_7454	3.36E-09
*Arvicola*_26217	3.44E-09
*Arvicola*_34108	3.45E-09
*Arvicola*_28823	3.50E-09
*Arvicola*_28389	3.52E-09
*Arvicola*_23533	3.53E-09
*Arvicola*_6124	3.71E-09
*Arvicola*_37324	3.78E-09
*Arvicola*_14628	3.79E-09
*Arvicola*_19415	3.83E-09
*Arvicola*_45177	3.94E-09
*Arvicola*_5737	4.11E-09
*Arvicola*_49442	4.17E-09
*Arvicola*_14128	4.18E-09
*Arvicola*_34910	4.19E-09
*Arvicola*_51131	4.22E-09
*Arvicola*_6366	4.23E-09
*Arvicola*_30646	4.29E-09
*Arvicola*_30182	4.45E-09
*Arvicola*_11439	4.58E-09
*Arvicola*_5712	5.02E-09
*Arvicola*_50070	5.33E-09

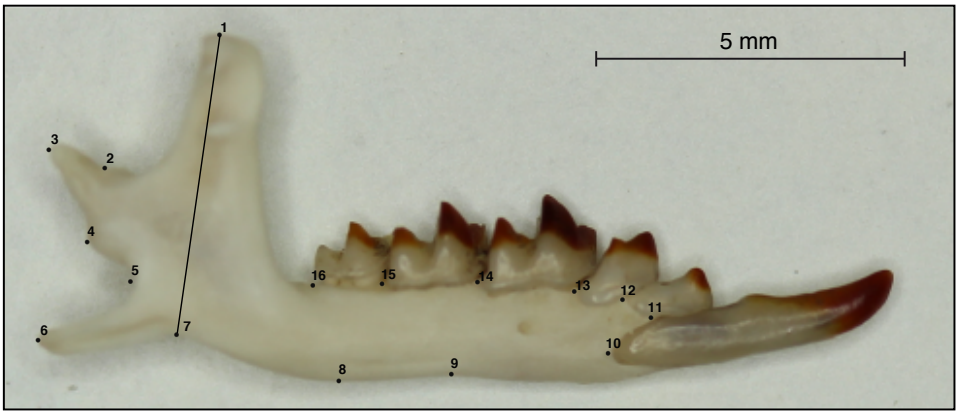

Figure S1. Landmarks selected in this study in order to estimate the centroid size and perform principal components analysis. Landmarks 1 and 7 were used to calculate the height of the coronoid process, as shown with the line.

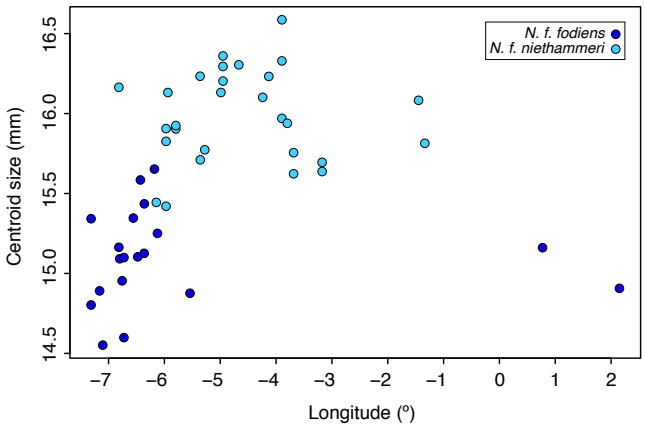

Figure S2. Plot across longitude showing differences in skull size of *N. fodiens* subspecies found in the Iberian Peninsula, as measured with the centroid size of the 16 landmarks selected.

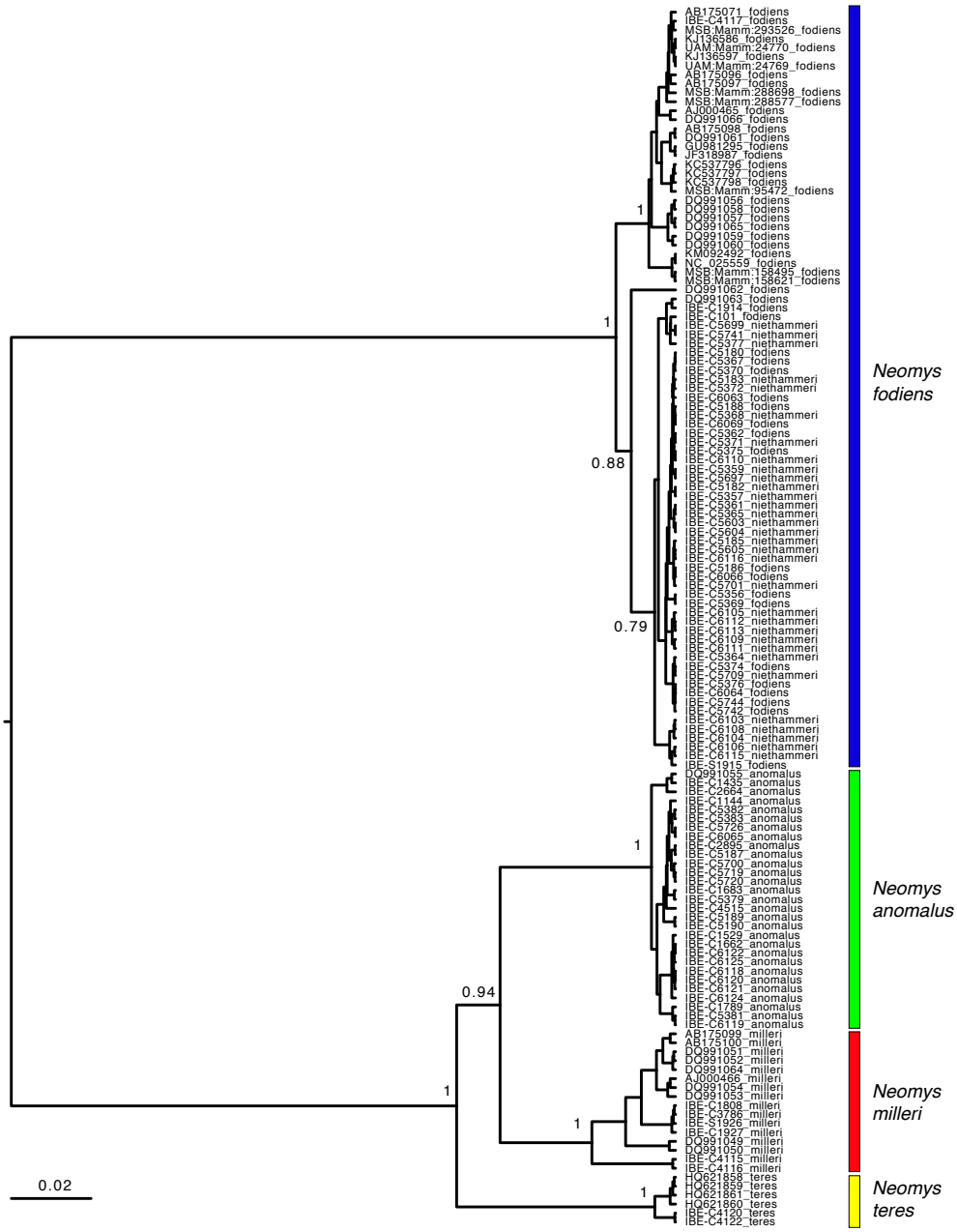

Figure S3. Bayesian phylogenetic tree of sequences obtained in this work plus sequences from Igea et al. (2015) and sequences downloaded from GenBank. The scale is in substitutions per position. Posterior probabilities are indicated for the species and the clades mentioned in the text.

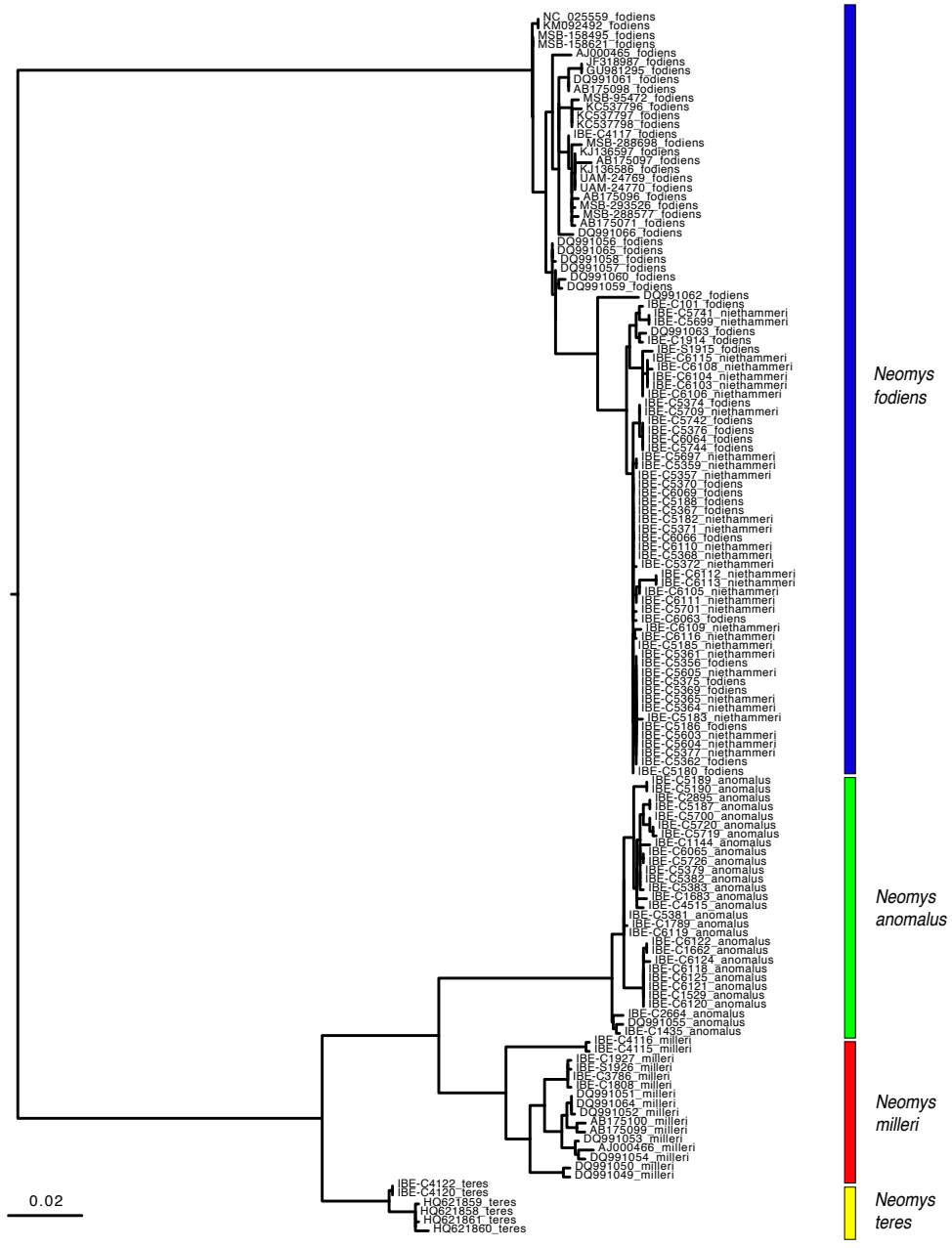

Figure S4. RAxML phylogenetic tree of sequences obtained in this work plus sequences from Igea et al. (2015) and sequences downloaded from GenBank, performed with 100 starting trees. The scale is in substitutions per position.

PUBLICATION

www.nature.com/scientificreports

SCIENTIFIC REPORTS
nature research

Corrected: Publisher Correction

OPEN

Size increase without genetic divergence in the Eurasian water shrew *Neomys fodiens*

Alfonso Balmori-de la Puente[1], Carlos Nores[2], Jacinto Román[3], Angel Fernández-González[4], Pere Aymerich[5], Joaquim Gosálbez[6], Lídia Escoda[1] & Jose Castresana[1*]

When a population shows a marked morphological change, it is important to know whether that population is genetically distinct; if it is not, the novel trait could correspond to an adaptation that might be of great ecological interest. Here, we studied a subspecies of water shrew, *Neomys fodiens nietham meri*, which is found in a narrow strip of the northern Iberian Peninsula. This subspecies presents an abrupt increase in skull size when compared to the rest of the Eurasian population, which has led to the suggestion that it is actually a different species. Skulls obtained from owl pellets collected over the last 50 years allowed us to perform a morphometric analysis in addition to an extensive multilocus analysis based on short intron fragments successfully amplified from these degraded samples. Interestingly, no genetic divergence was detected using either mitochondrial or nuclear data. Additionally, an allele frequency analysis revealed no significant genetic differentiation. The absence of genetic divergence and differentiation revealed here indicate that the large form of *N. fodiens* does not correspond to a different species and instead represents an extreme case of size increase, of possible adaptive value, which deserves further investigation.

Phylogeographic studies allow researchers to understand not only the geographical distribution of genetic diversity, but also the evolution of phenotypic differences that might have adaptive potential[1,2]. Changes in body size are among the most important sources of phenotypic variation in endothermic vertebrates[3,4]. They can occur across a clinal variation as a consequence of the changing environment[5], in islands due to ecological release[6], or be restricted to a limited region within a species' range due to local adaptation[7]. In some of these cases, populations with different body sizes are recognized as subspecies. Other instances of body-size modification in specific areas do not result in taxonomic changes as they are likely to correspond to ecotypes that can exploit new resources, more accessible to individuals with either smaller or larger body sizes[8–10]. Understanding the origin and evolution of such body size changes and whether these arose through a process of isolation or a rapid ecological adaptation requires a thorough phylogeographic and population genetics analysis, something that many studies on this topic lack.

The Eurasian water shrew (*Neomys fodiens*) is a good example of where the relationship between body size variation and phylogeography can be studied. This species has a Eurasian distribution, ranging from the northern Iberian Peninsula to eastern Asia[11]. It is a semi-aquatic species that inhabits water courses and other wetland habitats with abundant invertebrate prey[11,12]. Among the four species described in the genus[13], *N. fodiens* is considered the most aquatic due to its excellent diving ability, although it sometimes demonstrates terrestrial behavior[12,14].

Several subspecies have been proposed for *N. fodiens*, but none has been adequately assessed, with the exception of *N. f. niethammeri*[15]. This taxon is present in the north-central Iberian Peninsula, from the Cantabrian Range to the western end of the Pyrenees (Supplementary Fig. S1)[16–19], and is characterized by the largest skull size observed throughout the range of *N. fodiens*[19]. This size increase in a specific population is striking, as the morphology of this species is fairly stable across the rest of its European range[20]. *N. f. niethammeri* lives sympatrically with *N. anomalus*[21], which was recently separated from the European species *N. milleri*[13,22]. A population

[1]Institute of Evolutionary Biology (CSIC-Universitat Pompeu Fabra), Passeig Marítim de la Barceloneta 37, 08003, Barcelona, Spain. [2]Indurot, Universidad de Oviedo, Campus de Mieres, 33600, Mieres, Asturias, Spain. [3]Department of Conservation Biology, Doñana Biological Station, CSIC, Calle Americo Vespucio 26, 41092, Sevilla, Spain. [4]Biosfera Consultoría Medioambiental S.L., Calle Candamo 5, 33012, Oviedo, Spain. [5]Calle Barcelona 29, 08600, Berga, Barcelona, Spain. [6]Department of Evolutionary Biology, Ecology and Environmental Sciences, University of Barcelona, Avinguda Diagonal 645, 08028, Barcelona, Spain. *email: jose.castresana@csic.es

of the nominal subspecies *N. f. fodiens* is found beyond the range of *N. f. niethammeri*[12], making that the population of *N. f. niethammeri* is flanked by populations of *N. f. fodiens* (Supplementary Fig. S1). Coronoid height has been widely used to differentiate *Neomys* species in paleontological and neontological studies[17,23–25], and is also the main character to distinguish *N. f. niethammeri*[16–19]. Due to the much larger size of the latter, it has been suggested that it is a different species in numerous studies, including the most important reference works on mammals[11,15,18,19].

Improved laboratory techniques, many adopted from ancient DNA studies that target low quality and degraded DNA, have enabled the use of non-invasive and minimally invasive samples as well as different types of post mortem remains in phylogeographic studies[26,27]. This has made it possible to genetically analyze elusive and threatened species, as larger sample sets that do not require the manipulation or capture of specimens become available for study[22,28,29]. For example, skull bones obtained from owl pellets containing undigested material from small mammal prey have been used in various phylogeographic studies[30–32]. This material is very interesting as it can be used for both morphological and genetic work. However, despite this potential, few studies have taken advantage of skull bones from owl pellets for simultaneous genetic and morphometric analyses and, in particular, to recover nuclear data.

Mitochondrial DNA is more abundant than nuclear DNA in animal cells and can be more easily amplified from degraded samples. Nevertheless, mitochondrial introgression, which is a common phenomenon in mammals, may lead to erroneous conclusions if only mitochondrial genes are considered[33,34]. The development of highly variable nuclear markers avoids the problems of using solely mitochondrial sequences and allows the use of coalescent-based methods[35,36], thus leading to robust conclusions on the origin and evolution of biodiversity[13,33,37,38]. It is therefore important to develop nuclear markers that can be amplified from degraded samples, in which the DNA fragment size is shorter. In order to amplify these short fragments, primers need to be designed to reduce the size of the PCR product so that more DNA becomes available for amplification, thus exploiting the full potential of multilocus information.

The main objective of this work was to understand whether the size increase observed in *N. f. niethammeri* is linked to genetic distinctiveness. To discern this, we first designed novel nuclear introns that could be amplified using skull bones extracted from barn owl pellets collected over recent decades. From this material we then amplified mitochondrial and nuclear markers, and performed a morphological analysis as well as a multilocus study of genetic divergence, differentiation, and diversity. The results showed that the relationship between phenotypic novelty and phylogeography is not always easily predictable.

Results

Morphometric analyses of *Neomys* mandibles. Skull samples from 67 *Neomys* individuals (Supplementary Table S1) were obtained, primarily, from barn owl pellets collected over the last 50 years in the northern Iberian Peninsula. The samples came from approximately longitudes −7° to 2°, where two subspecies of *N. fodiens*, as well as *N. anomalus*, are present (Fig. 1). Landmarks were taken from each mandible (Supplementary Appendix S1) to measure the coronoid height and perform a geometric morphometric analysis. According to the coronoid height (Supplementary Fig. S2), 32 samples were classified as *N. f. niethammeri*, 19 as *N. f. fodiens*, and 16 as *N. anomalus* (Supplementary Table S2). Plotting these measurements against longitude, we confirmed an abrupt size increase in *N. f. niethammeri* in the north-central part of the Iberian Peninsula, approximately between longitudes −6.25° and −1° (Fig. 1c), corroborating previous work[17,18]. We found individuals of both sizes in the same locality, indicating a certain overlap in the distribution of the two groups. The skulls of the sympatric species *N. anomalus* were always smaller than those of *N. fodiens* (Supplementary Table S2). The centroid size of the mandibles provided similar results (Supplementary Fig. S3 and Supplementary Table S2). A principal components analysis of the landmarks allowed *N. anomalus* to be distinguished from *N. fodiens*, but not *N. f. niethammeri* from *N. f. fodiens* (Fig. 2), indicating that the two *N. fodiens* subspecies were similar in shape.

Mitochondrial phylogeny of *Neomys*. Both complete and partial mitochondrial cytochrome *b* sequences were obtained from 85 samples of *N. fodiens*, including all the mandibles used in the morphometric analysis plus additional tissue samples from Eurasia (Fig. 1 and Supplementary Table S1). Some primers were newly designed (Supplementary Table S3) so that sequences could be obtained from the majority of samples, including the oldest (Supplementary Table S1). The Bayesian mitochondrial tree reconstructed with the *N. fodiens* mitochondrial sequences can be subdivided into three main clades separated by relatively long branches and moderate or high support (Fig. 3): one includes the Iberian samples and a sample from a nearby locality in France; the second consists of a single sample from southern Italy; and the third comprises samples from the remaining Eurasian range of the species. Coronoid height measurements mapped into this tree indicated that individuals classified as *N. f. niethammeri* appeared randomly across the Iberian clade, reflecting the fact that the two subspecies were indistinguishable at the mitochondrial level. When additional sequences from other *Neomys* species were included in the Bayesian phylogenetic analysis to configure a dataset of 136 sequences, the tree perfectly separated the four species in the genus, but *N. f. fodiens* and *N. f. niethammeri* were once again intermixed in the tree (Supplementary Fig. S4). Similar results were obtained with a maximum-likelihood method (Supplementary Fig. S5).

Development of nuclear markers for degraded *Neomys* samples. We developed a set of six short intron markers (ASB6 intron 2, CSF2 intron 2, GDAP1 intron 1, JMJD intron 2, MYCBPAP intron 11, and TRAIP intron 8) that could be amplified using DNA extracted from the mandibles, despite the high degradation levels of some of them (Supplementary Table S4). For some introns, several rounds of primer design were performed to shorten the PCR product and allow the amplification of the most degraded samples (Supplementary Table S4). In this way, we obtained nuclear information from most of the recent samples, as well as from a good proportion of the older samples, including those collected during the 1970s (Supplementary Table S1). For some introns,

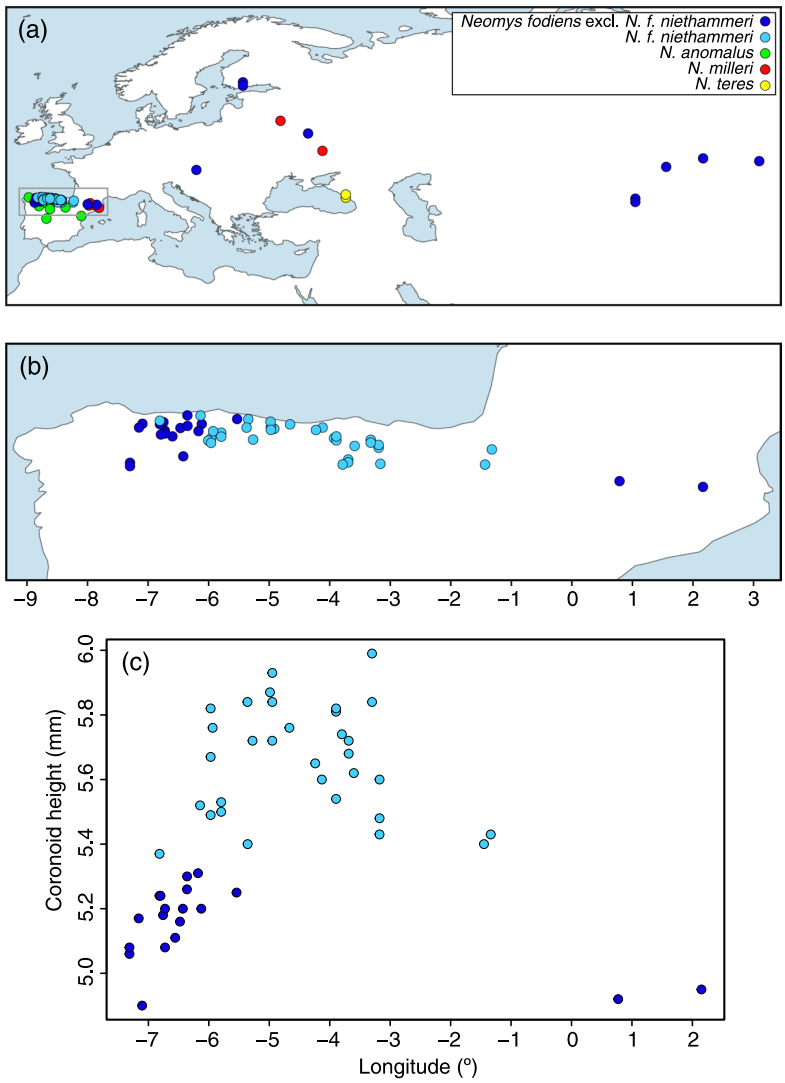

Figure 1. Distribution of the samples used in this study. (**a**) Map of all *Neomys* samples with the main study area highlighted, (**b**) enlargement of the northern Iberian Peninsula showing only *N. fodiens* specimens, and (**c**) plot across longitude in the Iberian Peninsula showing differences in skull size as measured using the coronoid height for *N. fodiens*. Samples from Igea *et al.*[13] are included but sequences from databases are not. Note that the samples of *N. fodiens* not corresponding to *N. f. niethammeri* may include several subspecies: the European specimens most likely correspond to *N. f. fodiens* but those from Central Asia may belong to other subspecies whose ranges are not clearly delimited.

allele-specific primers were designed to separate heterozygous sequences (Supplementary Table S5). A total of 58 samples with a minimum of four sequenced introns were used in further analyses, including 37 mandibles and 11 tissues, together with sequences from 10 samples taken from a previous work[13] (Supplementary Table S1). Considering all the introns together, 172 sequences were used from *N. f. niethammeri*, 250 from the other *N. fodiens* specimens, 158 from *N. anomalus*, 48 from *N. milleri*, and 24 from *N. teres*, totaling 123,556 bp of nuclear sequence information after alignment cleaning (Supplementary Appendix S2).

Multilocus phylogenetic analysis of *Neomys*. Haplotype genealogies derived from the maximum-likelihood trees of the nuclear sequences showed a low degree of allele sharing between the four *Neomys* species (Fig. 4a). On the other hand, *N. f. niethammeri* and the rest of *N. fodiens* shared the most frequent alleles (largest circles in Fig. 4a), although most minor alleles were exclusive to one group or the other (smaller circles in Fig. 4a). Since the mutational differences between the alleles were minimal, both groups were completely

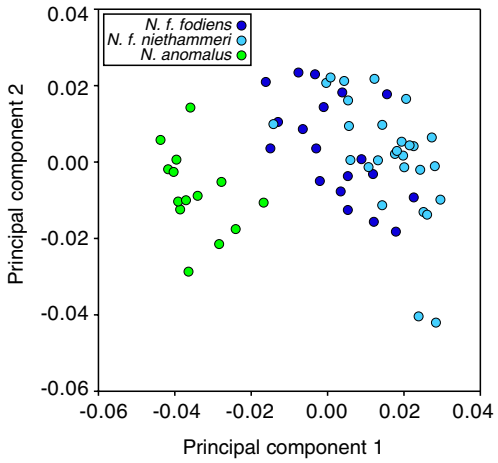

Figure 2. Principal components analysis of the mandible landmarks of Iberian *N. fodiens* and *N. anomalus* individuals.

intermixed in the phylogenetic tree reconstructed using the concatenated intron sequences (Fig. 4b). In fact, no clades within *N. fodiens* can be distinguished in the nuclear tree.

Genetic differentiation. To study the possibility that differentiated groups existed within *N. fodiens*, we next converted the six intron alignments into a multi-allelic data format. There were 22 different alleles and therefore the average number of alleles per locus was 3.7. Using this information, we calculated the F_{ST} distance between *N. f. niethammeri*, *N. f. fodiens* from the northern Iberian Peninsula, and *N. fodiens* from the rest of the range. The value obtained between *N. f. niethammeri* and Iberian *N. f. fodiens* was 0.040 and it was not significant (95% confidence interval: −0.005, 0.085). F_{ST} values between these and the other population were also non-significant.

Nuclear genetic diversity of *N. fodiens* populations. Individual heterozygosity estimated from the nuclear introns of *N. fodiens* specimens showed that the most heterozygous samples were from the northern Iberian Peninsula (Fig. 5). Thus, we found an average of 0.0013 heterozygous positions in the Iberian samples (including both *N. f. fodiens* and *N. f. niethammeri*) versus 0.0004 in the rest of the sampled range. When the nuclear data was analyzed at the population level, the average θ values were 0.0021 and 0.0014 for these two groups, respectively (Supplementary Table S6), showing the same trend. The same was found with the π parameter (Supplementary Table S6).

Discussion

The multilocus dataset used in this study of the Eurasian water shrew *Neomys fodiens* was based on the mitochondrial cytochrome *b* gene and six small intron fragments. The lengths of the newly designed introns (153–229 bp) were smaller than those of previously proposed intron markers[13,37], in order to facilitate the amplification of degraded DNA obtained from skulls from owl pellet material. Using the novel primers, we amplified between 4 and 6 introns from 37 mandible samples of *Neomys*, many of which had been collected during the 1970s (Supplementary Table S1). Despite their relatively short lengths, the intron markers were variable enough to detect mutational differences between species. They also enabled the reconstruction of a nuclear phylogenetic tree, which was compared with the mitochondrial tree and used to detect any possible occurrence of mito-nuclear discordance in *Neomys*. Finally, once these intron markers were converted to allele frequency data, and despite the small number of markers used, they allowed us to undertake a differentiation analysis of the main populations of *N. fodiens*. Therefore, thanks to the various genetic analyses performed, these novel markers were highly useful in unraveling the evolutionary history of *N. f. niethammeri* and, specifically, assessing whether the morphological differences observed (large skull size) arose through a long period of isolation and genetic differentiation. Furthermore, to our knowledge, this is one of the first studies where multilocus genetic data as well as morphometric information of skulls obtained from owl pellets has been fully exploited, showing the enormous potential of this type of non-invasive sampling for biodiversity studies.

The mitochondrial sequences of *N. f. fodiens* and *N. f. niethammeri* were intermixed in the phylogenetic tree, meaning that there was no evidence to suggest genetic divergence (Figs 3 and S4). This was a highly unexpected result for two populations with important skull size differences. Without further data, a possible explanation could be that, in fact, these two forms were more divergent at the nuclear level but, due to some recent unidirectional introgression event, *N. f. niethammeri* acquired the mitochondria of *N. f. fodiens*, a phenomenon that has been observed in many other species[33,34]. With *N. anomalus* living sympatrically with *N. fodiens* in the northern Iberian Peninsula, additional scenarios involving inter-specific introgression with this other species could not be discarded, demonstrating the need to carry out a nuclear analysis. The phylogenetic tree we obtained using nuclear data also revealed a lack of genetic divergence between the two *N. fodiens* subspecies (Fig. 4b). A first

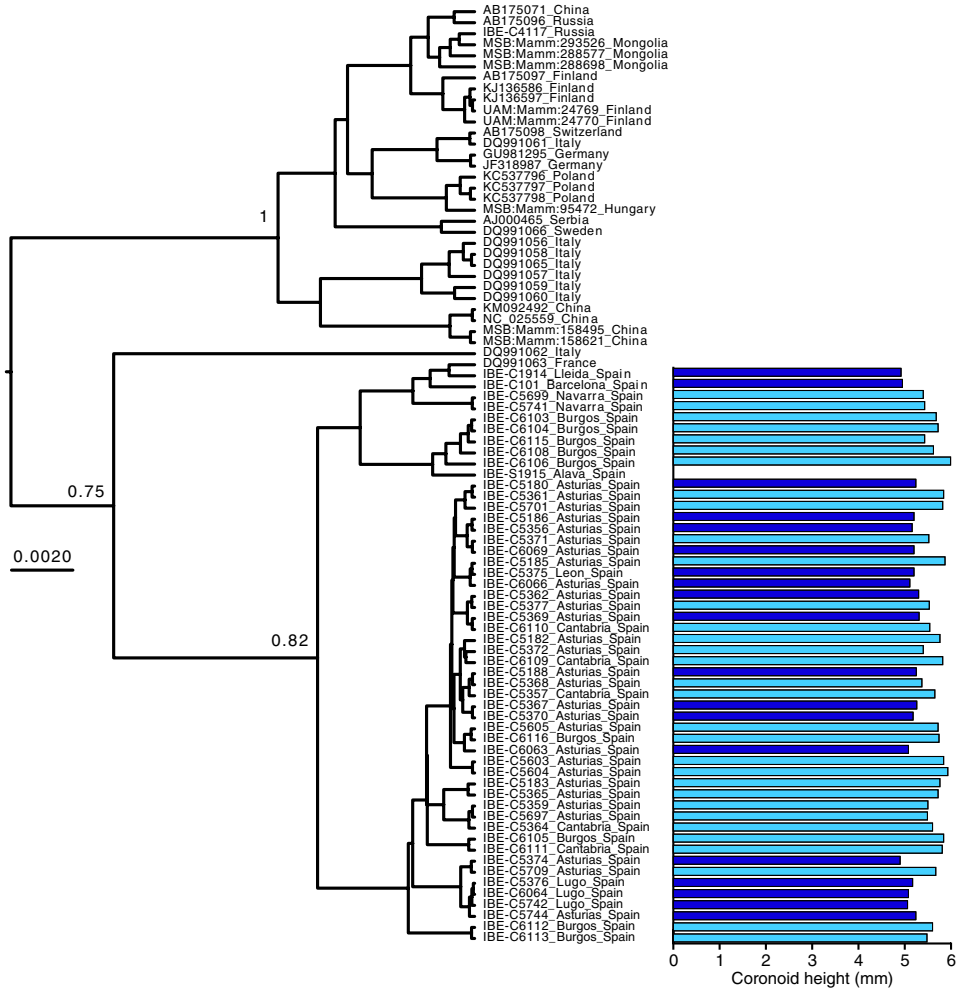

Figure 3. Bayesian tree of *N. fodiens* cytochrome *b* sequences. Samples with coronoid height measurement are represented with color-coded bars showing their skull size: dark blue for *N. f. fodiens* and light blue for *N. f. niethammeri*. The scale is in substitutions per position and posterior probabilities are indicated for the clades mentioned in the text.

conclusion from this work is, therefore, that our mitochondrial and nuclear data are consistent in highlighting a lack of support for genetic divergence between *N. f. fodiens* and *N. f. niethammeri*.

The mitochondrial and nuclear phylogenies showed that the four *Neomys* species were reciprocally monophyletic in both trees (Figs 4b and S4). This suggests that there has been no recent mitochondrial introgression, not only between *N. fodiens* groups, but also during the evolution of the *Neomys* species. Incidentally, the topological relationships between the four *Neomys* species were not coincident in the mitochondrial and nuclear trees, since *N. milleri* and *N. anomalus* group in the former, whereas *N. milleri* and *N. teres* appear as sister taxa in the latter. However, this could be a consequence of methodological difficulties in resolving old divergences in the tree or incomplete lineage sorting[39], and it does not affect the conclusion that there has been no recent introgression in *Neomys*. This reasonable mito-nuclear agreement enables the use of cytochrome *b* for species identification from non-invasive samples in further ecological studies of this genus[22].

Populations that have been isolated for a short period of time may not have accumulated enough mutations to reflect phylogenetic separation, but, if the gene flow between them is low, differences in allele frequencies may appear by genetic drift[40,41]. To test the possibility that *N. fodiens* populations showed some degree of differentiation, we computed F_{ST} statistics. No significant genetic differentiation was found. Thus, the increase in skull size of *N. f. niethammeri* (Fig. 1c) corresponded to neither a difference in shape (Fig. 2) nor mitochondrial (Fig. 3) or nuclear genetic divergence (Fig. 4b), nor genetic differentiation of nuclear allele frequencies. In this respect, it is interesting to note that fossil data of both forms have been found at ~40 kyr[24,25]. This would suggest that a large amount of gene flow must have occurred between the two forms to prevent genetic differentiation during all this time, indicating the lack of reproductive barriers between them.

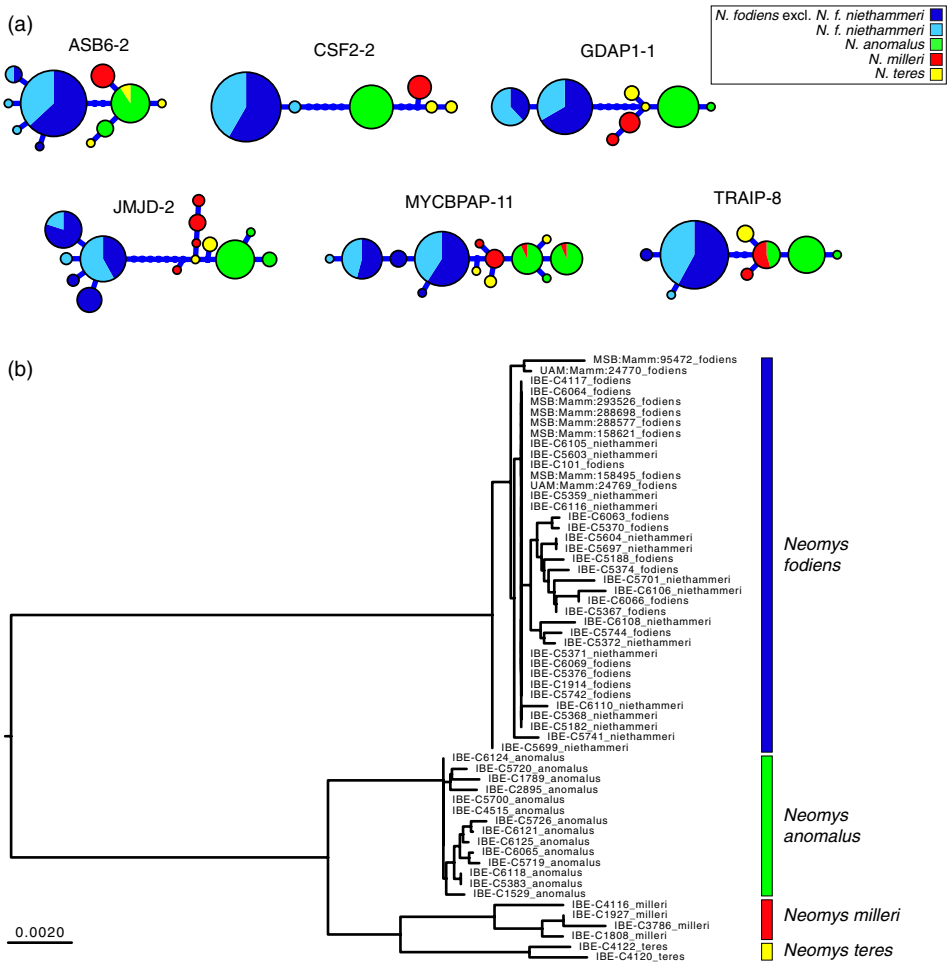

Figure 4. Phylogenetic information derived from the 6 introns amplified in the *Neomys* samples. (**a**) Haplotype genealogies where the size of the circles is proportional to the number of alleles detected. (**b**) Distance tree for the concatenated introns with the scale in substitutions per position.

The populations of *N. fodiens* of the northern Iberian Peninsula are at the edge of the Palearctic range of the species (Supplementary Fig. S1), which could lead to the hypothesis that this area was recently colonized from the multiple European glacial refugia that have been described for various taxa[42,43]. We found, however, that the nuclear genetic diversity was higher in the Iberian samples than in the rest of the Palearctic samples analyzed here (Fig. 5), something that is not consistent with the recent colonization of the Iberian Peninsula. The existence in this area of fossil *N. fodiens* dated at ~40 kyr[24,25,44] also supports the idea that the species was present in the Iberian Peninsula long before the Last Glacial Maximum and, consequently, that these populations are not the product of recent colonization. Instead, refugia in the Iberian Peninsula or nearby areas were likely to have been the source for the recolonization of at least some parts of the western Palearctic[45,46].

With regard to the taxonomic debate surrounding *N. f. niethammeri*, the phylogenetic analyses performed here, using mitochondrial and intron sequences, indicate that *N. f. niethammeri* has not accumulated measurable genetic divergence with respect to *N. f. fodiens*. There is also no significant genetic differentiation between them, meaning that also allele frequencies are similar. Taking all this information into account, it is clear that *N. f. niethammeri* cannot be considered an independent species, contradicting previous studies where it was suggested that *N. f. niethammeri* might warrant species status[11,15,18,19]. An alternative suggestion is that *N. f. niethammeri* is an ecotype, although further work would be required to corroborate this point.

Indeed, the lack of genetic divergence and differentiation revealed here suggests that the large skull of *N. f. niethammeri* possibly arose as an adaptation to the environment. Two main hypotheses can be used to explain this. Firstly, a previous hypothesis proposed that more calcareous substrates present in the central part of the Cantabrian Range could have resulted in rivers richer in nutrients and a consequent selection of individuals with better-developed mandibles to capture larger prey[17,18]. However, *N. fodiens* lives in other areas with calcareous

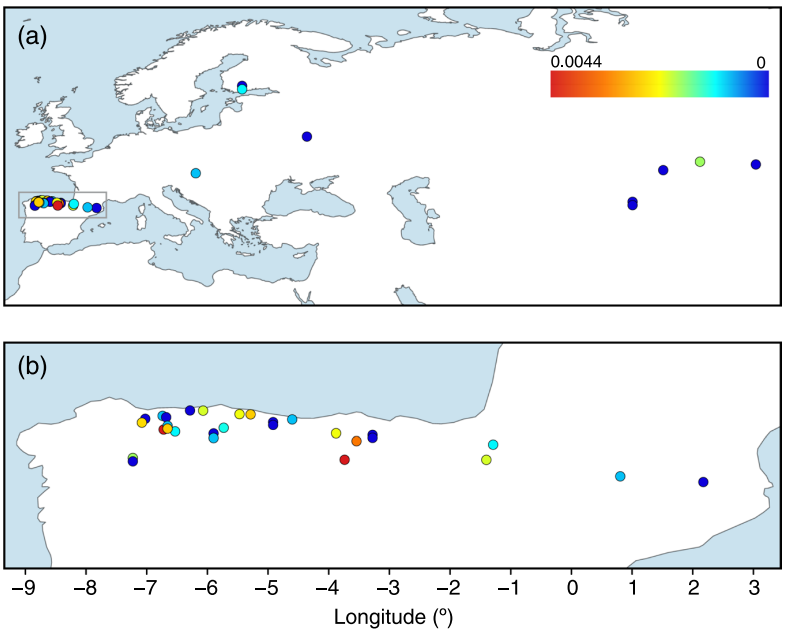

Figure 5. Map of color-coded individual heterozygosity rates in *N. fodiens*. (**a**) Map of all samples with the main study area highlighted, and (**b**) enlargement of the northern Iberian Peninsula. The scale is in number of heterozygous positions per base.

substrates where it displays no change in body size, so this is unlikely to have been the sole driver. Alternatively, the size increase of *N. f. niethammeri* could have resulted from ecological displacement due to competition with the Iberian endemic *N. anomalus*, similar to that observed in other mammals[47,48]. An increase in the size of *N. f. niethammeri* could have favored access to new resources, for example larger prey, thus limiting competition with *N. anomalus*. In principle, both species occupy the same aquatic habitat in the northern Iberian Peninsula and most of the range of *N. f. niethammeri* overlaps with that of *N. anomalus*[12,21], making competition between the two species possible. The interaction of *N. fodiens* with *N. milleri* has been studied in Europe, where both species live sympatrically[49]. However, the interaction of *N. fodiens* with *N. anomalus* when they live sympatrically has never before been studied, and this may be totally different to that which occurs when it coincides with *N. milleri*, so we do not know if and how this interaction could have stimulated a size increase in *N. f. niethammeri*. We therefore suggest that future studies be directed at understanding the micro-habitat and inter-specific interactions of these *Neomys* species. We hope that a combined genetic and ecological approach will help unravel why *N. f. niethammeri* experienced an abrupt increase in skull size across a narrow strip in the Iberian Peninsula, and reveal the evolutionary advantages and possible ecological consequences of this phenotypic novelty.

Methods

Sample collection. A total of 79 samples from the Palearctic range of the genus *Neomys*, with special emphasis on *N. f. niethammeri* and *N. f. fodiens* from the Iberian Peninsula, were analyzed (Fig. 1 and Supplementary Table S1). These included 68 skull samples from barn owl pellets collected in the field, of which 65 could be used for genetics and morphometry, and 3 could only be used for genetic analysis. Some of these samples had been analyzed in a previous morphological study of *N. f. niethammeri*[17]. In addition, 9 tissue samples were loaned from museums and colleagues, and 2 tissue samples were taken from our own collection.

To complete the phylogenetic analysis, cytochrome *b* and nuclear sequences of 18 *Neomys* samples were taken from Igea *et al.*[13] and 39 cytochrome *b* sequences were downloaded from GenBank[50]. Two of the *N. fodiens* skull samples available from Igea *et al.*[13] were used for morphometry.

Ethics statement. No live animals were collected for this study and therefore no ethics permit was necessary.

Measurements and geometric morphometric analysis. After cleaning the skulls extracted from the owl pellets, we used only one lower mandible per skull and the rest was stored. Images of the 67 mandibles, together with a scale, were taken with a Canon 100D camera and a Canon EF-S 60 mm f/2.8 macro objective. The ImageJ 1.50i[51] program was then utilized to take 16 landmarks from each sample (Supplementary Fig. S2 and Supplementary Table S2). Many of the mandibles were partially broken or without teeth due to the digestion process so that no landmarks were taken in teeth. Landmarks 1 and 7 were used to calculate the coronoid height (for six partial mandibles, only these two landmarks could be obtained). According to previous works, the coronoid height ranges considered to discriminate the different taxa were: ≤4.70 mm for *N. anomalus*; 4.80–5.35 mm for *N. f. fodiens*; and >5.35 mm for *N. f. niethammeri*[19,23]. With the coordinates of the 16 landmarks, and using MorphoJ

version 1.06d[52], we made a Procrustes fit, calculated the centroid size, and performed a principal components analysis from the covariance matrix. Landmark coordinates of the mandibles used in this study are available in TPS format in Supplementary Appendix 1.

DNA extraction, PCR amplification and sequencing. The photographed mandibles were then used for DNA extraction. They were first powdered using liquid nitrogen and a mortar after which genomic DNA was extracted with a QIAamp DNA Micro kit. In the case of tissues, DNA was extracted with a DNeasy Blood & Tissue Kit (QIAGEN) following the recommended protocol. Extractions of all degraded samples were performed in a separate room with UV irradiation to avoid contamination. Extraction blanks were always present in order to detect any possible contamination at each step. Additionally, pre-PCR procedures were developed in a dedicated UV-hood, in a controlled, sterile room.

Complete cytochrome *b* sequences (1140 bp) from *N. fodiens* samples were amplified in three fragments using already published primers[13] with slight modifications to improve amplification (Supplementary Table S3). In addition, primers for a smaller fragment of 226 bp were developed with the purpose of amplifying DNA from the most degraded samples (Supplementary Table S3). The length amplified in each sample is shown in Supplementary Table S1.

For the nuclear markers, a set of six new primer pairs were designed starting from intron markers previously developed for *Neomys*[13]. The primers were placed in conserved intronic regions or exons that spanned small fragments (between 153 and 229 bp) and flanked the highest possible number of polymorphic sites. Some markers were amplified with more than one primer pair in various samples, as we reduced the amplified intron length during the work to enable the amplification of degraded samples that failed with the initial primers (Supplementary Table S4). PCR reactions were performed in a final volume of 25 µl with 2–6 µl genomic DNA, 0.15 µl of Promega GoTaq DNA polymerase, and 1 µM of each primer. The cycling conditions included an initial denaturation step of 30 s at 95 °C, followed by 40 cycles of denaturation (30 s at 95 °C), annealing (60 s at 54 °C for cytochrome *b* and 65 °C for introns), and extension (60 s at 72 °C), as well as a final extension of 5 min at 72 °C. For the most degraded skull samples, an alternative protocol using the QIAGEN Multiplex PCR was performed in a final volume of 50 µl with 4 µl of genomic DNA, 0.3 µM of each primer, and 25 µl of PCR Master Mix. In this case, there was an initial heat activation step of 15 min at 95 °C, the denaturation step was at 94 °C, the annealing temperature was lowered to 63 °C for the introns, and the annealing time was extended to 90 s. PCR products were purified using ExoSAP-It (Affymetrix) and sequenced at Macrogen Inc. Sequences were assembled using Geneious Pro 5.1.7 (https://www.geneious.com).

In introns where two or more variable sites were present in a sample, PHASE version 2.1.1[53] with a threshold of 0.9 was used to phase the alleles. When the program did not produce results or length-heterozygous alleles were present, allele-specific primers were used to independently amplify the two alleles. Allele-specific primers consist of two primers that are identical to one another except for the last nucleotide, which is situated over a polymorphic position of the sequence to be phased. The use of this type of primers was suggested for the sequencing reaction[54], although in this work we used them both for amplifying and sequencing. To design them, a polymorphic position was selected and two 19–20 nucleotide primers were synthetized, each of which had one of the two possible nucleotides placed at the 3′ end. Then, two independent PCR reactions were performed, one for each allele-specific primer, and using the opposite original primer at the other side of the polymorphic region for amplification. In this way, two PCR products, corresponding to the two alleles, were obtained. Finally, each PCR product was sequenced with the corresponding allele-specific primer to obtain the resolved partial allele, which was then assembled with the original PCR sequence to obtain the complete allele[54]. The primers used for PCR allele-specific resolution are shown in Supplementary Table S5.

Phylogenetic analyses of cytochrome *b*. Since some cytochrome *b* sequences were completely amplified whereas others were only partial (Supplementary Table S1), they were aligned using MAFFT version 7.130[55] with the *maxiterate* option enabled.

A Bayesian tree of the cytochrome *b* sequences was built using BEAST version 2.5.0[56]. To select a statistically appropriate model, a Bayes factors approach based on path sampling[57] was used with 96 complete sequences. Markov chain Monte Carlo analyses were based on 100 steps of 10,000,000 generations sampled each 1,000 generations, 10% preburn-in, 10% burn-in, and an alpha parameter of the Beta distribution to divide steps of 0.3. The convergence of each tree was checked in Tracer v1.7.1, from the same software package. Different priors were tested for each parameter category, and a more complex model was selected only if it converged and improved the log marginal likelihood by more than 5, as recommended[57]. Using these criteria, the selected model was the following: HKY substitution model with estimated base frequencies and Gamma site heterogeneity for each partition (unlinked substitution models); a strict clock model for all partitions (linked clock model); and a coalescent constant size tree model. Once the best model had been selected, it was applied to the sequences of either all *Neomys* species or only *N. fodiens*. In these cases, 50,000,000 generations were run. Consensus trees were calculated using the TreeAnnotator program (BEAST2 package) with median heights.

For comparison, a maximum-likelihood tree of all sequences was reconstructed with RAxML version 8.0.19[58] using a GTR substitution model (as recommended in the manual of this program), rate heterogeneity modeled with a Gamma distribution, and 100 randomized maximum-parsimony starting trees. Mid-point rooting was used to represent the tree.

Multilocus analyses. The *Neomys* alleles showed some differences in length due to small indels. They were aligned with MAFFT version 7.130[55] with the *maxiterate* option enabled. Then, a few gap positions as well as a few positions with unknown nucleotides were removed from each alignment. The six final alignments are available in FASTA format in Supplementary Appendix S2.

A maximum-likelihood tree was reconstructed with RAxML[58] from each alignment as before. For each of these trees, haplotype genealogies were constructed using Haploviewer[59].

In addition, we reconstructed a phylogenetic distance tree from the intron alignments, as in Igea *et al*.[13]. First, pairwise distances were calculated in such a way that the two alleles of each sequence were taken into account by making all possible comparisons between alleles[60], and correcting for multiple substitutions using the Jukes-Cantor formula. The pairwise distance matrix was then utilized to construct a tree with the Fitch program of the Phylip software package[61]. Mid-point rooting was used to represent the tree.

Genetic differentiation. Intron alignments were converted to a diploid multi-allelic data format by assigning a number to each allele. Then, pairwise F_{ST} for all populations was calculated with the R package *hierfstat* version 0.04–22[62] using the *genet.dist* function with the WC84 method. Significance of the observed F_{ST} values was estimated by bootstrapping over loci using the *boot.ppfst* function of the same package with 100,000 replications and calculating the 95% confidence intervals. Significance was inferred if the confidence interval did not overlap zero.

Genetic diversity. Nuclear genetic diversity (π and θ) was calculated using the Bioperl library PopGen version 1.6924[63]. The number of heterozygous positions in each sample were counted across the different nuclear markers and divided by their respective lengths. A map of heterozygosity values was then represented with QGIS[64].

Data availability

A total of 611 new sequences were deposited in EMBL/GenBank with Accession Numbers LR585354-LR585964, using the European Nucleotide Archive. For introns amplified using various primer pairs, only the shortest sequence was deposited for all samples.

Received: 6 May 2019; Accepted: 6 November 2019;
Published online: 22 November 2019

References

1. Papadopoulou, A. & Knowles, L. L. Toward a paradigm shift in comparative phylogeography driven by trait-based hypotheses. *Proc. Natl Acad. Sci. USA* **113**, 8018–8024 (2016).
2. Zamudio, K. R., Bell, R. C. & Mason, N. A. Phenotypes in phylogeography: Species' traits, environmental variation, and vertebrate diversification. *Proc. Natl Acad. Sci. USA* **113**, 8041–8048 (2016).
3. McNab, B. K. Geographic and temporal correlations of mammalian size reconsidered: a resource rule. *Oecologia* **164**, 13–23 (2010).
4. Yom-Tov, Y. & Geffen, E. Recent spatial and temporal changes in body size of terrestrial vertebrates: probable causes and pitfalls. *Biol. Rev.* **86**, 531–541 (2011).
5. Ashton, K. G., Tracy, M. C. & de Queiroz, A. Is Bergmann's Rule Valid for Mammals? *Am. Nat.* **156**, 390–415 (2000).
6. Lomolino, M. V., Sax, D. F., Palombo, M. R. & Van Der Geer, A. A. Of mice and mammoths: evaluations of causal explanations for body size evolution in insular mammals. *J. Biogeogr.* **39**, 842–854 (2012).
7. Martinez, P. A. *et al*. The contribution of neutral evolution and adaptive processes in driving phenotypic divergence in a model mammalian species, the Andean fox *Lycalopex culpaeus*. *J. Biogeogr.* **45**, 1114–1125 (2018).
8. Paetkau, D., Shields, G. F. & Strobeck, C. Gene flow between insular, coastal and interior populations of brown bears in Alaska. *Mol. Ecol.* **7**, 1283–1292 (1998).
9. Shafer, A. B. A., Nielsen, S. E., Northrup, J. M. & Stenhouse, G. B. Linking genotype, ecotype, and phenotype in an intensively managed large carnivore. *Evol. Appl.* **7**, 301–312 (2014).
10. Docampo, M., Moreno, S. & Santoro, S. Marked reduction in body size of a wood mouse population in less than 30 years. *Mamm. Biol.* **95**, 127–134 (2019).
11. Burgin, C. J., *et al*. Species accounts of Soricidae. In *Handbook of the Mammals of the World. Volume 8. Insectivores*, Sloths *and Colugos* (eds. Mittermeier, R. A. & Wilson, D. E.) (Lynx Edicions, 2018).
12. Ventura, J. *Neomys fodiens* (Pennant, 1771). In *Atlas y libro rojo de los mamíferos terrestres* de España (eds. Palomo, J., Gisbert, J. & Blanco, J. C.) 111–113 (Dirección General para la Biodiversidad-SECEM-SECEMU, 2007).
13. Igea, J., Aymerich, P., Bannikova, A. A., Gosálbez, J. & Castresana, J. Multilocus species trees and species delimitation in a temporal context: application to the water shrews of the genus *Neomys*. *BMC Evol. Biol.* **15**, 209 (2015).
14. Mendes-Soares, H. & Rychlik, L. Differences in swimming and diving abilities between two sympatric species of water shrews: *Neomys anomalus* and *N. fodiens* (Soricidae). *J. Ethol.* **27**, 317–325 (2009).
15. Wilson, D. E. & Reeder, D. M. *Mammal species of the world. A taxonomic and geographic reference*. (Johns Hopkins University Press, 2005).
16. Bühler, P. *Neomys fodiens niethammeri* ssp. n., eine neue Wasserspitzmausform aus Nord-Spanien. *Bonn zool. Beitr.* **14**, 165–170 (1963).
17. Nores, C., Canals, J. S., Castro, A. D. & Gonzalez, G. Variation du genre *Neomys* Kaup, 1829 (Mammalia, Insectivora) dans le secteur cantabro-galicien de la péninsule Ibérique. *Mammalia* **46**, 361–373 (1982).
18. López-Fuster, M. J., Ventura, J., Miralles, M. & Castién, E. Craniometrical characteristics of *Neomys fodiens* (Pennant, 1771) (*Mammalia, Insectivora*) from the northeastern Iberian Peninsula. *Acta Theriol.* **35**, 269–276 (1990).
19. Bühler, P. Zum taxonomischen Status der Großkopf-Wasserspitzmaus (*Neomys fodiens niethammeri* Bühler, 1963), aus Spanien nebst Festlegung und Beschreibung eines Neotypus. *Bonn zool. Beitr.* **46**, 307–314 (1996).
20. Kryštufek, B. & Quadracci, A. Effects of latitude and allopatry on body size variation in European water shrews. *Acta Theriol.* **53**, 39–46 (2008).
21. Ventura, J. *Neomys anomalus* Cabrera, 1907. in *Atlas y libro rojo de los mamíferos terrestres* de España (eds. Palomo, J., Gisbert, J. & Blanco, J. C.) 114–116 (Dirección General para la Biodiversidad-SECEM-SECEMU, 2007).
22. Querejeta, M. & Castresana, J. Evolutionary history of the endemic water shrew *Neomys anomalus*: Recurrent phylogeographic patterns in semi-aquatic mammals of the Iberian Peninsula. *Evol. Ecol.* **8**, 10138–10146 (2018).
23. Blanco, J. C. *Mamíferos de España. Vol 1. Insectívoros, Quirópteros, Primates y Carnívoros de la Península Ibérica, Baleares y Canarias*. (GeoPlaneta, 1998).
24. Cuenca-Bescós, G., Straus, L. G., González Morales, M. R. & García-Pimienta, J. C. Paleoclima y paisaje del final del Cuaternario en Cantabria: Los pequeños mamíferos de la cueva del Mirón (Ramales de la Victoria). *Revista Española de Paleontología* **23**, 91–126 (2008).

25. Sesé, C. Los micromamíferos (Eulipotyphla, Chiroptera, Rodentia y Lagomorpha) del yacimiento del Pleistoceno Superior de la cueva de El Castillo (Cantabria, España). *Estudios Geológicos* **73**, e072 (2017).
26. Rohland, N. & Hofreiter, M. Comparison and optimization of ancient DNA extraction. *BioTechniques* **42**, 343–352 (2007).
27. Carroll, E. L. *et al*. Genetic and genomic monitoring with minimally invasive sampling methods. *Evol. Appl.* **11**, 1094–1119 (2018).
28. Waits, L. P. & Paetkau, D. Noninvasive genetic sampling tools for wildlife biologists a review of applications and recommendations for accurate data collection. *J. Wildl. Manage*. 1418–1433 (2005).
29. McCarthy, M. S. *et al*. Genetic censusing identifies an unexpectedly sizeable population of an endangered large mammal in a fragmented forest landscape. *BMC Ecol.* **15**, 21 (2015).
30. Taberlet, P. & Fumagalli, L. Owl pellets as a source of DNA for genetic studies of small mammals. *Mol. Ecol.* **5**, 301–305 (1996).
31. Poulakakis, N., Lymberakis, P., Paragamian, K. & Mylonas, M. Isolation and amplification of shrew DNA from barn owl pellets. *Biol. J. Linn. Soc.* **85**, 331–340 (2005).
32. Barbosa, S., Pauperio, J., Searle, J. B. & Alves, P. C. Genetic identification of Iberian rodent species using both mitochondrial and nuclear loci: application to noninvasive sampling. *Mol. Ecol. Resour.* **13**, 43–56 (2013).
33. Hailer, F. *et al*. Nuclear genomic sequences reveal that polar bears are an old and distinct bear lineage. *Science* **336**, 344–347 (2012).
34. Toews, D. P. L. & Brelsford, A. The biogeography of mitochondrial and nuclear discordance in animals. *Mol. Ecol.* **21**, 3907–3930 (2012).
35. Brito, P. H. & Edwards, S. V. Multilocus phylogeography and phylogenetics using sequence-based markers. *Genetica* **135**, 439–455 (2009).
36. Sánchez-Gracia, A. & Castresana, J. Impact of deep coalescence on the reliability of species tree inference from different types of DNA markers in mammals. *PLOS ONE* **7**, e30239 (2012).
37. Igea, J., Juste, J. & Castresana, J. Novel intron markers to study the phylogeny of closely related mammalian species. *BMC Evol. Biol.* **10**, 369 (2010).
38. Kearns, A. M. *et al*. Nuclear introns help unravel the diversification history of the Australo-Pacific *Petroica* robins. *Mol. Phylogenet. Evol.* **131**, 48–54 (2019).
39. Degnan, J. H. & Rosenberg, N. A. Gene tree discordance, phylogenetic inference and the multispecies coalescent. *Trends Ecol. Evol.* **24**, 332–340 (2009).
40. Knowles, L. L. The burgeoning field of statistical phylogeography. *J. Evol. Biol.* **17**, 1–10 (2004).
41. Omland, K. E., Baker, J. M. & Peters, J. L. Genetic signatures of intermediate divergence: population history of Old and New World Holarctic ravens (*Corvus corax*). *Mol. Ecol.* **15**, 795–808 (2006).
42. Stewart, J. R., Lister, A. M., Barnes, I. & Dalén, L. Refugia revisited: individualistic responses of species in space and time. *Proc. R. Soc. B* **277**, 661–671 (2010).
43. Schmitt, T. & Varga, Z. Extra-Mediterranean refugia: The rule and not the exception? *Front. Zool.* **9**, 22 (2012).
44. López-García, J. M. *et al*. Palaeoenvironmental and palaeoclimatic reconstruction of the Latest Pleistocene of El Portalón Site, Sierra de Atapuerca, northwestern Spain. *Palaeogeogr. Palaeoclimatol. Palaeoecol.* **292**, 453–464 (2010).
45. Hewitt, G. M. Post-glacial re-colonization of European biota. *Biol. J. Linn. Soc.* **68**, 87–112 (1999).
46. Schmitt, T. Molecular biogeography of Europe: Pleistocene cycles and postglacial trends. *Front. Zool.* **4**, 11 (2007).
47. Hulva, P., Horácek, I., Strelkov, P. P. & Benda, P. Molecular architecture of *Pipistrellus pipistrellus*/*Pipistrellus pygmaeus* complex (Chiroptera: Vespertilionidae): further cryptic species and Mediterranean origin of the divergence. *Mol. Phylogenet. Evol.* **32**, 1023–1035 (2004).
48. Biedma, L., Román, J., Calzada, J., Friis, G. & Godoy, J. A. Phylogeography of *Crocidura suaveolens* (Mammalia: Soricidae) in Iberia has been shaped by competitive exclusion by *C. russula*. *Biol. J. Linn. Soc*. 1–15 (2018).
49. Rychlik, L. & Zwolak, R. Interspecific aggression and behavioural dominance among four sympatric species of shrews. *Can. J. Zool.* **84**, 434–448 (2006).
50. Clark, K., Karsch-Mizrachi, I., Lipman, D. J., Ostell, J. & Sayers, E. W. GenBank. *Nucleic Acids Res.* **44**, D67–72 (2016).
51. Schneider, C. A., Rasband, W. S. & Eliceiri, K. W. NIH Image to ImageJ: 25 years of image analysis. *Nat. Methods* **9**, 671–675 (2012).
52. Klingenberg, C. P. MorphoJ: an integrated software package for geometric morphometrics. *Mol. Ecol. Resour.* **11**, 353–357 (2011).
53. Stephens, M., Smith, N. J. & Donnelly, P. A new statistical method for haplotype reconstruction from population data. *Am. J. Hum. Genet.* **68**, 978–989 (2001).
54. Scheen, A.-C. *et al*. Use of allele-specific sequencing primers is an efficient alternative to PCR subcloning of low-copy nuclear genes. *Mol. Ecol. Resour.* **12**, 128–135 (2012).
55. Katoh, K. & Standley, D. M. MAFFT multiple sequence alignment software version 7: improvements in performance and usability. *Mol. Biol. Evol.* **30**, 772–780 (2013).
56. Bouckaert, R. *et al*. BEAST 2: a software platform for Bayesian evolutionary analysis. *PLoS Comp. Biol.* **10**, e1003537 (2014).
57. Baele, G. *et al*. Improving the accuracy of demographic and molecular clock model comparison while accommodating phylogenetic uncertainty. *Mol. Biol. Evol.* **29**, 2157–2167 (2012).
58. Stamatakis, A. RAxML version 8: a tool for phylogenetic analysis and post-analysis of large phylogenies. *Bioinformatics* **30**, 1312–1313 (2014).
59. Salzburger, W., Ewing, G. B. & Haeseler von, A. The performance of phylogenetic algorithms in estimating haplotype genealogies with migration. *Mol. Ecol.* **20**, 1952–1963 (2011).
60. Freedman, A. H. *et al*. Genome sequencing highlights the dynamic early history of dogs. *PLOS Genet.* **10**, e1004016 (2014).
61. Felsenstein, J. PHYLIP-phylogeny inference package (version 3.4). *Cladistics* **5**, 164–166 (1989).
62. Goudet, J. HIERFSTAT, a package for R to compute and test hierarchical F-statistics. *Molecular Ecology Notes* **5**, 184–186 (2005).
63. Stajich, J. E. & Hahn, M. W. Disentangling the effects of demography and selection in human history. *Mol. Biol. Evol.* **22**, 63–73 (2005).
64. QGIS Development Team. QGIS Geographic Information System. Open Source Geospatial Foundation Project, http://qgis.osgeo.org (2019).

Acknowledgements

We thank the Museum of Southwestern Biology, the University of Alaska Museum, Adrián Álvarez Vena, Anna Bannikova and Juan Fernández Gil for samples, and Alfonso Balmori Martínez for help with field work and discussions. We also thank Link E. Olson and an anonymous reviewer for their helpful comments on this manuscript. This work was financially supported by research projects CGL2014-53968-P and CGL2017-84799-P of the "Plan Nacional I + D + I del Ministerio de Ciencia, Innovación y Universidades (Spain)", cofinanced with FEDER funds (AEI/FEDER, UE), to J.C. Support was also provided by grant 2017-SGR-991 of the "Generalitat de Catalunya". A.B.P. was supported by research contract BES-2015-074119 of the "Ministerio de Ciencia, Innovación y Universidades", cofinanced with FEDER funds.

Author contributions

J.C. designed the study with the help of A.B.P., C.N., A.F.G, P.A. and J.G. A.B.P., C.N. and J.R. collected samples. A.B.P. performed laboratory work and analyses. L.E. helped with laboratory work and J.C. with morphometric analysis. A.B.P. and J.C. wrote the paper with input from the other authors. All authors contributed to the interpretation of the results and approved the final version of the manuscript.

Competing interests

The authors declare no competing interests.

Additional information

Supplementary information is available for this paper at https://doi.org/10.1038/s41598-019-53891-y.

Correspondence and requests for materials should be addressed to J.C.

Reprints and permissions information is available at www.nature.com/reprints.

Publisher's note Springer Nature remains neutral with regard to jurisdictional claims in published maps and institutional affiliations.